



## Semiconducting polymer dots for multifunctional integrated nanomedicine carriers

Ze Zhang<sup>a</sup>, Chenhao Yu<sup>c</sup>, Yuyang Wu<sup>c</sup>, Zhe Wang<sup>c</sup>, Haotian Xu<sup>d</sup>, Yining Yan<sup>e</sup>, Zhixin Zhan<sup>b, \*\*</sup>, Shengyan Yin<sup>c,\*</sup>

<sup>a</sup> Department of Hepatobiliary and Pancreatic Surgery II, General Surgery Center, The First Hospital of Jilin University, Changchun, Jilin 130012, PR China

<sup>b</sup> Department of Neurosurgery, The First Hospital of Jilin University, Changchun, Jilin 130012, PR China

<sup>c</sup> State Key Laboratory of Integrated Optoelectronic, College of Electronic Science and Engineering, Jilin University, No.2699 Qianjin Street, Changchun, Jilin 130012, PR China

<sup>d</sup> Department of Hepatobiliary and Pancreatic Surgery, The Third Bethune Hospital of Jilin University, Changchun, Jilin 130000, PR China

<sup>e</sup> Department of Radiology, The Third Bethune Hospital of Jilin University, Changchun, Jilin 130000, PR China

### ARTICLE INFO

#### Keywords:

Semiconducting polymer dots  
Nanomedicine  
Bioimaging  
Biosensor  
Translational medicine  
Diagnosis  
Treatment

### ABSTRACT

The expansion applications of semiconducting polymer dots (Pdots) among optical nanomaterial field have long posed a challenge for researchers, promoting their intelligent application in multifunctional nano-imaging systems and integrated nanomedicine carriers for diagnosis and treatment. Despite notable progress, several inadequacies still persist in the field of Pdots, including the development of simplified near-infrared (NIR) optical nanopropes, elucidation of their inherent biological behavior, and integration of information processing and nanotechnology into biomedical applications. This review aims to comprehensively elucidate the current status of Pdots as a classical nanophotonic material by discussing its advantages and limitations in terms of biocompatibility, adaptability to microenvironments *in vivo*, etc. Multifunctional integration and surface chemistry play crucial roles in realizing the intelligent application of Pdots. Information visualization based on their optical and physicochemical properties is pivotal for achieving detection, sensing, and labeling probes. Therefore, we have refined the underlying mechanisms and constructed multiple comprehensive original mechanism summaries to establish a benchmark. Additionally, we have explored the cross-linking interactions between Pdots and nanomedicine, potential yet complete biological metabolic pathways, future research directions, and innovative solutions for integrating diagnosis and treatment strategies. This review presents the possible expectations and valuable insights for advancing Pdots, specifically from chemical, medical, and photophysical practitioners' standpoints.

### 1. Introduction

Semiconducting polymer dots (Pdots) can achieve unique optical characteristics by optimizing their  $\pi$ -conjugated structure [1]. By altering the composition of the conjugated chains within the Pdots and modifying the external surface of their spherical core architecture, advanced functionalities can be integrated into these nanoparticles, transcending their optical properties [2,3]. For instance, Pdots have shown potential as intelligent multifunctional integrated nanocarriers for applications such as detection sensing, signal conversion, environmental perception, disease diagnosis, tumor treatment, and more [4,5].

These nanoparticles are of significant value for further exploration, as illustrated in Fig. 1, which showcases the “hot research topics” surrounding Pdots in the optical field, nanomedicine and beyond, classified according to their functional modification purposes and application domains. The inspiration for this newsletter image stems from nearly two decades of research, summarizing widely recognized Pdots research outcomes, including synthetic pathways, biomedical imaging, high-sensitivity substrate detection nanopropes, and multifunctional integrated nano-drug carriers. Fig. 2A compares the research priorities and areas of expertise of various classical optical materials in optics, while Fig. 2B indicates that intrinsic brightness, plug-and-play

\* Corresponding author.

\*\* Corresponding author.

E-mail addresses: [zhanzx@jlu.edu.cn](mailto:zhanzx@jlu.edu.cn) (Z. Zhan), [syin@jlu.edu.cn](mailto:syin@jlu.edu.cn) (S. Yin).

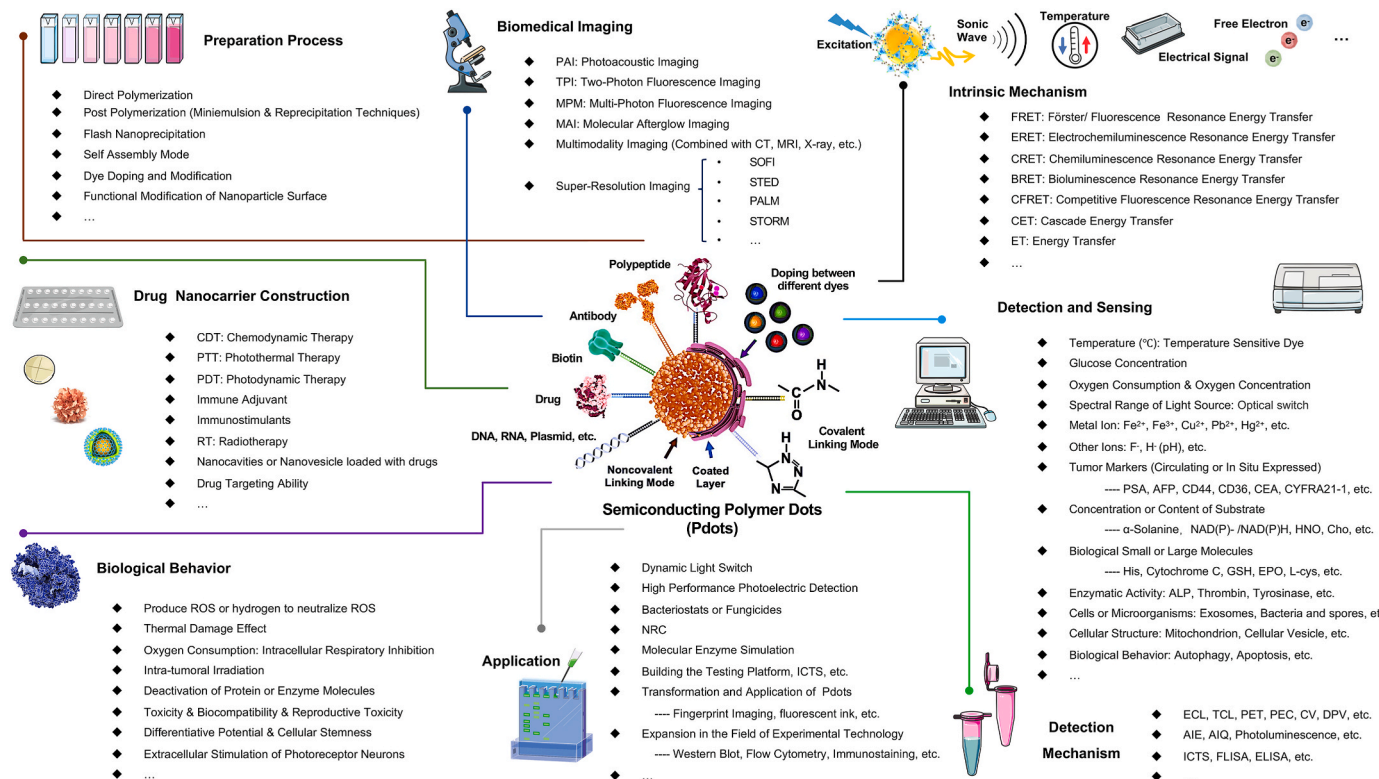


**Fig. 1. Newsflash Chart of Semiconducting Polymer Dots.** Progression and future of semiconducting polymer dots within and beyond the optical properties and toward the expanded applications in analytical testing and biomedical imaging. Starting from the preparation process, the wide application of visual signals in inspection, sensing, labeling probes, drug carriers, and other fields is elaborated, and the advantages and limitations of Pdots in optical properties, versatility, biocompatibility, and microenvironment adaptability are explained. Progression and future of Pdots within and beyond the optical properties and toward the expanded applications in analytical testing and biomedical imaging.

compatibility, blinking and photo-switching, cargo capacity, and particle size have reached maturity. However, improvements could be made in tap & labeling, surface chemistry, and resistance to photobleaching. The recent research trend has shifted towards a focus on exploring emerging optical materials with emission wavelengths in the near-infrared domain, extending beyond the visible light domain [6,7]. Reflecting the research history of other classic optical materials, emerging trends are likely to emphasize energy conversion, quantum yield, biomimetic material development, and medical application innovation [8]. Building on the high biocompatibility of Pdots, the emergence of an integrated nanotechnology platform for diagnosis and treatment, as well as the construction of nanozymes, have been recently reported as promising in current research.

Although the meticulous design of delocalized electrons and  $\pi$ -conjugated structures can generate a novel generation of Pdots, it is undeniable that the research and development of Pdots remains in its initial stages [2,9] (Fig. 2C - the number of research results released by different classical optical materials at different time nodes). Based on their distinctive optical properties, the color composition of these materials can be fine-tuned over a broad range, spanning from vibrant fluorescence in the visible light spectrum to imperceptible bands in the near-infrared region, from narrow reflection peaks in single-molecule structures to extensive reflection bands in various dye doping, from the inherent high brightness of Pdots to the signal-responsive modifications induced by external stimuli [10–12]. Particularly, introducing the nanoprecipitation method and developing water-soluble conjugated polymers have enabled Pdots to thrive in the fields of detection and imaging [13]. The ingenious design of Pdots enables these advanced functions through responsive materials or modification with groups possessing specific biological properties [14,15]. Intriguingly, the evolution of this functional Pdot system not only inherits the superior optical

characteristics of traditional optical materials but also endows it with excellent biocompatibility, laying the foundation for nanomedicine research and development.

The present review delineates a multitude of research domains associated with Pdots communication graphs (Fig. 1). The primary objective is to supply novel ideas and insights for designing and discovering next-generation Pdots boasting advanced functionalities. We have compiled the published structural formulas of Pdots and accentuated the distinctive optical properties and intricate structures achievable through doping dyes and modifying conjugated chains. The functional extension of Pdots beyond conventional optical nanomaterials in inspection and sensing, and the manner in which to visualize the substrate for detection through signal conversion, are also discussed. Additionally, we explore strategies to surmount the challenges of biocompatibility at cellular, tissue, organ, and individual levels, as well as the novel opportunities and difficulties that lie ahead in biomedical realms beyond disease diagnosis and treatment. By reviewing the progression of Pdots and summarizing their extensive applications in inspection, sensing, labeling probes, drug carriers, and other fields, we elucidate their merits and limitations in optical properties, versatility, biocompatibility, and microenvironment adaptability. Subsequently, we delve into the principal advancements of Pdots in various fields and anticipate that this review will furnish novel ideas and insights for materials science and biomedicine researchers.

## 2. Semiconducting polymer dots and preparation technology

Scientists have been actively engaged in the development of novel fluorescent nanoprobes characterized by high fluorescence brightness, exceptional light stability, and superior biocompatibility [16–18] (Fig. 2A & B), such as fluorescent dyes (FDs), inorganic quantum dots

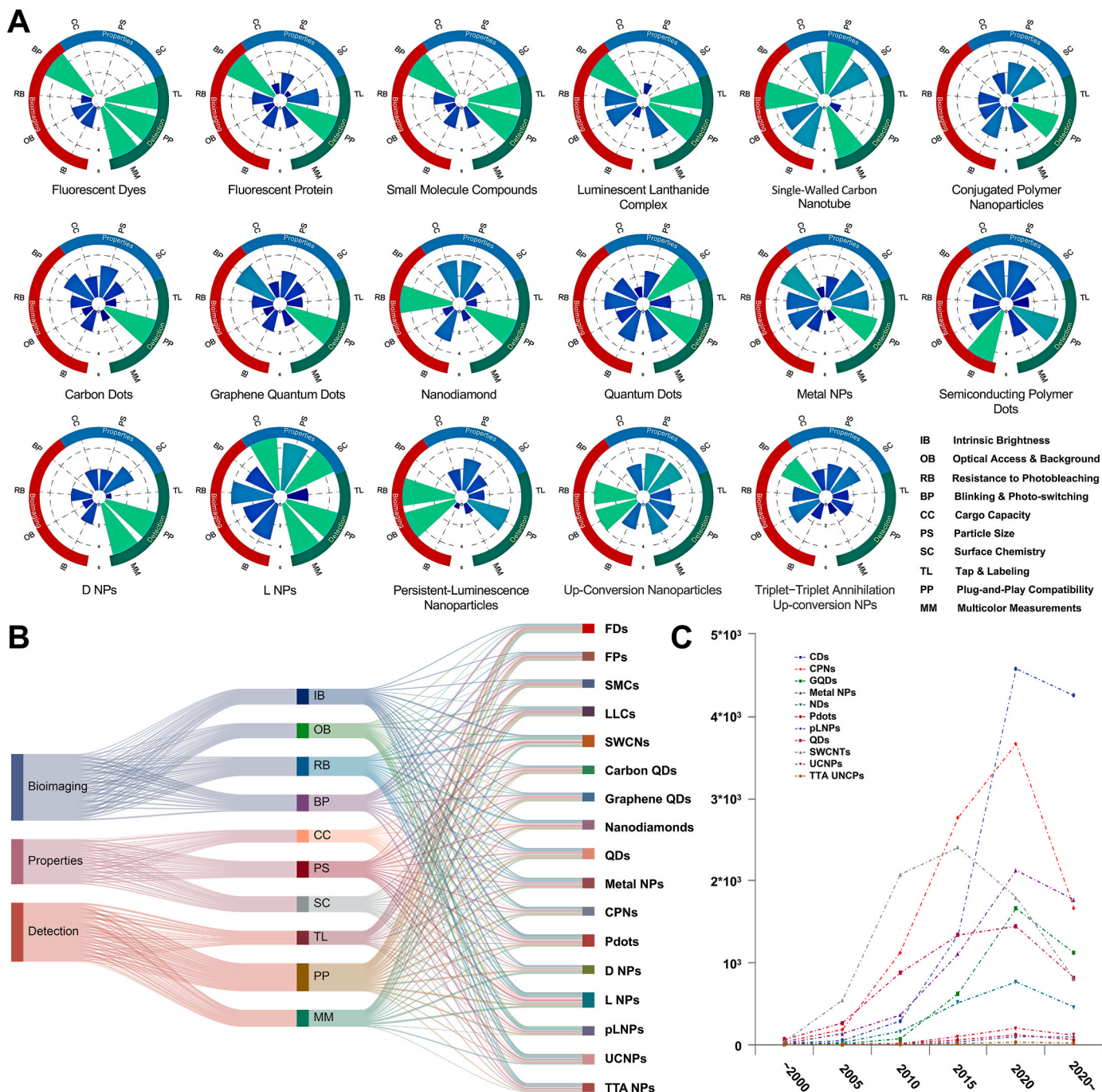


**Fig. 2. The research focuses on luminescent molecular nanomaterials, and the quantity trend of published literature. A.)** Qualitative scores for luminescent molecular nanomaterials (LMNs) in various functional categories are shown as radar plots. These qualitative scores might reflect variations in exploring potential, the difficulty of preparation, Spectral coverage range, medical-biological imaging, detection analysis, and achievement transformation, as discussed in the text. The higher the assignment scores, the more in-depth the research progress. Doped and labeled NPs are listed as D&L NPs. Drawing inspiration and reprinted with permission from Ref. [2]. Copyright 2020 American Chemical Society. **B.)** Sankey diagram based on the score of each LMN in Fig. 3A. Among the three areas, researchers pay more attention to the application of optical materials in analysis, monitoring, and biological imaging, while less energy is devoted to the properties of materials. **C.)** Approximate numbers of indexed publications per year of various optical nanomaterials. Abbreviations: SWCNT<sub>s</sub>, single-walled carbon nanotubes; CDs, carbon dots; CPNs, conjugated polymer nanoparticles; UCNPs, lanthanide-doped upconversion nanoparticles; metal NCs, metal nanoclusters; Pdots, semiconducting polymer dots; pLNP<sub>s</sub>, persistent-luminescence nanoparticles; TTA-NPs, triplet-triplet annihilation upconversion nanoparticles. Source: PubMed (<https://pubmed.ncbi.nlm.nih.gov>).

(Qdots), fluorescent proteins (FPs), carbon dots (Cdots), up-conversion nanoparticles (UCNPs), metal nanoparticles (metal NPs), and so on [2, 5, 19–23]. Among these, Pdots have garnered significant attention in the field of fluorescent chemical nanoprobes due to their exceptional fluorescence brightness, outstanding photostability, high quantum yield,

and commendable biocompatibility [24–27]. As defined, the core of Pdots consists of  $\pi$ -conjugated chains within hydrophobic polymers [28–30]. The mass fraction or volume fraction of  $\pi$ -conjugated polymers must exceed 50 %, as its interaction with delocalized electrons determines the quantum yield and fluorescence brightness of such probes.

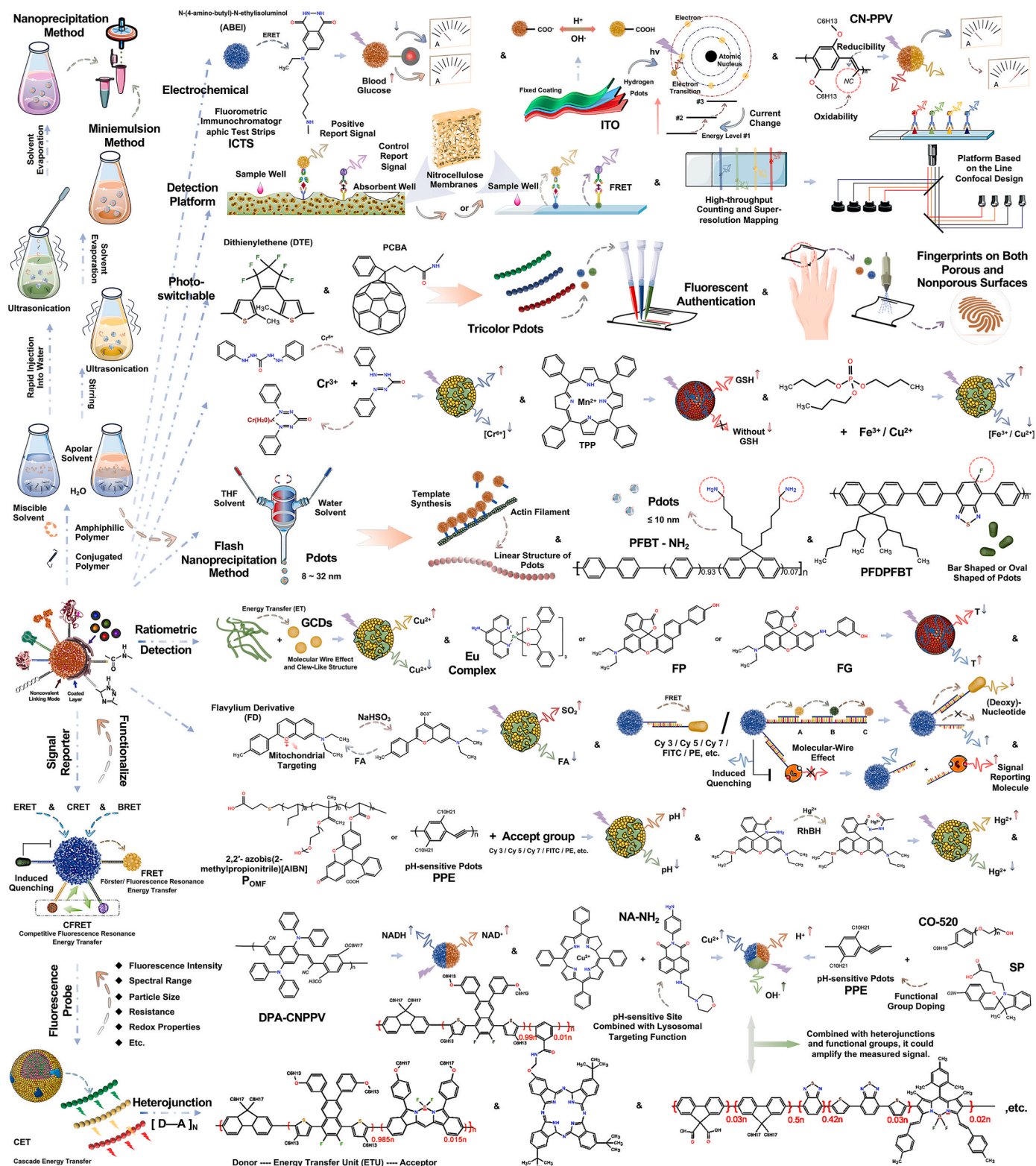


**Fig. 3. The preparation process of semiconducting polymer dots (Pdots), the mechanisms used in analysis and detection, and representative applications.**

Upper Left). Schematic diagrams of two common preparation processes. Left Lower). The inherent mechanism applied to substrate detection and analysis. Upper Right). Schematic diagram of electrochemical detection, ICTS and anti-counterfeiting stamp. Middle Part). Special preparation process. Right Lower). Schematic diagram of substrate detection based on energy transfer and heterojunction. Abbreviations: AIE, Aggregation-Induced Emission; AIQ, Aggregation-Induced Quenching; BRET, bioluminescence resonance energy transfer; CET, cascade energy transfer; CRET, chemiluminescence resonance energy transfer; CFRET, competitive fluorescence resonance energy transfer; CV, cyclic voltammetry; D-A: donor-(single or multiple) energy transfer unit (ETU)-accepter; DPV, differential pulsed voltammetry; ECL, electrochemiluminescence; ERET, electrochemiluminescence resonance energy transfer; FRET, Förster/fluorescence resonance energy transfer; ET, energy transfer; ICTS, fluorometric immunochromatographic test strips; NRC, nanoreactors; PEC, photoelectrochemical; TCL, thermochemiluminescence.

Furthermore, the diameter of Pdots should be  $< 100$  nm, typically distributed between 5–20 nm [31]. The incorporation of polyethylene glycol (PEG), poly (isobutylene-*alt*-maleic anhydride) (PIMA), poly (styrene-*co*-maleic anhydride) (PSMA), and other agents into the host chain during the preparation process also aids in forming a stable Pdots structure and a more concentrated distribution of particle size [32–35].

## 2.1. Miniemulsion and nanoprecipitation method

We present two prevalent preparation approaches for Pdots (Fig. 3, upper left), and enumerate several recently proposed innovative techniques (Fig. 3, middle area), including the fabrication of ultrasmall-sized and rod-shaped nanoparticles. The “Miniemulsion Method” and “Nanoprecipitation Method” (also known as the “Reprecipitation Method” in certain literature) are the most extensively employed strategies for constructing polymer nanoparticles [36–39]. These two conventional preparation strategies have been described in detail in several reviews and will not be stated too much in this article. Relevant information can be found in the following literature [3,40,41]. It is worth noting that for the former (Miniemulsion Method), due to variations in the concentrations of polymer precursor solution and surfactant during the preparation process, the final nanoparticle size distribution is comparatively broad, spanning approximately 40–500 nm. To achieve compact-sized Pdots end products, researchers drew upon the synthesis strategies of micelles and nanomedicines, incorporated spatial stabilizers into the synthesis process, and meticulously controlled the solution concentration at each stage. The inclusion of stabilizers can concentrate the final product’s particle size and reduce it to 10–20 nm [42]. And for the latter (Nanoprecipitation Method or Reprecipitation Method), owing to the absence of surfactants in the system, the particle size distribution of the final product can be narrowed down to some extent. The difference in solubility of polymers in various solutions can result in the collapse of the main chain, leading to the formation of more compact polymer nanoparticles due to the combined effects of significantly reduced solubility and water surface tension. The particle size distribution of these nanoparticles is primarily concentrated within the range of 5–30 nm. Factors such as the initial concentration of polymer in the premix, the temperature of the organic and aqueous phases, and the frequency and intensity of ultrasound can all influence the particle size distribution of the final product. The Pdots structure generated using the second method is more stable, characterized by smaller particle size, more concentrated distribution, and improved performance [24,37]. As such, it can be applied across a wider range of fields compared to other techniques.

Based on the two prevalent preparation techniques mentioned above, researchers have also proposed advanced methods such as the “Flash Nanoprecipitation Method” and the “Self-assembly Method (also known as the ‘Direct Synthesis’).” The self-assembly method is less renowned due to its inability to address the issue of relatively dispersed particle size distribution [3]. On the other hand, the flash nanoprecipitation method builds upon the nanoprecipitation technique and optimizes the preparation process [43]. In essence, researchers fabricated a self-oscillating container capable of simulating the effects of ultrasound. The container’s two input ends are separately fed with a premixed solution of the organic phase (e.g., containing tetrahydrofuran (THF), dimethylformamide (DMF), etc.) and an aqueous phase. These solutions rapidly mix within the container, leading to a chain collapse, and ultimately yield polymer nanoparticles with a particle size distribution range of 8–32 nm at the output end (the schematic diagram is shown in the middle of Fig. 3).

## 2.2. Novel preparation process and storage

Regardless of the method employed—miniemulsion, nanoprecipitation, flash nanoprecipitation, or self-assembly—the resulting Pdots nanoparticles are invariably spherical, making it challenging to

obtain nanoparticles with distinct macroscopic physical morphologies from these processes. The “Template Method” offers a unique solution to this issue, capable of producing chain-like polymers [44]. Oleg A Andreev et al. proposed utilizing actin filaments as templates to form nanowires, employing PEG-amine (polyethylene glycol containing NH<sub>2</sub> groups) modified quantum dots (Qdots), and utilizing EDC [1-ethyl-3-(3-(dimethylamino) propyl) carbodiimide] to generate peptide bonds with the carboxyl groups on the actin filaments. Although this technique employs Qdots instead of Pdots, it still provides valuable insights for devising new Pdots preparation strategies. Additionally, Daniel T. Chiu et al. discovered that utilizing functional polymer poly (isobutylene-*alt*-maleic anhydride) (PIMA) instead of poly (styrene-*co*-maleic anhydride) PSMA, namely NH-PIMA-modified PFBT (PFBT-NH-PIMA Pdots), led to smaller particle sizes, averaging less than 10 nm. Concurrently, this researcher also proposed employing a fluoride-based monofluoro-substituted benzothiadiazole-based polymer, namely PFDPFBT Pdots (previously known as PFDPBT) [45]. The introduced fluorine atoms, under the influence of the formed F–F or F–H bonds, can alter the spatial conformation of the host chain, resulting in a rod-like Pdots macrostructure (refer to Fig. 3 middle part). Regarding the storage and transportation of Pdots, this researcher suggested a freeze-drying process [46]. This method preserves the optical properties and physicochemical stability of Pdots while ensuring their cellular targeting ability. Freeze-dried under the protection of a high concentration of sucrose solution (v/v = 10 %), the rehydrated Pdots exhibited no signs of aggregation, and the brightness and quantum yield after treatment demonstrated some improvement.

## 3. Characterization and spectral properties of semiconducting polymer dots

### 3.1. Characterization

In preceding discussions, it was noted that during their synthesis, polymer chains are prone to bending and folding. These structures are vulnerable to environmental shifts, often leading to spherical nanoparticle formation [47,48]. During this formation, organic molecules or biomolecules might integrate into the core of these nanoparticles or attach chemically to the polymer’s main chain, thus forming a heterojunction structure [49–51]. However, incorporating external molecular groups into the polymer does not guarantee enhanced outcomes. For instance, adding AIE groups may result in reduced quantum yield and diminished fluorescence brightness due to perturbation relaxation and stress relaxation effects [52,53]. To overcome such challenges, it is advantageous to employ multiple energy transfer strategies. Of particular interest is the development of near-infrared (NIR) dyes, which will be elaborated in subsequent discussions about spectral characteristics. The introduction of molecular groups impacts the physicochemical stability of Pdots in various ways. At a macroscopic level, this includes influencing colloidal system stability, chain structure preservation, storage duration, and so forth [54,55]. At a microscopic scale, it affects quantum yields, fluorescence intensity, energy transfer efficiency, and the maintenance of the heterojunction structure. The incorporation of amphiphilic polymers at the macroscopic level markedly improves Pdot stability and confers hydrophilicity. Additionally, optimal surface charges (ranging from approximately –20 to –40 mV) are crucial for maintaining nanoparticle charge repulsion. Despite the flexibility of the chemical bonds within the conjugated chain, the main chain retains a degree of rigidity due to van der Waals forces, stacking forces, hydrogen bonds, ionic bonds, and other interactions. This rigidity becomes evident during the folding collapse, creating gaps that can be filled by amphiphilic polymers. These polymers enhance chain interactions and ensure the dense packing of the spherical core. For instance, quantum dots dissolved in high ionic strength solutions may lose colloidal stability due to ion-induced destabilization, leading to the leakage of dyes from the amphiphilic polymer-enveloped spherical structures and alterations in

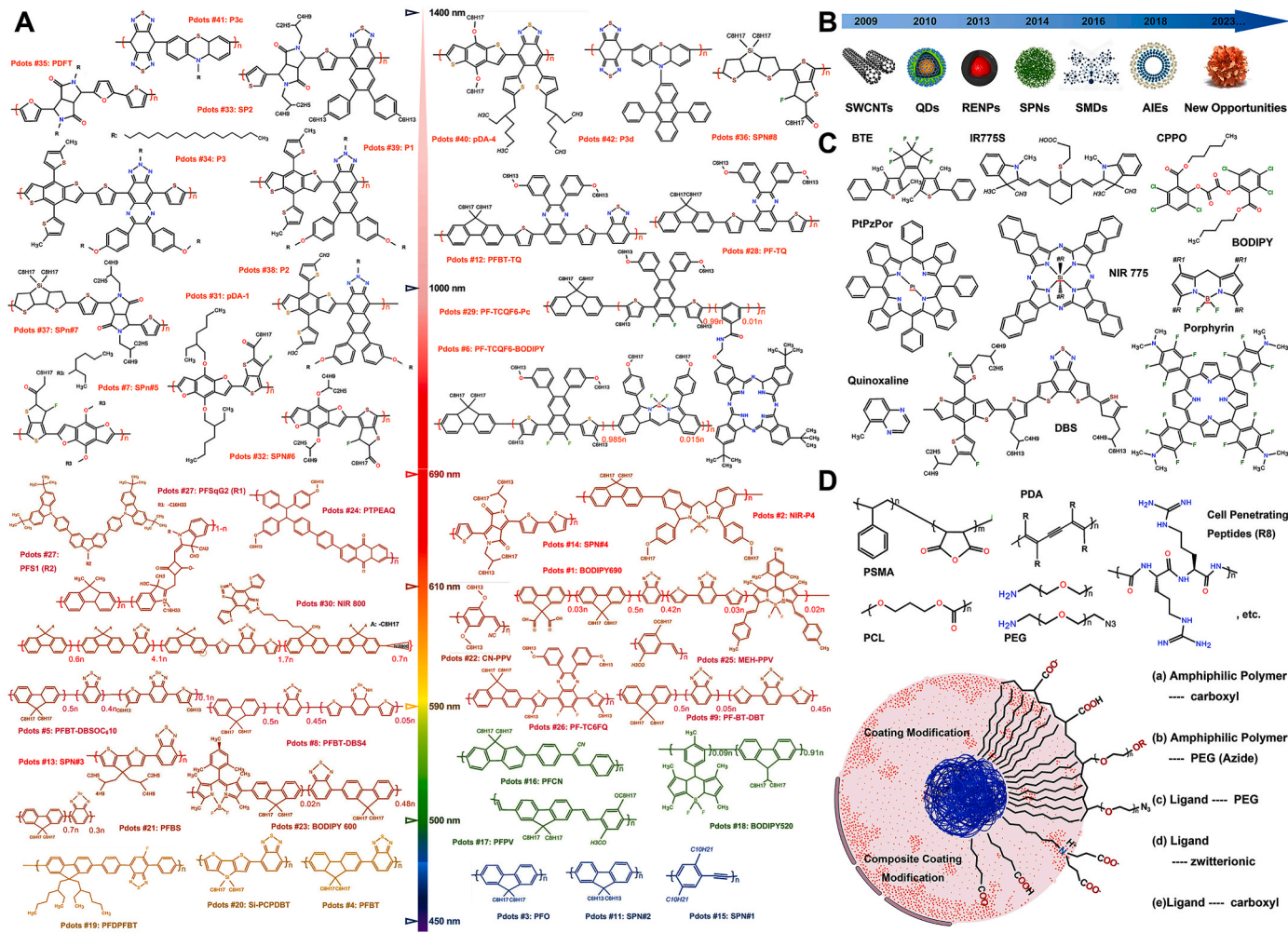


**Fig. 4. Molecular Design Strategies and Surface Modification.** A). Chemical structures of the published Pdots. The chemical structural formula's color represents the emission peak's spectral position.  $R_x$  represents the side chain chemical structural formula. Drawing inspiration and reprinted with permission from Ref. [65]. Copyright 2021 American Chemical Society. B). Hotspot optical nanomaterials at different time nodes. Abbreviations: SWCNTs, single-walled carbon nanotubes; QDs, quantum dots; RENPs, rare-earth-doped nanoparticles; SPNs, supramolecular polymer networks; SMDs, small-molecule dyes; AIEs, aggregation-induced emission luminogens. Drawing inspiration and reprinted with permission from Ref. [92]. Copyright 2020 American Chemical Society. C). The common doped and combined fluorescent dyes (donor-acceptor or donor-bridge-acceptor) inside or outside the  $\pi$ -conjugated chain. Abbreviations: BTE, (1,2-bis(2,4-dimethyl-5-phenyl-3-thienyl)-3,3,4,4,5,5-hexafluoro-1-cyclopentene; CPPO, Bis(3,4,6-trichloro-2-[(pentyloxy)carbonyl]phenyl) oxalate; BODIPY, 10-(4-(2,5-dioxo-2,5-dihydro-1H-pyrrol-1-yl)phenyl)-5,5; DBS, dithienyl-benzo selenadiazole; PtBzPor, (meso-tetraphenyl tetraazobenzoporphyrin platinum (II), etc. D). Common amphiphilic polymers or compounds used for surface chemical modification. Drawing inspiration and reprinted with permission from Ref. [2]. Copyright 2020 American Chemical Society. Abbreviations: PSMA, poly (styrene-co-maleic anhydride); PDA, polydiacetylene; PEG, polyethylene glycol; PCL, Poly (ε-caprolactone), etc. Exposed chemical groups that can be used for functionalization after modification, which could form a single or multiple layer surface modification coating. Or include processes such as electrostatic bonding and self-forming coating.

optical stability. Microscopically, an excessive number of hydrophilic groups can overly intensify interactions between the main chain and solvent. A balanced ratio of hydrophilic groups (conjugated polymer to amphiphilic polymer ratio of 4:1) is more effective in compacting the overall structure [56–59].

### 3.2. Energy transfer

Energy transfer (ET) is a ubiquitous phenomenon in both nature and materials science. It fundamentally involves the transference of energy from one entity or form to another [60,61]. In natural settings, this transfer manifests through the conversion of thermal energy into electrical or kinetic energy, facilitated by mechanical devices to propel production activities [62,63]. Its significance is paramount in the quest for advanced optical nanomaterials and their multifaceted applications. In the design of optical nanomaterials, efficient ET donors (D) transfer brightness effectively to acceptors (A) using various mechanisms,

including bioluminescence resonance energy transfer (BRET), cascade energy transfer (CET), fluorescence resonance energy transfer (CFRET), chemiluminescence resonance energy transfer (CRET), competitive electrochemiluminescence resonance energy transfer (ERET), and Förster/fluorescence resonance energy transfer (FRET) as depicted in Fig. 3 (lower left corner) [64–67]. This transfer is notably more pronounced in Pdots, which are substantially brighter than most fluorescent dyes [68–70]. This attribute significantly enhances detection sensitivity and expands probe spectral coverage. Efficient ET requires a close proximity between donor and acceptor molecules (the molecular-wire effect) and a substantial overlap between the emission spectrum of D and the absorption spectrum of A [58,71,72]. These principles have been extensively explored in the development of NIR Pdots. Furthermore, the large absorption cross-section and broad, tunable emission band of Pdots facilitate doping and integration with other fluorescent dyes (in donor-acceptor or donor-bridge-acceptor configurations) within or adjacent to the  $\pi$ -conjugated chain. This approach achieves spectral

**Table 1**  
Semiconducting polymer dots (Pdots) for applications.

No.	Pdots	$\lambda_{\text{max}}^{\text{abs}}$ (nm)	$\lambda_{\text{max}}^{\text{em}}$ (nm)	$\Phi$ (%)	Application	Ref.
01	APNs	700	720	N.A.	Cancer and Allograft	[93]
02	ASO	600	790	0.12	Tumor	[94]
03	ASPNC	~400	680	N.A.	Exosomes Sensing	[95]
04	Au@FP	~500	660	N.A.	Fluorescent Imaging	[96]
05	Au-NP-Pdots	525	~440/460	18	Multimodal Imaging	[97]
06	BODIPY	561	720	23.2	Fluorescent Imaging	[67]
07	BODIPY520 (Pdots #18)	378/504	516	35	N.A.	[4]
08	BODIPY600 (Pdots #23)	455/546	596	13	N.A.	[4]
09	BODIPY690 (Pdots #01)	450/538/653	688	19	N.A.	[4]
10	CL-BODIPY 565	330/380/480	564	32	Fluorescent Imaging	[98]
11	CN-PPV (Pdots #21)	374/494	600	11.22	Fluorescent Imaging	[99]
12	CR/TPP@Pdots	380	440/610	N.A.	pH monitoring	[72]
13	CSPN	403/660	830	N.A.	Cancer Treatment	[100]
14	DPA-CNPPV	294	627	10.8	NADH Sensing	[101]
15	DPP-BTzTD	~1000	N.A.	N.A.	Photoacoustic Imaging	[102]
16	DPP-DT	630~811	N.A.	N.A.	Photothermal Therapy/Photoacoustic Imaging	[103]
17	DQ-CD@Pdots	450	541	N.A.	GSH	[71]
18	FCPNPs-GSH, GNPs@PEI	470	500~600	N.A.	GST	[104]
19	FH	N.A.	425/590	N.A.	Fluorescent Imaging/Photodynamics Therapy	[105]
20	GCDs@RSPN	380	501/625	N.A.	Copper Ions Detection	[106]
21	HA-BSe NPs	452	760/825	0.33	Photothermal Therapy	[107, 108]
22	L-Pdots	N.A.	425	N.A.	MicroRNA-21	[109]
23	Lu-SPN-GIP	808	N.A.	N.A.	Photothermal Therapy	[110]
24	MEH-PPV (Pdots #25)	504	776	N.A.	Fluorescent Imaging	[111]
25	MiRNA-122 Nanoprobe	N.A.	543	N.A.	MicroRNA-122	[112]
26	MMPF NPs	680	810	N.A.	Tumor	[113]
27	m-PBTQ4F	946	980/1150 (1123)	3/3.2	Fluorescent Imaging	[114]
28	NIR800 (Pdots #30)	350/470	800	8	Fluorescent Imaging	[50]
29	NIR-P4 (Pdots #02)	690	720	30	Fluorescent Imaging	[115]
30	N-Pdots	N.A.	672	N.A.	MicroRNA-205	[109]
31	OSPS	403/660	830	N.A.	Cancer Treatment	[100]
32	P2,7-CZBT	315/434	587	2	Fluorescent Imaging	[116]
33	P3,6-CZBT	468	612	3	Fluorescent Imaging	[116]
34	P1 (Pdots #39)	923	1095	0.92	Fluorescent Imaging	[117]
35	P2 (Pdots #38)	870	1063	N.A.	Fluorescent Imaging	[117]
36	P3 (Pdots #34)	703	1058	N.A.	Fluorescent Imaging	[117]
37	P3C (Pdots #41)	740	1000~1450	1.7	Fluorescent Imaging	[51]
38	PBD-CD36	850~1100	N.A.	N.A.	Photoacoustic Therapy	[118]
39	PCPDFT	395/602	758	2	Fluorescent Imaging	[116]
40	PCPDFTBT@MnO <sub>2</sub> @@Ce3+ Ce4+	404/650	840	N.A.	Photodynamics Therapy	[119, 120]
41	pc-PFO	435	439	9~24	Photocrosslinking	[121]
42	PD4Gx	380	425/672	11.5	Blood Glucose Monitoring	[122]
43	pDA-1	654	1047	1.7	Fluorescent Imaging	[123]
44	pDA-4 (Pdots #40)	1000~	1348	N.A.	Fluorescent Imaging	[123]
45	PDDB@RhBH	380	557/580	N.A.	Mercury Ion Detection	[124]
46	PDFT	809	1032	N.A.	Fluorescent Imaging	[125]
47	Pot@Fe@GOx	~850	N.A.	N.A.	Cancer Treatment	[126]
48	Pdots@hydrogel	800~900	600	N.A.	Photothermal Fluorescence Therapy	[127]
49	Pdots-C6	745	1055	N.A.	Fluorescent Imaging	[128]
50	Pdots-Eu	342	350/650	26	Temperature Sensing	[129]
51	PDTTB	314/459	674	1	Fluorescent Imaging	[116]
52	PEPV-TPP@MnO <sub>2</sub>	458	656	N.A.	GSH	[130]
53	PFBT (Pdots #04)	450	550/640~820	20~40	Fluorescent Imaging/Hydrogen therapy	[131, 132]
54	PFBS (Pdots #22)	488	600	60	Fluorescent Imaging	[133]
55	PFBT@TPP	400~500	660	N.A.	Bioanalysis/Photodynamics Therapy	[134, 135]
56	PFBT-DBS	320~397	709~760	1~20	Fluorescent Imaging	[136]
57	PFBT-DBS4 (Pdots #08)	323/450/680	438/702	11.7	Fluorescent Imaging	[136]
58	PFBT-DBSIC <sub>6</sub> X	322~373/ 450~500	672~702	2~12	Fluorescent Imaging	[136]
69	PFBT-DBSOC <sub>6</sub> 10 (Pdots #05)	321~367/ 458~557	701~724	2~36	Fluorescent Imaging	[136]
60	PFBT-DBT (Pdots #09)	465	650	N.A.	Fingerprint detection	[137]
61	PFBT-Py	~500	530	N.A.	Fluorescent anti-counterfeiting	[138]
62	PFBT-RhB	470	580	30	Temperature sensing	[139]
63	PFBT-SP	~450	550	N.A.	Fluorescent Anti-counterfeiting	[138]
64	PFBT-TQ (Pdots #12)	350	680	N.A.	Fingerprint Detection	[137]
65	PFCN (Pdots #16)	~390	~450	N.A.	AFP Detection	[140]
66	PF-DNAP CPNs	390	530	N.A.	ssDNAC	[141]
67	PFDPFBT (Pdots #19)	410	510	46	Fluorescent Imaging	[45]
68	PFO (Pdots #03)	~350	~490	N.A.	ROS & CEA Detection	[142]

(continued on next page)

**Table 1** (continued)

No.	Pdots	$\lambda_{\text{max}}^{\text{abs}}$ (nm)	$\lambda_{\text{max}}^{\text{em}}$ (nm)	$\Phi$ (%)	Application	Ref.
69	PFO/CN-PPV@Tyr-Ome	380	586	N.A.	TR	[143]
70	PFO/PSMA-NA	N.A.	435	N.A.	Antibacterial	[144]
71	PFO-BODIPY	375	520/680	34/16	Cell Tracking	[145]
72	PFO-DPC	380~400	440/470	N.A.	Chromium ion detection	[146]
73	PFODTB	200	N.A.	N.A.	Hydrogen therapy	[131]
74	PFO-PCBA Pdots	405	440/470	N.A.	Super-Resolution Imaging	[147]
75	PPFV (Pdots #17)	455~460	510~520	N.A.	Fluorescent Imaging	[148]
76	PPFV-RhB	450	550~590	10	Temperature Sensing	[139]
77	PF-TAZ-BODIPY	339/418	717	9	Fluorescent Imaging	[149]
78	PF-TAZ-Pc	337/433	715	2	Fluorescent Imaging	[149]
78	PFTBT5	300~400	430/650	N.A.	Fluorescent Imaging	[150]
80	PF-TBT-BODIPY	371/518	719	13	Fluorescent Imaging	[149]
81	PF-TBTOC6-BODIPY	365/497	718	15	Fluorescent Imaging	[149]
82	PF-TBTOC6-Pc (Pdots #29)	367/500	715	8	Fluorescent Imaging	[149]
83	PF-TBT-Pc	367/517	718	8	Fluorescent Imaging	[149]
84	PF-TC6FQ (Pdots #26)	362	652	47	PSA Detection/Fluorescent Imaging	[151]
85	PF-TC6FQ-BODIPY (Pdots #06)	362/495	723	33	Fluorescent Imaging	[149]
86	PF-TC6FQ-Pc	361/496	722	18	Fluorescent Imaging	[149]
87	PF-TFQ	379/511	664	11	Fluorescent Imaging	[151]
88	PF-TFQ-BODIPY	380/512	724	7	Fluorescent Imaging	[55]
89	PF-TQ (Pdots #28)	389/529	712	9	Fluorescent Imaging	[151]
90	PF-TTFQ	392/531	695	8	Fluorescent Imaging	[151]
91	PFV	~450	500	N.A.	pH Response	[152]
92	PFV@BDMO-PPV	~550	524	N.A.	pH Response	[152]
93	PFS1 (Pdots #27)	375	693	30	Fluorescent Imaging	[153]
94	PFSqG2-5% (Pdots #10)	379/433/680	438/701	11.7	pH Response	[154]
95	PHIDT-DBT	575	783/793	1~10	Fluorescent Imaging	[155]
96	PHIDT-DFDBT	558	720/779	2~21	Fluorescent Imaging	[155]
97	PHIDT-HBT	558	733/784	5~14	Fluorescent Imaging	[155]
98	PNDI-2F@CN-PDHVF	430	500/540	N.A.	Fluorescent Imaging	[75]
99	PNDI-2F@CN-PPV	450	610	N.A.	Fluorescent Imaging	[75]
100	PNDI-2F@F8BT	330/470	530	N.A.	Fluorescent Imaging	[75]
101	PNDI-2T@PFPV	450	550	N.A.	Fluorescent Imaging	[75]
102	PPE Gd-SPNs	388	440/470	22	Multimodal Imaging	[156]
103	PS-SH co PPE	N.A.	430/460	N.A.	pH Sensing	[157]
104	PTPEAQ-NPs (Pdots #24)	440	680	N.A.	Fluorescent Imaging (Photosensitizer)	[158]
105	Pttc-SeBta-NIR	1082~1290	1125	1.2	Fluorescent Imaging	[159]
106	Pttc-TaQ-NIR	~400/550~950	810/855/917	2/12/14	Fluorescent Imaging	[160]
107	Pttc-TFQ-BODIPY	361/490	724	51	Fluorescent Imaging	[55]
108	PTTPA/PFTBTA	450	490/597	N.A.	Hydrogen therapy	[161]
109	RB@CD	560	544/582	N.A.	Cho Detection	[162]
110	RET <sub>2</sub> IR NPs	503	778	0.18	Fluorescent Imaging	[163]
111	rSPN2	~680	840	2.7 ± 0.014	Multimodal Imaging	[164]
112	Si-PCPDBT (Pdots #20)	314/505	720	10	Fluorescent Imaging	[116]
113	Si-PFBT	316/430	570	20	Fluorescent Imaging	[116]
114	SPN-I (Pdots #32)	654	1048	1.7	N.A.	[165]
115	SPN-I-C (Pdots #13)	460/488/550~900	501	N.A.	Photodynamics Therapy	[166]
116	SPN-II (Pdots #33)	N.A.	1064	N.A.	Vessels	[165]
117	SPN-IV (Pdots #14)	748	N.A.	0.001	Fluorescent Imaging	[125]
118	SPN-NIR	452/773	507/775	51	Chemiluminescent Imaging	[167]
119	SPN-PT	1064	N.A.	N.A.	Photoacoustic Imaging	[168]
120	SPN-DT	710	820	N.A.	Brain Vasculature	[168]
121	SPNRs	450/460/580	520/540/700	2.12	Chemiluminescent Imaging	[169]
122	SPNs	~490	780	N.A.	Afterglow Imaging	[170]
123	SPNs-PEG	330/440	540	N.A.	Cancer Treatment	[171]
124	SP-PPE	N.A.	466	12	Copper Ion Detection	[172]
125	SPPVN	500/775	775	N.A.	Afterglow Imaging	[173]
126	TADF	862~900	1064~1100	0.4~1.58	Fluorescent Imaging	[174]
127	TBDPSCA	400	520	N.A.	Fluoride ion detection	[175]
128	TPE-TFQ-BODIPY	365/493	725	37	Fluorescent Imaging	[55]

overlap and enables emission at higher wavelengths through cooperative exciton diffusion and hole polaron action [73].

### 3.3. Spectral properties

Optical imaging technology has become a critical research tool in life sciences, materials science, and other disciplines [74–76]. The enhancement of material properties enables researchers to investigate life processes at a more microscopic level, detect subtle environmental changes, and visualize specific information [18,77–79]. Fluorescence imaging technology's potential is particularly evident in the properties and characteristics of luminous nanoparticles (NPs), including inherent

brightness, stability, spectral coverage, and tissue penetration depth [80–82]. Furthermore, advancements in computer technology, software, interactive programming, and the application of artificial intelligence (AI) in image processing present new challenges and opportunities for optical imaging technology [83–86]. The integration of multimedia technologies and software such as augmented reality (AR), virtual reality (VR), point capture, point-cloud reconstruction, digital modeling, and virtual reconstruction has led to innovations like 3D modeling of frame structures and CT 3D reconstruction in medical imaging [87–89]. With ongoing developments in Pdots preparation strategies, researchers have been incorporating chemical groups, rare earth elements, or specific valency metal ions into the main chain

architecture [3,15]. This approach aims to address the limitations of these optical nanomaterials, thereby enhancing their applicative value across various research fields (refer to Fig. 4A). The latest generation of Pdots features a narrower emission spectrum peak width, with a full width at half maximum (FWHM) of approximately 45–85 nm, which is about half to a third of that of the first-generation Pdots. This advancement enables the use of this molecular dye in applications like protein/nucleic acid labeling imaging, flow cytometry, confocal microscopy, multi-dimensional detection, and multi-composite imaging. Additionally, by modifying the molecular structure of the conjugated chain, researchers have expanded the emission spectrum coverage range from the visible region (400–700 nm) to the near-infrared (NIR) regions, including NIR-I (700–1000 nm), NIR-II (1000–1700 nm - further subdivided into NIR-IIa, 1000–1500 nm, and NIR-IIb, 1500–1700 nm), and the current research focus, the NIR-III region (1700–2500 nm). This expansion facilitates fluorescence imaging or targeted molecule labeling in deep tissues and organs. As documented in numerous studies, the spectral profiles of polymer dots (Pdots) predominantly feature absorption and emission wavelengths within the visible and near-infrared spectrum [3,13,90,91]. This spectral positioning is crucial for their applications. Fig. 4A and Table 1 provides a detailed representation of the structural formulas for most of the documented Pdots & Pdots@dopant.

In this analysis, significant examples include polymers such as polyfluorene, poly (phenylene ethynylene), poly (phenylene vinylene), fluorene-based copolymers, and their derivatives, namely PFO [176], CN-PPV [32], PFPV [177], PFCN [178], PFBT [179], and PFDTBT [180]. The quantum yields of these polymers vary considerably, typically ranging from above 20% to around 50% [34]. With advancements in diagnostic technology and materials science, photoluminescent dots (Pdots) with emission peaks in the near-infrared (NIR) region have gained increasing attention. These Pdots are characterized by lower tissue attenuation, enhanced signal-to-background ratio (SBR), and deeper penetration depths (NIR-I: 3.0–4.0 mm, NIR-II: approximately 5.0–20 mm) [181–183]. Traditional visible-light optical nanoparticles (NPs) are effective for cell smears and tissue sections, but NIR probes offer superior performance for *in vivo* imaging. NIR probes are particularly adept at overcoming inherent challenges such as spontaneous fluorescence and tissue scattering, and researchers have also developed these wavelength specific probes based on different types of optical materials (Fig. 4B). As Fig. 4A illustrates, Pdots with visible range emission peaks typically have simpler structures, like PFO and PFBT [133]. Pdots with emission peaks below 610 nm usually contain a singular repeating conjugated structure. As emission peak values increase, the complexity of embedded repeating structures also increases, highlighting the importance of heterostructures in optical materials research [184–186]. The concept of heterostructures, involving the interface of two materials with differing properties, imparts unique physical and chemical properties to the resulting composite. In semiconductors, heterostructures allow for the manipulation of current, voltage, and energy, essential for energy transfer (ET) [187–189]. In optical devices, combining materials with varied refractive indices or absorption coefficients in heterostructures enables functions like modulation and detection of optical signals [190]. For instance, laser diodes utilize reverse-biased PN junctions between p-type and n-type semiconductors to generate stimulated emission effects and laser output. Heterostructures are also employed in energy conversion technologies, such as in solar cells, where they convert light into electrical energy [191]. The “D-A Strategy” is commonly used in preparing NIR optical nanoprobes [49,192]. Pdots with simpler structures serve as energy donors (D), and the introduction of molecular groups with higher emission peaks as acceptors (A) facilitates NIR emission through ET strategies, as shown in Fig. 4C. This approach is a primary method in NIR optical nanoprobe preparation. Modifying the side chains of the conjugated backbone helps reduce  $\pi$ - $\pi$  stacking, maintaining a loose spatial structure through spatial occupancy effects and chemical bond formation to mitigate aggregation-caused quenching (ACQ) effects [133,193]. For example,

Pdots with emission peaks in the 1000–1500 nm range incorporate multiple benzene ring-based side chain groups to prevent excessive stacking of conjugate repeat units, as depicted in Fig. 4A.

Utilizing the D-A strategy (Fig. 3–left lower), Hong et al. pioneered the synthesis of conjugated polymers (CPs) suitable for the NIR-II range [123]. These CPs/SPNs were transformed into Pdots in an aqueous solution via a nanoprecipitation method, achieving an emission peak exceeding 1000 nm. The hydrophobic conjugated polymer, poly (benzo [1,2-b:3,4-b']difuran-fluorothieno [4,4-b]thiophene) (pDA-Pdots), was encapsulated with hydrophilic units (DSPE-mPEG 5000 phospholipid) to enhance biocompatibility and water solubility. Chen et al. proposed a ternary component (D#1/D#2-A) strategy for narrow-band NIR emission [49,67]. This approach involved the integration of a BODIPY [10-(4-(2,5-dioxo-2,5-dihydro-1H-pyrrol-1-yl)phenyl)-5,5] group-assisted polymer as the acceptor (A) to create bright long-wavelength excitable Pdots (LWE-Pdots) based on the principle of cascade energy transfer. In this system, D#1 and D#2 facilitated weak ET, which was amplified by their combined action, leading to a stronger initial energy input and subsequent NIR emission through the bonded BODIPY auxiliary group. Additionally, the strategy of aggregation-induced emission (AIE) luminescence has proven effective. For instance, using phenothiazine as an electron donor and benzobisothiazole (BBTD) as a strong electron acceptor, the AIE mechanism facilitated NIR emission in the second region. Crucially, this AIE approach hinges on meticulous design. In another study, the introduction of side-chain groups mitigated inter- and intra-chain  $\pi$ - $\pi$  stacking in the conjugated chains due to their spatial arrangement effect, with phenothiazine's non-planar structure (characterized by a dihedral angle) playing a key role. This arrangement helped prevent the inner-filter effect of fluorescence (IFE) and aggregation-caused quenching (ACQ), culminating in the preparation of P3c-Pdots with superior optical properties [51]. Subsequent experiments demonstrated these Pdots' exceptional SBR and imaging clarity, particularly in imaging the whole body and subcranial vascular structures of mice, thus marking them as an ideal choice for imaging applications.

### 3.4. NIR conversion of visible fluorescent pdots based materials

For deep tissue and organ imaging in individual organisms, fluorophores that emit at longer wavelengths are essential to enhance tissue transmission depth (also referred to as imaging depth) and minimize interference from spontaneous tissue fluorescence, such as SBR [63, 194]. In fluorescent nanoprobe research, the near-infrared region is typically categorized into two segments: the first near-infrared region (NIR-I) and the second near-infrared region (NIR-II), based on the tissue transparency window (600–960 nm) and the water resonance wavelength (1400 nm) [195–197] [according to the IEC (International Electro Technical Commission) 60050–845:2007 standard]. Achieving longer wavelength emission with conjugated polymer chains, composed of simple, repeating monomers, poses a challenge. A viable strategy involves introducing composite monomer structures or side-chain modifications to the conjugated chains, a technique prevalent in the development of NIR dyes, including quantum dots and carbon dots [63, 198,199]. The groups amenable to modification include: 1). Xanthene derivatives: By altering the amino position, adjusting the central atomic structure, and changing the conjugated chain length, the maximum emission wavelength can be red-shifted [200]. Classic examples are rhodamine B and rhodamine 6G [201]. Substituting the central atom to alter the group structure results in a red shift in the emission wavelength in the order of N, O, S, C, Si, and P [202–204]. Primarily, oxaanthracene derivatives are used to form composite monomer structures that extend the  $\pi$ -conjugated length of the luminescent group, thereby modifying the absorption/emission maximum of the new dye [205,206]. 2). Coumarin: The emission wavelength is red-shifted by extending the  $\pi$ -conjugated length and enhancing the donor/acceptor capability [207–209]. The modification strategy for coumarin derivatives typically involves

donor/acceptor modifications, as seen in classic coumarin dyes (D-A). Instead of merely extending  $\pi$ -conjugation, the approach for coumarin derivatives includes expanding the  $\pi$ -conjugation, which involves side-chain modifications or the secondary introduction of auxiliary side chains, coupled with increased electronic delocalization to achieve a red-shifted emission wavelength [210]. However, this NIR emission often necessitates stronger interferometric contrast transfer (ICT) and a robust electron acceptor group [211]. 3). Naphthalene-based fluorescent molecules: Like the aforementioned dyes, NIR emission can be achieved by modifying the electron donor/acceptor and increasing the  $\pi$ -conjugation length (NIR dye doping strategy #1~#3 please see Fig. 4C) [212].

### 3.5. Surface modification and biocompatibility

Surface modification is a widely utilized technique that enhances the macroscopic morphology, physicochemical properties, or functionality of Pdots through various methods such as coating, chemical bonding, and molecular docking [13,213–215]. This technique finds extensive applications in diverse fields, including industrial manufacturing, materials science, and biomedicine [216–218]. By incorporating exogenous compounds, functional macromolecules, chain-like nucleotides, and exposed groups into the material's surface, microstructures or functional domains are formed. These modifications impart properties to Pdots like hydrophilicity, bondable sites, targeting capabilities, and energy conversion [26,32,34,219]. The addition of amphiphilic polymers, for instance, can confer more carboxyl or hydroxyl groups on the surface of quantum dots, facilitating interaction with water molecules. This results in effective water adsorption and stable colloidal formation in aqueous solutions (Fig. 4D) [2]. In drug delivery, NPs can serve as carriers, with surface modifications like specific nucleotide chains, ligands, and antibodies enabling targeted delivery. This allows NPs to selectively bind to target cells and release drugs for therapeutic effects. Techniques such as layer coating and functional macromolecular protein modification can also facilitate efficient transmembrane transport and intracellular subcellular localization [220,168]. Additionally, surface modification plays a critical role in optoelectronic devices, where it is used to regulate charge transport and excitation state transition processes. Functional domains created by surface modification interact with the internal spherical core structure to form a signal reporting cycle (Fig. 3-Right Lower). In optoelectronic devices, analysis or visualization of substrates is achieved by measuring parameters such as current transmission rate, photoluminescence efficiency, emission peak shifts, and fluorescence intensity (Fig. 4) [2]. Some common strategies for modifying exposed chemical groups include the use of PSMA and PIMA for providing carboxyl groups, NH-PIMA and polypeptides for amino groups, and N<sub>3</sub>-PEG and N<sub>3</sub>-PCL for azide functional groups [25,221]. These modifications facilitate cycloaddition reactions with active alkynes or aromatic molecules under copper ion catalysis, enabling precise regulation and modification of NP surfaces. The paramount function of surface modification is to impart excellent biocompatibility to Pdots. This involves assessing the interaction between nanoparticles and various biological aspects, such as genetics, morphology, physiology, and pathology. For biological entities, Pdots represent exogenous substances. When introduced into a living system, it is crucial to evaluate their impact on internal microenvironment homeostasis and potential alterations to physiological activities [222–225]. Incompatibility between Pdots and the organism can lead to tissue and organ disease or even systemic collapse (this part will be discussed in the 6th section).

Appropriately structured conjugated chains, synthesis strategies, low-toxicity reagents, and surface modifications can augment the biocompatibility of Pdots with cell membranes or tissue organs, simultaneously mitigating the inherent toxicity of nanoparticles (NPs) [10,13,226]. This enables Pdots to stably exist within the microenvironment of a biont and be subject to metabolic control, offering potential for long-term labeling of target cells and organs. Wu et al.'s study highlights

the need to consider the body's complex microenvironment, including the blood sinus structure, biological barriers, charge barriers, and efficient foreign body metabolism, when employing NIR-775 Pdots for long-term labeling and imaging [50]. Cellular efflux systems play a crucial role in mediating the intracellular metabolism of labeled probes, facilitating the removal of unwanted or harmful substances. For larger nanoparticles, a common mechanism involves isolating these substances from the cytosol, encapsulating them with a membrane coating, and expelling them via exocytosis. Lysosomes are pivotal for smaller nanoparticles, particularly those with biological coatings, where the process of autophagy degrades and removes excess or deposited NPs [227]. However, excessive NP accumulation can lead to necrosis and other forms of non-programmed cell death. Additionally, exogenous foreign body excretion mechanisms in the liver, kidney, and lungs also play a significant role. The long-term exposure of Pdots and their potential toxic side effects remain a subject of debate. Upon intravenous injection in mice, Pdots initially accumulate in the liver and lung capillaries due to venous circulation. The pulmonary capillary's outer basement membrane leads to more Pdots accumulating in the lungs, influenced by charge dynamics. Over 4–7 days, Pdots undergo multiple rounds of internal circulation, concentrating more in the liver and kidneys, causing reduced liver weight, transient increases in transaminase levels (ALP, AST, & ALT), and fluorescent signals in the renal cortex. A week later, non-macrophage-cleared NPs remain in the mice, having undergone several cycles in the cells or body, with most of the biological coatings on their surface shed or consumed by macrophages [228,229]. Pdots, being nearly non-volatile, primarily rely on hepatic (bile circulation–intestinal pathway) and renal (renal filtration–urine formation) pathways for metabolism. Theoretically, the renal basement membrane's charge (negative, filtering positively charged substances) and mechanical barriers (filtration) are significant factors, but Pdots may not fall within this range. The negative surface charge and substantial molecular weight of Pdots present challenges for biological metabolism. Therefore, a thorough exploration of Pdots' absorption, distribution, metabolism, and excretion processes, particularly their selective distribution and physical transformations (such as dissolution, aggregation, or morphological changes), remains an imperative and complex issue [230–234]. This encompasses the toxicological effects and safety of nanoparticles, a crucial concern for researchers.

## 4. Sensing and detection

Sensing involves converting the attributes of a measured object into observable signals through physical, chemical, or biological means [14, 235,236]. Detection encompasses the analysis and interpretation of these signals using various instruments and equipment to extract required information [237]. Traditionally, sensors are categorized into active sensors, which actively detect and sense physical or chemical quantities in the environment, converting them into useable signals with high sensitivity and accuracy; passive sensors, typically not requiring an external energy source and generating output signals based on measured physical quantities; and digital sensors, which usually comprise micro-electronic components, optical components, and mechanical structures [238,239]. Digital sensors convert measurable physical quantities into digital information processable by computers, thereby facilitating intelligent control [240,241]. Optical sensors based on Pdots are generally classified as active sensors, often requiring external light or energy sources to produce variable signals [13,139]. Due to their high sensitivity, precision, and non-invasive nature, optical sensors are widely applied in environmental monitoring and biomedicine. They measure changes in light intensity or wavelength in response to specific substances. For instance, fluorescence-based optical sensors can detect minute quantities of mercury and chromium ions with remarkable sensitivity and selectivity. In life sciences, optical sensing technology enables researchers to observe and analyze changes at cellular, tissue, and molecular levels, finding applications in disease diagnosis and

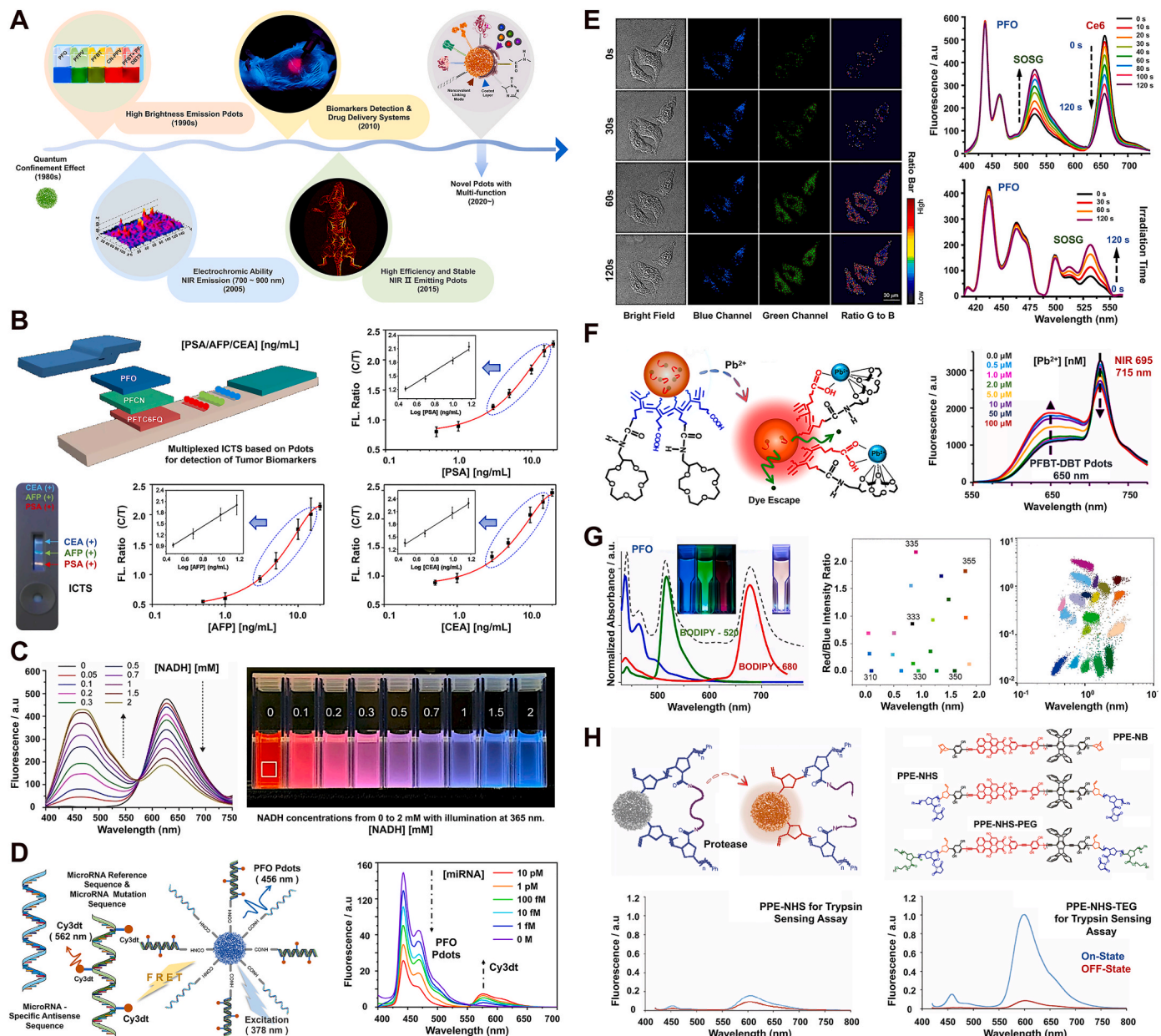


**Fig. 5. Multifunctional Pdots through the design of  $\pi$ -conjugated chains and surface functionalized modification to reflect unique sensor architecture for special functions categories of use.** A). Five representative nodes of time for Pdots with optical sensing performance, including (i) the fabrication of high-brightness Pdots, (ii) the concept of Pdots in the first region of the NIR-I, (iii) in vivo applications of biosensors based on Pdots, (iv) the concept of Pdots in the second region of the NIR-II, and (v) proposal of the concept of intelligent nano platform. Reprinted with permission from Refs. [3,248]. Copyright 2013 John Wiley and Sons Ltd. & Reprinted with permission from Refs. [249,114]. Copyright 2016 and 2023 American Chemical Society. B). The structure and principle of multiplexed ICTS based on PFO/PFCN/PFTC6FQ Pdots for detecting [CEA/AFP/PSA]. The graph in the lower corner represents the detection results of multiplexed CTMs concentration (0/0/5, 0/5/0, 5/0/0, 5/5/5 ng/mL). C). Emission spectra of DPA-CN PPV Pdots with 0~2 mM [NADH] (left). DPA-CN PPV Pdots' color gradient law at 0~2 mM [NADH] with excitation at 365 nm under UV light (right). Reprinted with permission from Ref. [101]. Copyright 2021 John Wiley and Sons Ltd. D). The structure and principle of multiplexed Pdots-anti miRNAs based on PFO/PFBT/PFDTBT/CN PPV Pdots for detecting the pathological grade specific miRNAs (left). High sensitivity tests spectral results based on energy transfer models (right). E). Fluorescence imaging of intracellular  $^1\text{O}_2$  detection using SOSG-Pdots with 10  $\mu\text{g}/\text{mL}$  [ $\text{Ce}^{6+}$ ] after different irradiation times at 0/30/60/120 s (LEFT). Spectral changes of the SOSG-Pdots in the presence of  $^1\text{O}_2$  (right, [ $\text{Ce}^{6+}$ ] contain oxidizing properties). F). Schematic diagram of color changes with increasing concentrations of  $\text{Pb}^{2+}$  and the fluorescence spectra of PFBT-DBT Pdots with different concentrations of  $\text{Pb}^{2+}$ . G). Fluorescence spectra of the three Pdots formed from PFO Pdots and Pdots doped with BODIPY 520 & BODIPY 680 (left). The 2D distribution of 20 Pdots spectral-intensity barcodes plotted against the green-to-blue (x-axis) and red-to-blue (y-axis) fluorescence intensity ratios. The excitation wavelength was 405 nm, and blue, green, and red fluorescence were collected through the band-pass of 450/50 nm, 525/50 nm, and 670/30 nm, respectively, by flow cytometry (right). H). The structure and principle of protease sensor based on Pdots (upper). Protease-triggered "Switch on or off" leads to a change in fluorescence spectra. Fluorescence spectra of shell cross-linked Pdots before (red) and after (blue) incubation with trypsin (lower). Reprinted with permission from Refs. [180,140,142,145,250], and [251]. Figure B and D ~ H Copyright 2012, 2015, 2017, 2018, and 2022 American Chemical Society.

treatment [242–244]. For example, functionalized Pdots can bind to target molecules and generate specific frequency signals upon excitation, thus facilitating rapid quantitative detection of these targets (Table 1). Furthermore, optical sensing technology has achieved significant advancements in drug development [245–247]. During new drug screening, holographic image processing algorithms combined with specially designed Pdots fluorescent probes can be employed for large-scale sample screening and high-resolution imaging in protein-ligand interaction testing. Fig. 3 (Right Half) and Fig. 5 provide a comprehensive overview of the design concepts and classic cases of optical sensors based on Pdots.

#### 4.1. Biomacromolecule

Pdots, recognized for their intense luminescence, are pivotal in the realm of bioanalysis and biosensing, marking a transformative milestone in fluorescence-based technologies (refer to Fig. 5A) [114,248,249,252]. This section contrasts the progression, along with the merits and limitations, of Pdots against traditional optical nanoparticle varieties within the scope of biological detection. Discussed applications encompass multiplexed detection, biosensing, point-of-care diagnostics (PCD), and immunochromatographic test strips (ICTS). For instance, Fang and colleagues engineered a Pdots-enhanced ICTS, enabling swift (within 10 min), quantitative detection of biomarkers like PSA (Prostate Cancer), AFP (Hepatocellular Carcinoma), and CEA (Gastrointestinal Neoplasms), as illustrated in (Fig. 3-ICTS Part and Fig. 5B) [140]. Despite these advancements, Pdots-based systems have yet to achieve the clinical breakthroughs seen with electrochemical point-of-care tests, largely due to the limitations of optical sensors and the cumbersome nature of associated equipment. In such substrate detection, a prevalent approach involves modifying Pdots surfaces with ET model-based reporter molecules, subsequently amplifying the signal. This methodology aligns with techniques used in enzyme-linked immunosorbent assays and fluorescence quantitative PCR for RNA detection [253]. The second approach involves selecting substances that directly react with biological macromolecules to modify the main chain of the π-conjugated polymer, primarily due to the weak physicochemical properties of the substrate itself. This approach includes selecting biochemical reactions that can be simulated extracellularly, such as those involving reactive oxygen species (ROS),  $\text{Fe}^{2+}/^{3+}$ ,  $\text{Cu}^{2+}$ ,  $\text{Pb}^{2+}$ ,  $\text{Hg}^{2+}$ ,  $\text{Ce}^{6+}$ , etc [3,142,254] (Fig. 5 E & F). These reactions are converted into chemical equations, facilitating simulation and measurement of substrate concentration changes in test tubes or cuvettes. In their research, Chen et al. demonstrated the versatility of ratiometric NADH-sensitive Pdots [101]. A significant achievement includes developing a system for NADH imaging using a smartphone, tailored for point-of-care applications, as illustrated in Fig. 5C. Moreover, this team successfully integrated an ultrasensitive optical transducer into a wireless glucose monitoring system, operable through a smartphone interface [255]. Zhang et al. employed a strategy of multiple Pdots-anti miRNAs staining combined with a FRET model for highly sensitive labeling and quantitative determination of cell-specific miRNAs. This method effectively eliminates the interference of subjective factors under single and double staining, enhancing detection specificity to the miRNAs (fM) level (Fig. 5D) [180]. Meanwhile, traditional electrochemical sensors remain a reliable option in the field. Wang and associates have developed an innovative NADH-sensitive electrochemiluminescence (ECL) biosensor based on Pdots, efficiently detecting NADH and its related metabolic precursors and products [256]. Separately, You and the team have combined highly luminescent Pdots with gold nanorods exhibiting strong plasmonic effects, creating a fusion known as Pdots-Au nanoparticles [253]. This combination offers dual capabilities of colorimetric and fluorescent detection, enabling direct identification of circulating tumor markers (CTMs) in blood samples without prior processing. This breakthrough positions Pdots-based ICTS as a frontrunner for immediate point-of-care diagnostics. Further, Yang and colleagues have engineered a fluorometric

ICTS using Pdots, producing traffic light-like signals through energy transfer, contingent on target analyte concentrations, marking the first instance of a Pdots-based immunoassay test strip with such a traffic light-like mechanism and multiplexing functionality [257]. Schüller's team encapsulated two distinct Pdots varieties - poly-(9,9-dioctyl-fluorenyl-2,7-diyl) (PDOF) and poly-(2,5-di-hexyloxy-cyanoterephthalylidene) (CN-PPV) - within silica shell-crosslinked Pluronic® micelles (Si-NP). Their research focused on examining NP brightness relative to the concentration of conjugated polymers [258]. Remarkably, the detection sensitivity of Pdots in flow immunoassays (LFI) was significantly higher than that of Si-NPs and other reference nanoparticles, requiring considerably less Pdots mass for effective detection. Additionally, a less commonly used method involves leveraging the substrate properties to change the spatial conformation or interchain stacking force of the polymer chain, thereby altering the fluorescence reporter signal intensity of Pdots (mean fluorescence intensity, MFI) (Fig. 5G). For instance, Pdots functionalized with dextran (Dex-Pdots) have shown enhanced particle stability across various pH levels and in high ionic strength conditions [259]. Furthermore, Cordovilla et al. employed a protease sensing scheme as a 'turn-on' mechanism, wherein the protease cleaves peptide cross-linkers within the fluorescence-quenched shell cross-linked NPs (OFF state), resulting in the formation of highly emissive non-cross linked NPs (ON state) (Fig. 5H) [251]. This stability is evident when forming immune conjugates with substrates, leading to changes in the folding conformation of the conjugated chains. Significantly, the advancement of Pdots for point-of-care biosensing and in vivo bioanalytical applications marks their emergence as a formidable category within the realm of optical diagnostic technologies, particularly in clinical settings [14].

#### 4.2. Physical quantity

Physical quantities, which are crucial for quantifying physical phenomena and objects [260], such as temperature and luminous intensity, can be effectively detected using Pdots. The ease of surface and internal modifications of Pdots allows for the detection of a wide array of physical parameters, including reactive oxygen species (ROS), common metal ions, pH values, temperature, and various biomolecules [226]. For instance, Ye and colleagues developed highly luminous single nanoparticle ratiometric temperature sensors utilizing Pdots [139]. This team ingeniously incorporated the temperature-sensitive dye Rhodamine B (RhB) into Pdots' matrix, observing a decrease in emission intensity with rising temperature (see Fig. 3 for the schematic diagram and detection strategy). Sun and team reported the synthesis of Pdots for single-molecule imaging and biosensing applications [261]. They successfully attached streptavidin to the surface of Pdots, enhancing their specificity for subcellular labeling and targeting. Additionally, TPP-Pdots, known for their biocompatibility, exceptional light-harvesting capability, and superior photothermal conversion efficiency, were employed to capture SA antibodies, serving as a dual-functional bioprobe for generating photocurrent and temperature signals (refer to Fig. 3, top right corner) [262]. More recently, He and associates introduced a ratiometric nanoprobe based on Pdots-Eu for temperature sensing (featured in Fig. 3, center section) [129]. The red/blue fluorescence intensity ratio of Pdots-Eu inversely correlated with temperature, facilitating the ratiometric monitoring of temperature variations. Fig. 3 comprehensively summarizes these detection strategies, encompassing proportion sensing, signal intensity analysis, and the utilization of specific functional groups.

#### 4.3. Chemical properties

Pdots have emerged as a novel category of intensely luminous nanoprobes, instrumental for biosensing and bioimaging applications [10]. However, controlling the surface chemistry and bioconjugation of Pdots has presented significant challenges, limiting their broader

utilization in substrate detection and various biological research areas. Addressing this issue, Yuan and colleagues, in the 2010s, introduced an efficient and potent conjugation technique [13]. This method, outlined in Fig. 3-top left corner, synergizes the nanoprecipitation approach with the incorporation of amphiphilic polymers, effectively resolving the aforementioned challenges.

**Metal Ion:** The determination of metal ion concentrations represents a significant area of exploration. Maintaining appropriate ion concentrations both inside and outside cells is crucial for the normal physiological functioning of organisms [263–265]. The detection of such substrates typically hinges on the redox properties of metal ions, which lead to the formation of metal complexes and chelates in solution systems. The impact of these ions on the fluorescence signal of Pdots can vary, with some ions exhibiting a linear effect on the reported signal, while others demonstrate a nonlinear relationship [9]. To enhance sensitivity to redox properties, functional groups are often introduced into the side chains or modified on the surface of Pdots (Fig. 3 illustrates the determination methods for ions like  $\text{Fe}^{3+}$  and  $\text{Cu}^{2+}$ ) [106]. The substrate under test specifically interacts with oxidation- or reduction-sensitive groups, influencing the fluorescence signal of Pdots. The formation of metal complexes and chelates can result in light shielding or conformational changes of the  $\pi$ -conjugated chains, thereby masking the fluorescent signal of the core or causing leakage of encapsulated dyes. For instance, the fluorescence of PFP-Pdots can be quenched through coordination between polyethylene glycol (PEG) and  $\text{Fe}^{3+}$  [266]. Li et al. developed a ratiometric fluorescent sensor utilizing Pdots coordinated with terbium ions ( $\text{Tb}^{3+}$ ) for the detection of bacterial spores in aqueous environments [267]. This  $\text{Tb}^{3+}$ -chelated Pdots sensor exhibits potential for both sensitive and rapid identification of bacterial spores. Additionally, this material can act as a versatile host for loading various metal ions, allowing for adjustable quantities and types of metal ions. This capability facilitates the preparation of evenly dispersed single or multiple metal catalysts. In another study, Kuo and team engineered a visual sensor based on Pdots, specifically targeting  $\text{Pb}^{2+}$  detection (as shown in Figs. 3 and 5F) [250]. A ratiometric approach to sense  $\text{Cu}^{2+}$  was proposed, leveraging variations in the fluorescence intensities of donors and acceptors in response to different concentrations of  $\text{Cu}^{2+}$ . This  $\text{Cu}^{2+}$  sensor demonstrated a reliable linear detection range between 0.05 and 5  $\mu\text{M}$ , with a detection limit of 15 nM.

[ $\text{H}^+$ ]: Chan and colleagues have pioneered the use of poly (2,5-di(3',7'-dimethyloctyl)phenylene-1,4-ethynylene) (PPE) Pdots as a foundation for FRET-based ratiometric pH nanoprobes [157]. These Pdots, coupled with fluorescein, exhibit a linear pH sensing range from 5.0 to 8.0, apt for most cellular studies. Additionally, Xu's team innovated novel Pdots functionalized for concurrent intracellular pH and oxygen imaging [268]. These Pdots contain a semiconducting poly [9, 9-dioctylfluorenyl-2,7-diy] (PFO) polymer, amino-terminated polystyrene, fluorescein isothiocyanate (FITC) as a pH-sensitive dye, and  $\text{Pt}^{2+}$  mesotetra (pentafluorophenyl) porphine (PtTFPP) as an oxygen-sensitive dye. Meanwhile, Sun and associates devised a unique ratiometric fluorescent chemical nanoprobe for monitoring and imaging mitochondrial pH in live cells, utilizing congo-red (CR)-modified dual-emission Pdots through a competitive fluorescence resonance energy transfer (CFRET) mechanism [72]. This probe offers excellent biocompatibility, a broad pH detection range (2.57–8.96), reversibility, selectivity, and photostability. Following this, Shi et al. introduced a photoelectrochemical (PEC) pH sensor that leverages PEC-Pdots for sensitive and extensive pH measurement [269]. The pH value alters the redox properties of the Pdots, consequently modifying the photocurrent response. Ou et al. created a blend polymer dot, employing poly [(9, 9-dihexyl-9H-fluorene-2,7-vinylene)-co-(1-methoxy-4-(2-ethylhexyloxy)-2,5-phenylenevinylene)] (PFV) as the donor and poly [2,5-bis(3',7'-dimethyloctyloxy)-1,4-phenylenevinylene] (BDMO-PPV) as the acceptor, along with polystyrene graft EO functionalized with carboxy (PS-PEG-COOH) for surface carboxyl groups [152]. These Pdots-20% exhibit spectral, intensity, and

fluorescence lifetime changes in pH values as low as 1 or 2, enabling pH sensing applications. Gao et al. detailed a novel approach to creating highly efficient ECL materials using trace  $\text{Ir}^{3+}$ -end capped AIE-active polymer dots [270]. The hybrid Pdots, characterized for cell imaging and exclusive ratiometric sensing of intracellular pH, were prepared via nanoprecipitation. Lastly, Li et al. proposed a simple yet sensitive method for ratiometric fluorescent detection of nucleic acids, based on pH-dependent adsorption of dye-labeled DNA on polymer dots [271]. This mixture shows the fluorescence of Pdots at neutral pH, while acidic pH leads to FRET from Pdots to the reporter molecule, thus illuminating the reporter molecule's fluorescence.

**[ROS]:** Reactive oxygen species (ROS) encompass a range of oxygen-containing free radicals and peroxides, closely associated with oxygen metabolism in organisms. These typically include peroxides, superoxides, hydroxyl radicals, singlet oxygen, and  $\alpha$ -oxygen [272,273]. The detection of ROS primarily relies on the oxidative properties of the substrate. For instance, peroxides are molecules with two adjacent oxygen atoms forming an 'O–O' bond within a diatomic or polyatomic bond structure. These can generate highly reactive free radicals through photolysis or catalysis on a sensing surface based on Pdots, subsequently affecting the reporting signal. Other types of ROS are superoxide ( $\text{O}_2^- \bullet$ ), a negatively charged and unstable ion; hydroxyl radicals, highly reactive molecules with one unpaired electron attached to a water molecule's center; singlet oxygen, an active molecule in an excited state with an unpaired electron; and alpha-oxygenated carbonyl compounds, molecules containing  $\alpha$ -oxygenated carbonyl compounds with functional groups like aldehydes/ketones [274–276]. ROS encompasses various highly reactive molecules capable of causing cellular damage or significantly impacting cell function regulation. While they are crucial in normal metabolism, excessive accumulation can lead to cellular damage and disease [277]. In the context of Pdots research, Wu et al. introduced a novel synthesis approach, while Li and colleagues explored the interaction of Pdots with human gastric adenocarcinoma (SGC-7901) cells and human gastric mucosal (GES-1) cells, focusing on cellular uptake and viability [278]. They extended their study to the generation of ROS and changes in mitochondrial membrane potential (MMP), uncovering a relationship between cellular proliferation, mitochondrial stability, and ROS and MMP levels. In 2018, Cai et al. developed a hemin-Pdots system, based on chemiluminescence resonance energy transfer (CRET) principles, composed of hemin and a fluorescent conjugated polymer [279]. Hemin-Pdots exhibited exceptional biocompatibility, stability, emission wavelength shift, and hypersensitivity to ROS, facilitating real-time imaging of ROS levels in mouse peritoneal cavities and in both normal and tumorous tissues. Concurrently, in the field of photocatalytic hydrogen production, driven by advances in catalysts and perovskite solar cells, Zhang et al. described a therapeutic application of Pdots involving in situ photocatalytic hydrogen generation [131]. This process, initiated by photon absorption in Pdots, mimics electrolytic water decomposition within an aqueous environment, with the generated hydrogen diffusing through the lipid bilayer to counteract ROS overexpression in diseased tissues. Furthermore, Xu et al. investigated the phototriggered inhibition of amyloid-beta ( $\text{A}\beta$ ) aggregation and cytotoxicity using Pdots modified with agents like rhodamine B (RhB), methylene blue (MB), and riboflavin (RF) [280]. Their findings indicated significant suppression of  $\text{A}\beta$  aggregation under light exposure with these modified Pdots. However, the oxidative by-products in photocatalytic hydrogen production pose concerns about energy and matter conservation. Addressing this, recent studies have turned to bionics, adopting strategies from the mitochondrial oxidative respiratory chain model. This approach categorizes electron transfer, substrate oxidation, and reduction hydrogenation processes, allowing efficient utilization of various end products and by-products, each playing distinct biological roles [131,281].

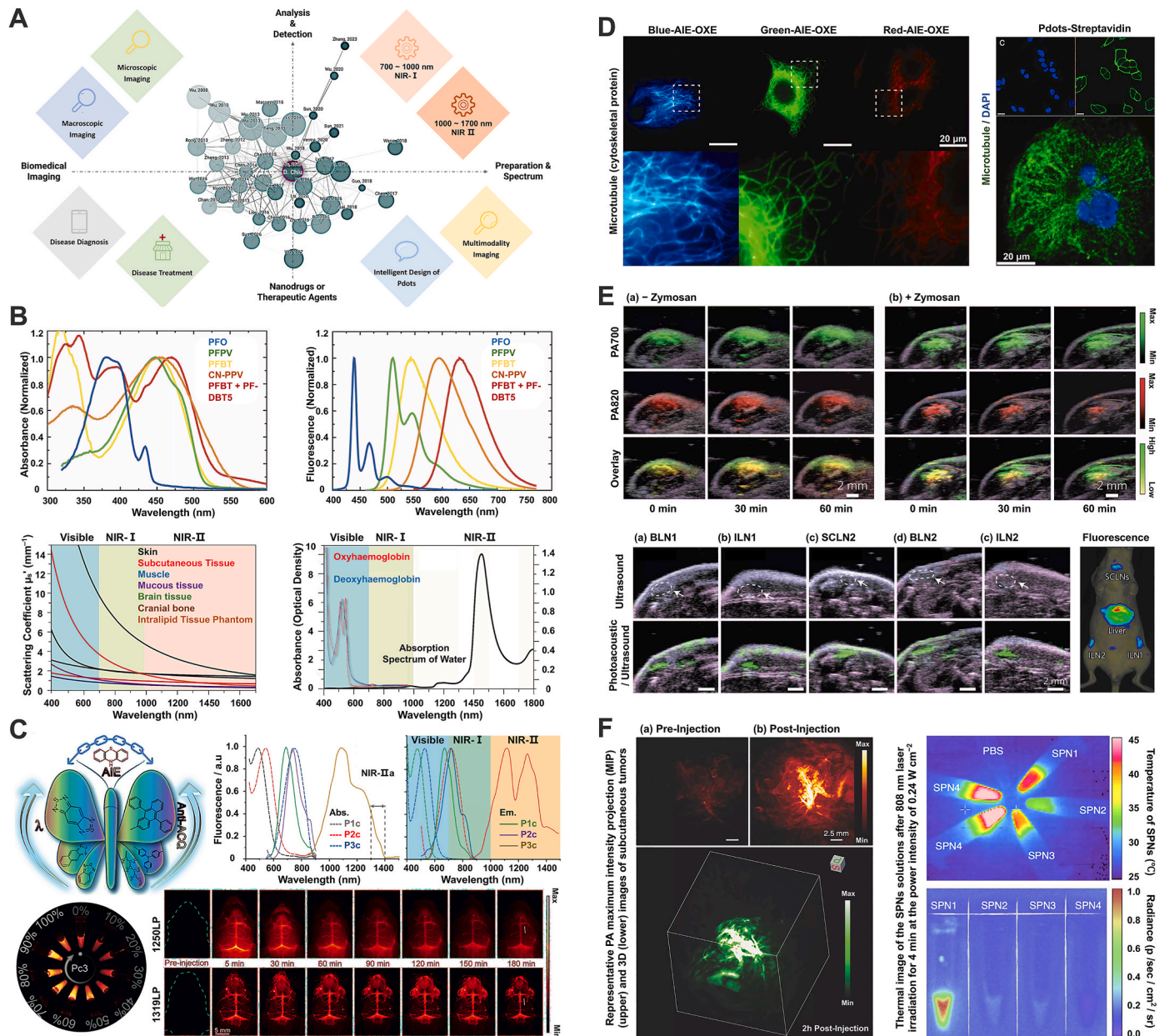


**Fig. 6. Multiple imaging methods and classic cases for Pdots of the  $\pi$ -conjugation chain.** A). Pdots-related developments and applications are typically implemented on a nano- or microscale, including (i) preparation and spectrum, (ii) analysis and detection, (iii) biomedical imaging, and (iv) nanodrugs or therapeutic agents. The squares in the figure represent the main influencing factors in these practical applications. Source: Connected Papers (<https://www.connectedpapers.com/>). B). Typical representative of Pdots whose emission spectra lie in the visible range of light. And the challenges to be faced in the development of NIR Pdots nanoprobes. Absorption spectra - upper left, emission spectra - upper right, scattering coefficients of different biological tissues & intralipid - lower left, absorption spectra of oxyhaemoglobin (red), deoxyhaemoglobin (blue) and water (black) through a 1-mm-long path in human blood - lower right. Reprinted with permission from Refs. [297,298]. Copyright 2008 and 2015 American Chemical Society. C). Method for NIR NPs synthesis of visible light fluorescent materials - aggregation-induced emission (AIE). Absorption and fluorescence spectra of P1c, P2c, and P3c polymers in water & THF - upper right. Fluorescence intensity changes of P3a, P3b, and P3c in THF/water mixtures containing different water fractions (v/v % = THF/water %). In vivo NIR-II fluorescence imaging of mouse brain at designated time points after intravenous injection of P3c Pdots - lower right. Reprinted with permission from Ref. [51]. Copyright 2020 John Wiley and Sons Ltd. D). Applications of Pdots in the field of super-resolution imaging. Fluorescence images of microtubules in HeLa cells labeled with the AIE Pdots - left. And the same cells were incubated with both biotinylated anti- $\alpha$ -tubulin and PFBT-NH-PIMA Pdots-streptavidin - right. Reprinted with permission from Refs. [35,299]. Copyright 2012 and 2017 John Wiley and Sons Ltd. E). In vivo photoacoustic imaging of tumor (liver), bronchial lymph nodes (BLN), inguinal lymph nodes (ILN), supraclavicular lymph nodes (SLN) and lymph nodes (LN) (lower). Reprinted with permission from Ref. [300]. Copyright 2013 Springer Nature, & F). In vivo PA imaging and 3D images of tumor incubated with Pdots (SPN4) - left. Thermal image of the SPNs solutions after 808 nm laser irradiation for 4 min. Reprinted with permission from Ref. [301]. Copyright 2015 John Wiley and Sons Ltd.

## 5. Image formation

Optical imaging technology, a vital tool in medical biology and materials science, employs imaging probes and related instruments to

visualize information of research interest [238,282,283]. Commonly utilized imaging instruments include fluorescence inverted microscopes, confocal fluorescence microscopes, and cryo-electron microscopes. However, with advances in the performance of optical imaging probes,

life science has transitioned into the era of molecular biology [284]. This shift, coupled with the growing application of biological histology parameters in disease diagnosis and prognosis, has heightened the development of biomedical imaging technology [285,286]. Consequently, researchers now have more detailed and stringent requirements for imaging and visualization technologies (Fig. 6A). The current research focus in this field centers on two primary areas: ultra-high-resolution microscopic imaging of intricate subcellular spatial structures and macroscopic multi-dimensional analysis of multicellular structural tissue blocks [287–290]. This analysis ranges from two-dimensional (2D-conventional planar imaging) to three-dimensional (3D-stereo imaging), encompassing visualization of protein spatial conformation and noninvasive imaging of deep tissues [87,291]. For subcellular imaging, common techniques include fluorescent antibody immunoabsorption, fluorescein or isotopic labeling, autofluorescent protein target cell transfection, and the use of certain lipophilic membrane-embedded dyes. In contrast, X-ray, computed tomography (CT), magnetic resonance imaging (MRI), and ultrasound imaging are predominantly utilized for macroscopic analysis. These self-luminous or indirectly luminescent dyes or labels, whether employed for ultra-microscopic *in situ* labeling of individual cells or gross visualization of target proteins within tissues, are crucial in life science and biomedicine [292]. Given the specificity of biomedical imaging, researchers employ various dyes, each with unique physical and chemical properties. These include organic small molecule dyes, luminescent nanoparticles, fluorescent proteins, organic dye droplets, and quantum dots [71,195,293,128]. While their clinical or translational medicine applications are still limited, the research and application potential of these imaging agents continues to be a subject of exploration and discovery. Additionally, advancements in computer hardware technology, software development, interactive programming, and the application of Artificial Intelligence (AI) in image processing have paved the way for 3D imaging of specific structures [294]. Utilizing multimedia technology and software like Augmented Reality (AR), Virtual Reality (VR), point-of-capture, point cloud reconstruction, digital modeling, and virtual reconstruction, researchers can deconstruct structural features unobservable in 2D planes [295,296]. Examples include 3D modeling of paleontological or paleoanthropological skeletons in archaeology, framework structure modeling in architecture, and CT three-dimensional reconstruction in medical imaging. These developments indicate the immense potential of biomedical imaging and optical imaging technology for multi-field applications.

### 5.1. Fluorescence nanoprobe

The fluorescence nanoprobe, a widely utilized optical imaging tool in scientific research and medical diagnostics, labels or detects target substances by emitting light signals at specific wavelengths upon external energy stimulation [297,302,303]. This facilitates the monitoring of the location, quantity, and activity of these substances. In 2013, Wu C.F., D.T. Chiu, and colleagues presented a comprehensive review on the photophysical properties of Pdots, underscoring their efficacy as fluorescent labels [3]. This review revealed that Pdots-based nanoprobes exhibit low cytotoxicity, a broad absorption spectrum, resistance to photodegradation, and excellent water dispersibility, as shown in Fig. 6A & B. Contrasting with traditional multiphoton probes, Hassan et al. demonstrated that Pdots' extensive multiphoton absorption spectrum enables imaging at longer wavelengths ( $\lambda_{ex} = 1060$  and  $1225$  nm) [304,305]. Their research in deep tissue imaging of cortical rodent microvasculature illustrated Pdots' versatility in bioimaging, attributed to their remarkable brightness and broad absorption capabilities, allowing for the exploration of deep biological structures [148]. In simpler terms, a fluorescence nanoprobe based on Pdots primarily consists of two components: a core formed from a fluorescent dye derived from Pdots, and a ligand that interacts with target substances, modifying the fluorescence signals. These ligands selectively bind to

targets, producing detectable fluorescence signals upon excitation [226, 249,105]. Additionally, fluorescence probes have crucial applications in various fields. In life sciences, for instance, they are extensively employed for cell imaging, protein localization and functional studies, and gene expression analysis [124,306,307]. In medical diagnostics, these probes are utilized for tumor detection, pathogen identification, and therapeutic effect evaluation. Furthermore, innovative and emerging applications of fluorescence probes continue to expand their utility. In environmental monitoring, they assist in tracking pollution sources [308]. In food safety, they are employed for detecting harmful additives or toxins [309]. Creatively, fluorescence probes are also integrated into artistic ventures, such as the application of fluorescent paints and inks in pattern drawing and painting creation [178,138]. In 2022, our research group introduced a groundbreaking method to develop multifunctional Pdots-based fluorescent probes through sophisticated molecular engineering. This approach enables precise imaging of biomolecules in living systems, addressing challenges related to the Abbe diffraction limit and signal-to-noise ratio [180]. We developed Pdots nanoprobes linked by specific miRNA antisense sequences (Pdots-anti miRNA), facilitating monitoring of pathological gradations via miRNA expression variation. Employing the Förster (or fluorescence) resonance energy transfer (FRET) model, combined with Pdots and Cy3dt tags, we demonstrated the enhanced sensitivity and specificity of these nanoprobes for *in vivo* miRNA detection simulations. In 2022, Peng et al. introduced a surface plasmon-enhanced NIR-II fluorescence technique, integrating silica-coated gold nanorods (GNRs) with Pdots into a sophisticated multilayer nanostructure [310]. This innovative technique extends surface plasmon enhancement to various Pdots fluorophores with NIR-II emission. More recently, Lu et al. unveiled the first Golgi apparatus-targeted NIR fluorescent nanoprobe, Golgi-Pdots [311]. Their research confirmed the excellent biocompatibility and targeted capability of Golgi-Pdots for the Golgi apparatus. Despite these significant advancements, challenges such as photobleaching and fluorescence scintillation continue to present limitations in terms of imaging resolution, penetration depth, and signal-to-noise ratio for quantum dots. To tackle these issues, researchers are exploring and developing a range of imaging technologies based on the unique photophysical properties of Pdots, striving to meet the escalating demands and stringent technical requirements of modern imaging technology.

### 5.2. NIR imaging

Imaging based on electromagnetic radiation in the near-infrared (NIR) spectral range enables the acquisition of detailed information on the surface or interior of an object, rendering it widely applicable across various fields [312,313]. For instance, in medical diagnostics, near-infrared emitting nanoprobes combined with corresponding detectors can obtain images of internal lesions in human tissues or organs. This facilitates clinicians in making early noninvasive diagnoses of diseases [314,315]. Additionally, near-infrared imaging is extensively used in detection sensing, such as atmospheric pollution monitoring, where near-infrared light sources with specific frequency bands are employed alongside sensors to assess air quality [298]. The preparation and spectral properties of NIR nanoprobes based on Pdots are discussed in Sections 3.3 and 3.4. As previously mentioned, the fundamental strategy for preparing NIR probes involves the combination of strong donor-acceptor (D-A) pairs, where judicious design significantly reduces quenching or post-filtering effects caused by the aggregation of conjugated chains [316]. However, energy transfers within NIR Pdots through single or multiple D-A pairs, along with exciplex formation, can substantially impact quantum efficiency and fluorescence yield, presenting a challenge yet to be perfectly resolved. Zhang et al. designed conjugated polymer PBT Pdots with phenothiazine as the donor and benzothiazole as the acceptor, using steric hindrance to reduce the dense stacking of conjugated chains. This approach improved the quantum effect of the AIE-Pdots to 23%, as illustrated in Fig. 6C [51]. Despite this

progress, a gap remains when compared to Qdots or Cdots, known for their high fluorescence quantum yield. Other notable research includes Li and team's 2016 unveiling of a novel photothermal therapy (PTT) material based on Pdots [317]. These Pdots, characterized by strong NIR absorption and exceptional photostability, demonstrated a photothermal conversion efficiency of 65% when illuminated with an NIR laser. In 2017, Ke and collaborators engineered Pdots with a donor-bridge-acceptor structure, yielding narrow-band emissions, ultrahigh brightness, and large Stokes shifts in the NIR spectrum, suitable for multiplexed biological applications [149]. Chen et al. introduced a new category of high NIR fluorescent Pdots, comprising two polymers (PTPE-DTNT2 and PTPE-DTNT4) with side chains containing cross-conjugated aggregation-induced emission fluorogens [318]. These Pdots displayed photoluminescent quantum yields (PLQYs) up to 31.8% and an NIR emission peak at 716 nm, ranking among the highest for NIR Pdots to date. In 2020, Zhang et al. developed NIR-IIa Pdots through a dual fluorescence enhancement mechanism, enhancing small animal imaging with notable improvements in penetration depth and signal-to-background ratio in cerebral vasculature imaging through skulls and scalps in live mice [51]. Liu and colleagues, in 2020, proposed a fluorination strategy in semiconducting polymers to create highly bright NIR-II probes, providing crucial insights for accurate brain tumor malignancy diagnosis [319]. Recent advancements in Pdots for the 'second near-infrared window' (NIR-II), specifically between 1000 and 1700 nm, have established them as a groundbreaking optical transparent imaging technology in living bodies. More recently, Dai et al. introduced an innovative approach for creating tumor microenvironment (TME)-activated NIR-II phototheranostic nanoprobes, further expanding the potential applications of Pdots in medical diagnostics and therapy [320].

**TP - two photon imaging:** TP imaging utilizes NIR light sources with wavelengths ranging from 700 to 1300 nm, distinct from the common single-photon microscopes in laboratories that use visible light sources between 400 and 700 nm [321,322]. Single photons with their shorter wavelength and higher energy can excite the fluorescent reporter group into an excited state. In contrast, TP microscopy employs two infrared photons simultaneously to stimulate the fluorescent reporter group due to the longer wavelength and lower energy of NIR light, making it challenging to achieve energy level transitions with single NIR photon excitation [323,324]. TP imaging technology often combines ultrafast pulsed infrared lasers with infrared correction objectives to image tissues with significant thickness and depth. When integrated with NIR Pdots nanoprobes, this technology enables imaging of samples with large depth and thickness [325]. The pulsed excitation of the light source reduces phototoxicity and enhances spatial localization, making it suitable for long-term specimen observation [326]. In 2015, He et al. explored the potential of water-soluble Pdots for TP bioimaging, focusing on their strong nonlinear optical phosphorescence [327]. They found that these small phosphorescent Pdots, emitting intense red luminescence at 620 nm, exhibit notable nonlinear optical properties. Living cell imaging experiments with these Pdots demonstrated their effectiveness in two-photon time-resolved phosphorescent microscopy. Concurrently, Liu and team developed a new method for accurately quantifying the particle sizes of these highly luminous Pdots, showing the importance of selecting Pdots with optimal sizes (~30 nm) for single-particle imaging and tracking [328]. In 2017 and 2018, Hassan and his workmates achieved deep imaging of the cortical microvasculature in C57 mice using Pdots. They investigated the two-versus three-photon power dependence, observing a distinct three-photon excitation signature at wavelengths beyond 1300 nm, and a transition from two-photon to three-photon excitation within the 1060–1300 nm range [305,329]. In 2021, Zhang et al. synthesized NIR-IIa Pdots using a dual fluorescence enhancement mechanism, significantly improving penetration depth and signal-to-background ratio in small animal imaging, evidenced by through-skull and through-scalp fluorescent imaging of cerebral vasculature in live mice [159]. Another research team

also created HClO-sensitive integrated polymers and corresponding Pdots through molecular engineering, effectively detecting and imaging HClO [330]. In TP imaging in HeLa cells, these Pdots showed promising results in both one- and two-photon imaging in acute inflammation models in mice. Recently, Mayder et al. reported on designing deep blue fluorophores, incorporating hexamethylazatriangulene to enhance photobleaching resistance, increase two-photon absorption cross-sections, and boost fluorescence quantum yields [331]. In addition, the resulting BF@Pdots nanoprobes demonstrated exceptional performance in detecting dynamic fluctuations of SO and FA, exhibiting precise mitochondrial targeting in cancer cells, self-calibrating ratio-metric analysis, long-wavelength excitation for two-photon emission, and rapid reversible response [332].

### 5.3. Super-resolution imaging

Super-resolution imaging represents a sophisticated image processing technology that enables researchers to obtain precise, detailed, high-resolution images [333]. This is achieved through the integration of advanced computer algorithms with high-performance fluorescent nanoprobes. The technology holds vast application potential across numerous fields, notably in medical and biological imaging [334]. Its significance lies in its ability to provide more accurate and detailed image data [335]. This ranges from analyzing the activity characteristics of intracellular biomolecules to assisting physicians in diagnosing diseases and formulating treatment plans [290,336]. As an emerging technology, super-resolution imaging increasingly offers novel methods and possibilities for addressing scientific challenges and enhancing experimental accuracy.

**STED - stimulated emission depletion super-resolution imaging:** STED is a far-field super-resolution imaging technique that employs purely optical methods to overcome the diffraction limit [337]. This technique is based on the phenomenon of stimulated emission, where a fluorescent molecule, upon returning from the excited state to the ground state, absorbs a second photon. This photon possesses energy equivalent to the energy level difference between the ground and excited states. The fluorescent molecule then simultaneously emits two photons, each mirroring the energy, frequency, phase, and propagation direction of the absorbed second photon, thereby suppressing spontaneous emission [338]. Utilizing this principle, STED employs two light sources: an excitation light source and a depletion light source, to regulate fluorescent molecules between bright and dark states. The technique employs a point spread function to surpass the conventional diffraction limit of 200 nm. In theory, increasing the power of the depletion light source can indefinitely enhance the resolution of STED [339]. However, practical limitations such as phototoxicity, the inherent particle size of the fluorescent molecule, and photobleaching constrain the lateral resolution of imaging to a range between 30 and 80 nm [340]. Addressing the limitations imposed by the diffraction barrier in far-field light microscopy, notably the Abbe diffraction limit, Wu et al. advanced the field by introducing two distinct types of nanoscale fluorescent polymer dots (Pdots) for enhanced bioimaging. These Pdots, specifically CN-PPV (poly [2-methoxy-5-(2-ethylhexyloxy)-1,4-(1-cyanovinylene-1,4-phenylene)]) Pdots and PDFDP (poly [{9,9-diethyl-2,7-bis(1-cyanovinylene)fluorene}-{2,5-bis('1-diphenylamino)-1,4-phenylene}]) Pdots, were developed for dual-color stimulated emission depletion (STED) bioimaging and cellular tracking [341]. Their implementation overcomes the conventional constraints of raster image correlation spectroscopy, such as distinguishing only larger regions of interest (around 200 nm) and requiring low fluorophore concentrations in the nanomolar range. Additionally, Fang et al., harnessing the AIE principle, developed Pdots characterized by NIR emission and a high fluorescence quantum yield, as shown in Fig. 6D [299]. These findings underscore the potential of Pdots as effective nanoprobes for live-cell multicolor STED nanoscopy, offering a significant advancement in imaging capabilities beyond the conventional optical resolution limits.

**SOFI - super-resolution optical fluctuation imaging:** Super-Resolution Optical Fluctuation Imaging (SOFI) is based on the scintillation characteristics of fluorescent molecules. This technique involves recording sequential images at different time points and conducting statistical analysis and superimposition calculations on fluorescence fluctuations [342]. It calculates the convolution distribution of fluorescence images through the point spread function and reorganizes pixel points to surpass the diffraction limit [343]. In 2009, T. Dertinger initially proposed the concept of SOFI imaging technology and outlined three essential conditions for its implementation: the scintillation characteristics of the light source, the independent existence of the radiation source, and a particle size distribution smaller than the diffraction limit [344]. The Fourier weight redistribution algorithm, an advancement over the original second-order algorithm, significantly reduces the diffusion function of effective points. This algorithm replaces the conventional interpolation method with virtual pixels that accurately reflect fluorescence signal information, thus yielding more detailed high-resolution images. In 2012, Dertinger and his colleagues demonstrated the inherent three-dimensional optical tomography capabilities of SOFI, which effectively reduces the equipment requirements for imaging [345]. Polymer nanoparticles, specifically Pdots wrapped by conjugated chains, exhibit substantial energy transfer influenced by their spatial conformation. To induce scintillation characteristics in Pdots, it is often necessary to introduce auxiliary groups or impose strict restrictions on their particle size distribution. In 2017, Chen and his team innovated by introducing two types of small photo-blinking Pdots with distinct colors and narrow emission spectra: blue-emitting PFO Pdots and carmine-emitting PFTBT5 Pdots [150]. These Pdots were utilized for blinking-based statistical nanoscopy, proving to be highly effective labels for dual-color super-resolution optical fluctuation imaging of specific subcellular structures. This innovation indicated their potential in facilitating long-term multicolor SOFI nanoscopy with enhanced spatiotemporal resolution. Further advancements were made in 2020 by Liu et al., who reported on the creation of two types of BODIPY-based Pdots [346]. These Pdots featured narrow-band emissions, significant fluctuations, and notable photostability, which enabled sophisticated, high-order, dual-color SOFI nanoscopy. Comparisons in single-particle and subcellular SOFI analysis revealed that these BODIPY Pdots outperformed conventional streptavidin-conjugated Alexa dyes in terms of performance, setting a new standard for precision in nanoscale imaging.

**STORM - stochastic optical reconstruction microscopy imaging:** This technique employs optical principles and computer algorithms to reconstruct high-resolution images [347]. It involves performing multiple exposures and multidimensional imaging of the sample, followed by the superimposition and processing of collected data using computer algorithms. A specialized microscope captures incomplete projection images of the sample from various dimensions or angles. These projection images are then digitally processed for algorithmic superimposition, background noise elimination, pixel distortion correction, and exposure adjustment [348]. The iterative optimization process gradually restores the high-resolution two-dimensional or three-dimensional details of the original sample. This approach enables the acquisition of clear images beyond the diffraction limit without the need for specific labeling or staining [349]. Predominantly, researchers utilize PFBT in Pdots for STROM imaging due to its high photostability and distinct emission peaks. Furthermore, Pdots display scintillation characteristics when the diameter of their spherical core, formed by entangled conjugated chains, is under 10 nm. This property remains consistent even with stable light sources, facilitating the capture of multi-dimensional signal reporting points. Jiang et al. enhanced the resolution of conventional inverted microscopes to approximately 30 nm by integrating PCBM into PFBT Pdots nanoparticles for STROM imaging of *E. coli* [350]. Similarly, Ye et al. labeled the  $\beta$ -amyloid peptide with PFBT Pdots, attaching a reporting molecule to the polypeptide chain's end [351]. This enabled STROM imaging of Alzheimer's disease markers

with a resolution of 20 nm.

**PALM - photoactivated localization microscopy imaging:** PALM and STORM imaging, two ultra-high-resolution optical microscopy techniques, share a common imaging principle and were developed independently by various research teams, from single-molecule localization microscopy (SMLM) imaging [352]. The essence of this principle involves accurately locating individual fluorescent sources in a sample, such as quantum dot-based fluorescent reporter groups, by fitting a two-dimensional Gaussian function to the centroid of the light spot formed by fluorescent reporter molecules under a microscope [353]. The introduction of light-switching molecules into the conjugated chains allows reporter molecules to emit strong but transient fluorescence signals post-excitation, quickly reverting to a stable dark state. Effective reactivation of fluorescent nanoprobes like photo switchable Pdots is achieved with laser irradiation matching their excitation peak. These reactivated photo-switchable Pdots molecules can be detected and localized before they revert to their dark state [354]. The emitted signal from reporter molecules is either pulsed or continuous, and its intensity is adjustable. Thus, within each imaging cycle in the microscope's field of view, only a minimal fraction of photo-switchable Pdots is activated, allowing the distinction of individual activated photo-switchable Pdots from the non-activated ones. Before final photobleaching occurs, thousands of localized images collected during these switching cycles are integrated. An algorithm then reconstructs these signal images at a specific spatial resolution, culminating in the generation of a super-resolution image.

#### 5.4. Photoacoustic imaging

Photoacoustic imaging (PA/PAI) represents an advanced non-contact imaging technology that integrates optical and acoustic principles [355]. This technology involves irradiating the target probe entity with laser pulses and detecting the resultant echo signal to acquire macroscopic morphology, detailed features, and structural information of the target [356,357]. The process can be outlined as follows: Initially, a near-infrared (NIR) laser source, ranging from 680 to 1400 nm, generates a high-energy, short-pulse laser beam focused on the target [358]. Interaction of the probe entity within the target with this laser beam induces local temperature fluctuations. These fluctuations prompt volume changes in the surrounding medium due to temperature-mediated effects, leading to mechanical vibrations [359]. Consequently, these vibrations cause the medium to emit ultrasound signals. Captured by sensors, these signals are transformed into electrical signals. Subsequently, these electrical signals are processed and analyzed by a computer system to reconstruct the image of the target object. Photoacoustic imaging offers several advantages over traditional imaging techniques: it enables high-resolution three-dimensional imaging, employs non-contact detection methods, utilizes nanosecond-level laser pulses, and minimizes tissue damage [360]. In 2016, Zhang et al. conducted research that illustrated the superior photoacoustic conversion efficiency of Pdots at 532 nm, surpassing that of gold nanoparticles (GNPs) [361]. Furthermore, at 700 nm and identical mass concentration, Pdots exhibited comparable photoacoustic efficacy to GNRs. This study highlighted the potential of Pdots as highly efficient contrast agents in photoacoustic imaging (PAI) and multiscale PAI (MSPAII), facilitating precise lesion localization in relation to blood vessels. Subsequently, Chen and team demonstrated that the optical absorption of polymer nanoparticles, with a single conjugated backbone, could be effectively modulated by judiciously designing particle morphology and polymer persistence length. This discovery positioned Pdots-based platforms as promising candidates for photothermal agents and photoacoustic probes in cancer theranostics. Another research group developed a novel PIID-DTBT-based Pdots, characterized by broad and strong optical absorption in the visible light spectrum (500–700 nm) [362]. In 2018, Chang et al. introduced a new type of Pdots for multifunctional applications in photoacoustic imaging-guided PTT. Notably, in vivo

experiments showed that BDT-IID Pdots provided enhanced photoacoustic contrast along with an effective photothermal effect [363]. More recently, a novel approach involving near-infrared (NIR) light activation of Pdots within thermosensitive hydrogel nanostructures was introduced for multimodal imaging-guided synergistic chemo-photothermal therapy. This innovative Pdots@hydrogel nano platform was shown to be an effective theranostic agent, enabling enhanced trimodal photoacoustic (PA)/computed tomography (CT)/fluorescence (FL) imaging and synergistic chemo-photothermal treatment of tumors [127].

In the realm of photoacoustic imaging, Pu et al., in 2014, made a significant contribution by introducing near-infrared (NIR) light-absorbing semiconducting polymer nanoparticles (SPNs) as a novel class of contrast agents for molecular imaging. Their findings established SPNs as an ideal platform for developing photoacoustic molecular probes, as illustrated in Fig. 6E and F [300,301]. Later, in 2016, Lyu et al. advanced the field by developing an intraparticle molecular orbital engineering technique to simultaneously enhance the photoacoustic brightness and photothermal therapy efficacy of SPNs [364]. This approach yielded theranostic SPNs with a dual optical component nanostructure, combining a NIR-absorbing semiconducting polymer and an ultrasmall carbon dot (fullerene) to trigger photoinduced electron transfer upon irradiation. They also innovated biodegradable SPNs with improved photoacoustic and photothermal therapy efficiency for cancer treatment. These SPNs, based on a biodegradable semiconducting polymer (DPPV), transform into water-soluble nanoparticles (SPNV), leveraging the enzymatically oxidizable nature of vinylene bonds. In real-time photoacoustic imaging systems, these nanoparticles enabled precise glioma localization up to 3 mm deep through the scalp and skull, exhibiting an ultrahigh signal-to-background ratio of 90. In 2017, Stahl et al. introduced a series of endogenous contrast agents for *in vivo* photoacoustic imaging [365]. Utilizing SPNs, they achieved wavelength-dependent differential contrast between vasculature and nanoparticles, aiding in unambiguous *in vivo* identification of the contrast agents. Guo et al., in 2019, demonstrated that NIR-II SPNs are valuable for precise imaging and treatment of brain tumors, marking the first series of metabolizable NIR-II photoacoustic agents based on SPNs [366,367]. Jiang et al. presented a generalized molecular design for organic metabolizable semiconducting materials, suitable for biophotonic applications in the NIR-II window [168]. SPNs with  $\pi$ -electron delocalized backbones can be tailored to enhance their photoacoustic imaging and photothermal therapy performance due to their distinct structure-property relationship and versatility in molecular structure modification. The most recent study by Sun et al. presents an innovative multicolor photoacoustic volumetric imaging technique that utilizes Pdots imaging information to visualize mitochondria within cells [368]. Comprehensive reviews by Zhen et al. and Huang et al. summarize recent advances in photoacoustic imaging and photothermal therapy applications of SPNs, with a focus on signal amplification and NIR-II (1000–1700 nm) window construction [369,370]. SPNs containing benzo(1,2-;4,5-)bis (1,2,5)thiadiazole (BBT) units have emerged as quintessential NIR-II (1000–1700 nm) photoacoustic contrast agents (Fig. 4). These agents achieve effective light absorption in the NIR-II region, reducing dilution loss in biological tissues and enhancing imaging resolution. Recent strategies in designing BBT and its derivatives for second near-infrared photoacoustic imaging have also been advanced.

### 5.5. Multimodal imaging

The synthesis and functional modification processes of Pdots fluorescent nanoparticles endow them with diverse properties. These include chain-like winding cores, side chains with differential structures for additional functionality, and numerous functional modification sites on the particle's outer surface. Pdots have broad applications across various fields. In environmental contexts, they are used in water media,

aerosols, soil, etc. In the biomedical sphere, applications include targeting molecule proteins, reactive oxygen species (ROS), DNA, RNA, and organelles. Additionally, Pdots are employed in chemical contexts for detecting special valence metals and specific elements, as well as in monitoring sensing. Their applications extend to fluorescence imaging, encompassing macroscopic anatomical structure identification and super-resolution imaging within cellular sub-spaces. Pdots are also instrumental in drug targeted delivery, nano-carrier construction, and tumor treatments such as photodynamic and photothermal therapy. While no single imaging method is universally superior, the combination of multiple imaging modalities enables researchers to obtain more comprehensive image information and detailed structural insights [371]. Employing basic fluorescence imaging as a foundation, and supplementing it with other modalities like CT, MRI, and ultrasound, allows for the synergistic visualization of specific anatomical structures and the tracking and detection of targeted molecules [372].

Currently, the field of super-resolution imaging, as introduced in the previous summary, is in need of further research, yet it holds significant promise. This technique addresses the challenge of capturing fine structural details in microscopic imaging. Multimodal imaging may prove crucial for comprehending comprehensive information in macro imaging. In the realm of clinical medicine, medical imaging has evolved into a relatively mature discipline. The introduction and widespread adoption of high-resolution CT and MRI have facilitated the development and application of numerous nano-scale innovations. For instance, modifying Pdots with paramagnetic nano iron or ions such as  $\text{Fe}^{3+}$ ,  $\text{Zn}^{2+}$ , and  $\text{Ga}^{3+}$  [373], commonly used in solid-state nuclear magnetic resonance technology, enables the acquisition of distinct fluorescence signals, photoacoustic signals, and nuclear magnetic signals, thereby enhancing MRI capabilities.

### 5.6. Virtual imaging

Virtual imaging represents a largely unexplored domain. In traditional imaging, signals are real and objective, reflecting the presence of fluorescent nanoprobes in specific spatial conformations within a substrate [374]. The integration of computer algorithms facilitates super-resolution (microscopic) and multi-modal (macroscopic) imaging [375,376]. These algorithms can be collectively referred to as "pre-imaging algorithms." Despite advancements in super-resolution imaging, the inherent limitation of the fluorescent nanoprobe's particle size and the halo formation around nanoparticles during excitation precludes surpassing the nanoparticle size limitation. To achieve higher resolution, material scientists face the challenge of reducing the size of fluorescent nanoprobes while simultaneously enhancing their inherent brightness. This endeavor significantly escalates the complexity of material preparation. Furthermore, in macroscopic imaging scenarios, such as imaging organoids or complex *in vivo* tumor microenvironments, researchers often resort to multi-batch, relatively independent labeling imaging or detection analysis. This approach aims to simplify the dimensionality of the anticipated data, facilitating the understanding of multi-dimensional parameters [377]. This advancement not only necessitates a solid professional knowledge base but also presents challenges to traditional imaging technology.

Virtual imaging, an emerging field in imaging technology, is yet to be clearly defined. Our research group conceptualizes it as "post-imaging algorithms," which involve the post-processing of existing signals or secondary imaging of images. Advancements in multimedia computing technology have led to the availability of numerous open-source acquisition tools, including augmented reality (AR), virtual reality (VR), mechanical model, theoretical calculation, parametric data set construction, bionic computer, digital reconstruction of pixel points, and so on [378–380]. These tools enable the addition of secondary signals to existing "non-real" signals post-imaging or the deletion of "real" but irrelevant signals. Essentially, it is possible to extract independent signal channels from labeled sites or dyes in specific cells or tissues, followed

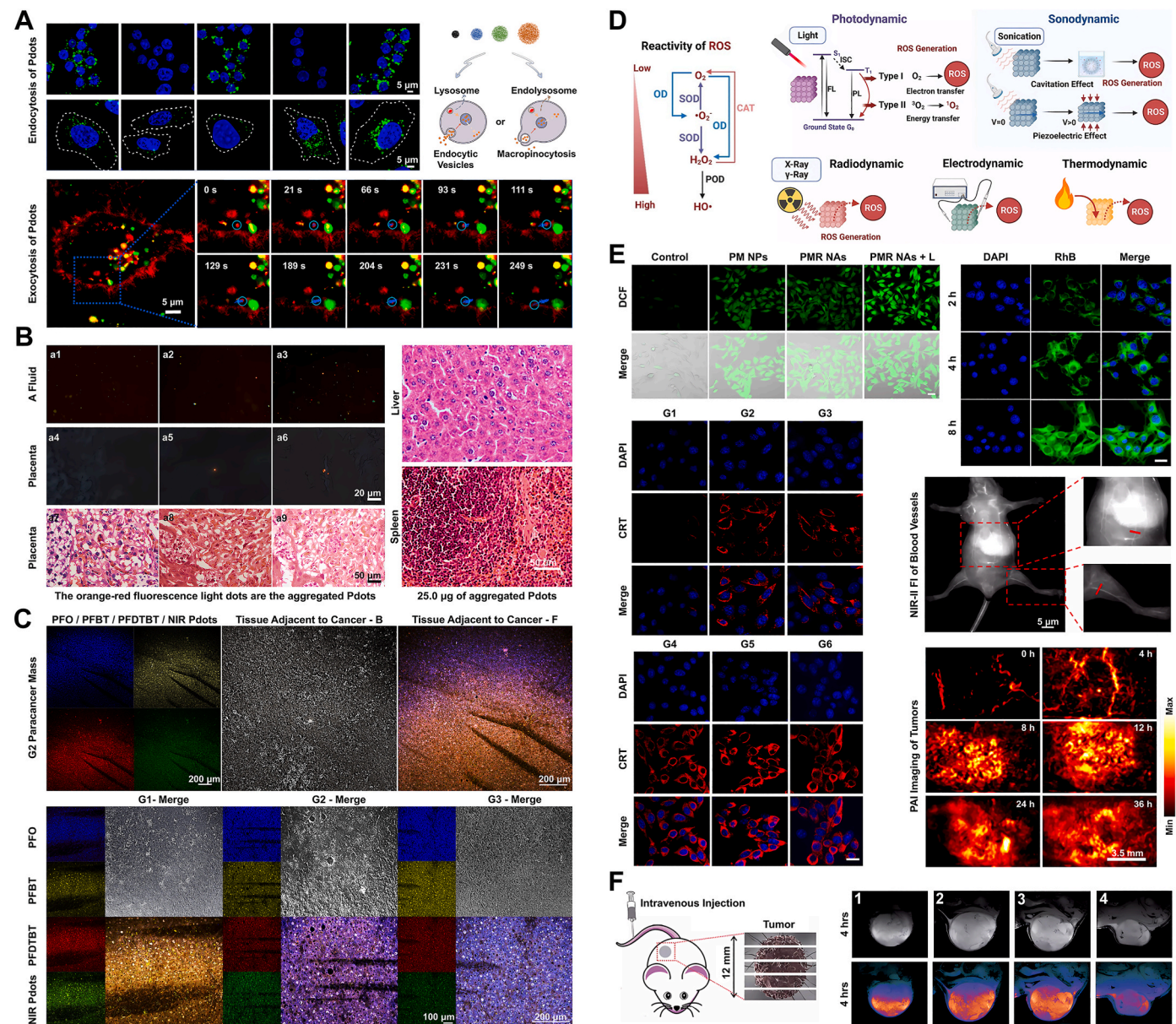


**Fig. 7. Multiple disease diagnosis & treatment methods and classic cases for Pdots of the  $\pi$ -conjugation chain.** A). Pdots with small particle size and spherical physical morphology largely depend on the clathrin-mediated endocytic pathway for transmembrane transport, and Pdots with large particle size or surface functionalized modification mainly rely on the macropinocytosis pathway for transmembrane transport. Reprinted with permission from Ref. [401]. Copyright 2017 American Chemical Society. B). Reproductive toxicity of Pdots. By tail vein injection, Pdots accumulated mainly in the liver and spleen, with no significant effect on maternal body weight or organ coefficient (note: A Fluid: amniotic fluid). Reprinted with permission from Ref. [400]. Copyright 2017 Iivyspring International Publishers. C). The staining ability of pathological grading with multi-Pdots-anti miRNAs. As the cell source gradually changed from normal tissue to malignant hepatocellular carcinoma, the color palette, after calculation and stacking, showed a gradual transition from bright orange for approximately normal tissue to violet-blue for cancerous tissue (upper part). The lower part shows bright orange-G1 (cell morphology is like normal tissue), violet-G2 (highly differentiated tumor cells), and dark blue or blue-yellow-G3 (poorly differentiated tumor cell) channel images to show pathology grading. Reprinted with permission from Ref. [180]. Copyright 2022 American Chemical Society. D). Schematic representation of photodynamic therapy (PDT). Photosensitizers generate ROS via light-induced electron transfer or energy transfer. Other effects, such as energy production and internal irradiation, are also included. Reprinted with permission from Ref. [406]. Copyright 2023 John Wiley and Sons Ltd. E). To improve the efficacy of immunotherapy, using  $Mn^{2+}$  ions as a coordination node, self-transferring NIR-II phototherapeutic nano adjuvants (PMR-NAs) were successfully prepared through the coordination self-assembly of ultrasmall NIR-II Pdots with toll-like receptor agonist resiquimod (R848). PMR-NAs can achieve TME-responsive drug release and tumor-targeted delivery of NIR-II fluorescence/photoacoustic/magnetic resonance imaging-mediated drugs and complete photothermal synergistic chemotherapy, stimulating effective anti-tumor immune responses through ICD effects. Reprinted with permission from Ref. [407]. Copyright 2023 Elsevier. F). The pH/hypoxia programmable triggered cancer photo-chemotherapy based on a Pdots hybridized mesoporous silica framework. Reprinted with permission from Ref. [408]. Copyright 2018 Royal Society of Chemistry.

by the application of traditional imaging methods. Subsequent to imaging, secondary algorithms like super-resolution pixel point addition, bionic iterative computation, 3D reconstruction, and digital model construction are introduced. Utilizing the advanced computational capabilities of modern computers, researchers can perform secondary

processing on collected fluorescence signals and virtually reconstruct required imaging components. This approach transforms stringent dye requirements into pixel or point cloud matrix sequences, which are easily computable and recognizable by computers [381]. The final step involves the application of secondary coloring or rendering models for

imaging. Our research group has made preliminary efforts in this imaging mode (Fig. 9E) [227], demonstrating that algorithmic support can enhance super-resolution imaging details by 2–3 times and facilitate 3D imaging of disordered cell clusters, such as organoids.

However, it is undeniable that as biological imaging experiments continue to increase in scale and complexity, the task of emulating human vision remains a formidable challenge for computers [382]. Initially, researchers relied on extensive high-quality imaging datasets to refine computer algorithms; however, in cell imaging, issues such as voluminous data and manual annotation are inevitable (e.g., **CellProfiler** [383] - an image analysis tool, and **ilastik** [384] - an image simplification tool), both requiring manual parameter adjustments for experiment-specific optimization. To address these challenges, scholars have introduced learning frameworks like **U-Net** [385] and neural networks to tackle multi-probe labeling (identifying numerous probe data) and the segmentation problem (cell nucleus organization identification) in cell images. In contrast, 3D spatial imaging and volume analysis of multi-dimensional tissue blocks using optical microscopy are relatively straightforward. Over the past few years, researchers have proposed a new solution - Transformers, which utilizes the integration of large language model **ChatGPT** and the core architecture of protein structure prediction algorithm **AlphaFold** to improve imaging resolution and processing ability of multi-dimensional data [386,387]. In the future, virtual imaging, with the intervention of AI, can better integrate new technologies such as high-performance optical imaging materials, more advanced imaging equipment, deep transcriptomics, and proteomics analysis, providing researchers with more powerful and convenient tools to process and analyze complex biological image data.

## 6. Nanomedicine based on pdots

With the synergistic advancement of modern medical technology and nanoscience, nanomedicine has emerged as a vital branch of contemporary medicine [388]. Utilizing “nanoparticles” as a medium, novel disease evaluation model has been developed, contributing to significant advancements in early diagnosis, efficacy determination, disease monitoring, and prognosis evaluation [389–391]. This progress supports the strategic integration of diagnosis and treatment [392]. Researchers are continually developing new therapeutic and diagnostic methods based on the diverse physical and chemical properties of Pdots, aiming to extend life expectancy and enhance the quality of life for patients. As innovative nano-dye particles, Pdots have been employed in fluorescence imaging, target molecule labeling, and other applications due to their exceptional spatial and temporal resolution, cost-effectiveness, non-radiative nature, high sensitivity, and detection specificity. Through redesign and optimization of preparation processes, followed by functional modifications, Pdots have been adapted to serve various roles across different fields [13,15,215,255,134,122]. For instance, (i) in biomedical imaging, modification with specific proteins or molecules facilitates early diagnosis, disease monitoring, and efficacy assessment; (ii) leveraging antigen-antibody specific adsorption enables targeted drug delivery and precise body distribution; (iii) controlling the synthesis pathway and doping with substances of varying physical and chemical properties permits internal tumor irradiation or photodynamic therapy; (iv) exploiting the optical characteristics of nanoparticles allows for real-time tracing or long-term labeling imaging, enhancing treatment precision and individualization; (v) and in combination with various treatment modalities, Pdots contribute to multi-level and multi-dimensional disease management.

### 6.1. Metabolism and cytotoxicity

Nano-biological interfaces arise when nanomaterials interact with biological systems, entailing nanoscale material interactions within the body's microenvironment [393,394]. Pdots nanomaterials, as evidenced in various studies, are extensively employed in bio-sensing, drug

delivery, tissue engineering, among other areas (Fig. 6A) [306,395,396]. Precise manipulation of cellular behavior and molecular processes is achievable through the detailed design and control of macroscopic structures, molecular composition regulation, surface chemical modification, and nanoscale structural optimization. However, conventional nanomedicine literature in databases often follows a predictable pattern [222,282,397–399]. They introduce novel concepts or materials using illustrative diagrams, substantiated by cell culture data and animal models, showcasing impressive *in vivo* outcomes. Despite their innovative nature, the translation of many nanomedicine materials into clinical practice is limited, with insufficient research addressing disease pathophysiology.

Pdots stand out in nanomedicine due to their distinctive optical properties, versatile structures, ease of surface modification, and notable biocompatibility, distinguishing them from traditional organic small molecules, quantum dots, and inorganic nanomaterials. In 2017, Wu et al. undertook a study using pregnant mice to assess the reproductive toxicity of Pdots [400]. Their findings indicated no significant adverse effects on maternal body weight and organ coefficients, suggesting a favorable safety profile. Concurrently, Han et al. conducted real-time imaging studies on the endocytosis and intracellular trafficking of a fluorescent Pdots type, confirming its excellent biocompatibility across various cell types [401,402]. These studies collectively revealed that Pdots primarily accumulate in the liver and spleen, organs with sinusoidal structures, without causing substantial physiological disruptions. Importantly, only trace amounts of Pdots were found to enter the amniotic fluid, without altering placental functionality or hindering early fetal development [400]. This body of research underscores the potential of Pdots as safe and effective agents in biomedical applications. Pdots, exhibiting specific targeting capabilities, are endocytosed by targeted cells. Smaller Pdots traverse cell membranes via vesicular transport along microtubules, contrasting with larger nanoparticles that undergo phagocytic endocytosis (as shown in Fig. 7A) [401], ultimately localizing in lysosomes [17,403,404]. Studies reveal Pdots' entry into human gastric adenocarcinoma (SGC-7901) and gastric mucosal (GES-1) cells. MTT assay results indicate a significant proliferative effect of Pdots on both cell lines [278]. Further analysis demonstrates a correlation between cell proliferation and the levels of intracellular ROS and mitochondrial membrane potential (MMP). An increase in Pot concentration corresponds to a decrease in protein kinase B (Akt) expression, while the levels of phosphorylated Erk (*p*-Erk) and c-Jun N-terminal kinase (*p*-JNK) increase. These findings suggest that Pdots promote SGC-7901 and GES-1 cell growth by modulating Akt, *p*-Erk, and *p*-JNK protein expression. However, recent studies in our group reveal that PFBT Pdots and PFDTBT Pdots may induce nonspecific detachment in primary endothelial cells, particularly in those with low adhesion properties [227]. Prolonged high-dose exposure to Pdots can initiate autophagy, evidenced by increased autophagosome formation. This excessive autophagy may result in apoptosis or necrosis in cells with limited resistance, such as mesenchymal stem cells. Notably, Pdots demonstrate excellent biocompatibility and no reproductive toxicity at the tested doses, as illustrated in Fig. 7B [400]. This positions Pdots as promising candidates for preclinical applications. Additionally, recent investigations by Guo et al. provide pivotal data on the biological effects and safety of variously surface-modified Pdots, paving the way for their potential biomedical applications [220,405].

### 6.2. Disease diagnosis

The new disease evaluation model based on “histological parameters” has been essential in various standard and rare clinical situations in modern medicine [409–412]. Detailed and precise observation of human tissue samples can effectively assist doctors in making correct and rapid clinical judgments. In the quantitative and qualitative determination of histological parameters, optical probes are also an essential medical tool that can assist clinicians in observing and analyzing the

general morphology, pathophysiology, structure, and function of human tissue and organs to help medical staff diagnose diseases [413–415]. In addition, histological parameters also play an essential role in disease treatment [416,417]. Doctors can further evaluate the patient's treatment response and prognosis by observing and analyzing specific prognostic markers. For example, in cancer treatment, doctors can judge whether the patient has an excellent response to therapy by following the expression level of circulating tumor markers labeled by optical probes, the cell composition of tumor microenvironment, and the functional storage level of target organs, and adjust the treatment plan based on these parameters to achieve the “individualized and precise” modern medical diagnosis and treatment thinking [417,418]. In 2020, Liu and colleagues developed a novel approach for creating NIR-II probes by implementing a fluorination strategy in semiconducting polymers. The resulting brightly fluorescent NIR-II polymer dots achieved through this fluorination process have proven to be crucial in accurately diagnosing brain tumor malignancies [319]. In a subsequent study conducted in 2022, Men et al. focused on biomimetic semiconducting polymer dots for precise NIR-II fluorescence imaging of gliomas [128]. They engineered conjugated polymer dots coated with C6 cell membranes (Pdots-C6), which were specifically designed for targeted glioma tumor detection. The incorporation of the C6 cell membrane onto the surface of these conjugated Pdots significantly enhanced their specific targeting abilities, both *in vitro* and *in vivo*. Recently, our experimental group also proposed some ideas for disease diagnosis [180]. We constructed a reading scheme for tissue staining slides labeled with multiple miRNA-sensitive nanoprobes - Pdots-anti miRNA, explored the significance of this scheme in the early diagnosis or prognosis evaluation of hepatocellular carcinoma (HCC), and established a new basis for pathological grading diagnosis. In Fig. 7C, we used Pdots-anti miRNA nanoprobes to independently and compoundly image frozen ultrathin sections of HCC, and the results showed significant regular changes. When the cell source transitions from low-grade malignant paracancerous cells to malignant cells, the combined color palette information gradually transitions from the initial “bright orange” to the “dark blue” of cancerous tissue. This indicates that the designed labeling probes have good binding ability to specific short single-stranded miRNA in tissues and pathological grading diagnosis ability.

### 6.3. Disease treatment

The application of optical probes for qualitative, quantitative, and range detection of histological parameters is crucial in disease treatment [419,420]. It aids physicians in determining the extent and method of surgery and managing potential post-surgical recurrence. Particularly in areas like tumor treatment, inflammation management, and large-area tissue dysfunction, where traditional methods fall short, nanoscale materials delivering drugs to specific tissues or cells have shown promising results [421–423]. Drug release from Pdots-based nanodrugs can be precisely controlled by manipulating particle size, morphology, and surface chemistry. Furthermore, functionalized targeted biomacromolecules can directly convey drugs to the required tissues or organs, enhancing therapeutic efficacy and minimizing side effects [59, 92,424]. In neurology, researchers propose utilizing the optical properties of Pdots to generate artificial exogenous light stimulation, potentially preserving optic nerve function and treating retinal diseases [425]. However, challenges persist in nanodrug clinical applications, such as ensuring stable nanoparticle delivery to targeted areas, maintaining specific half-lives, and preventing drug accumulation or toxic side effects [426–428]. The integration of nanodrug research with modern medicine has led to novel clinical technologies, offering clinicians more varied, precise, and personalized treatment strategies (Fig. 7D) [406]. A key challenge in advancing nanomedicine is ensuring the stability of nanocarriers. Li et al. introduced a novel PTT material primarily composed of Pdots [429], characterized by robust NIR

absorption and outstanding photostability. These Pdots have proven effective in photothermal ablation of cancer cells both *in vitro* and *in vivo*, highlighting their potential in clinical therapy. Photodynamic therapy (PDT), a recognized treatment for various diseases including superficial tumors, has advanced significantly. In 2017, Tang et al. developed photo-cross-linkable semiconductor polymer dots with the photosensitizer Chlorin e6 (Ce6) [430]. This approach resulted in an optimized nanoparticle platform for photodynamic therapy. The research indicates that Ce6-doped photo-cross-linkable Pdots are promising for effective photodynamic cancer treatment.

Individualized, precise, and multimodal treatment of diseases is an important research direction in the current medical field [431–433]. With the continuous advancement of science and technology, people's demand for treating different conditions is also increasing. Developing personalized treatment plans for each patient's specific situation can improve the cure rate and quality of life. Individualized treatment determines the best treatment strategy based on the patient's characteristics. In contrast, precise treatment emphasizes using advanced technology for accurate evaluation during diagnosis and monitoring. It makes corresponding adjustments based on the evaluation results for better clinical therapeutic effects. In Fig. 7E and F, we show some classic cases of Pdots-based multimodal treatment of tumors [407,408]. In addition, there are several classical works on the development of nano-drugs based on Pdots. Such as the research work described by Qian et al., which shown the metallophorphyrin-loaded Pdots for PDT applications [434]. Researchers evaluated the photodynamic efficiency of Pdots doped with metalloporphyrins through various cellular assays, assessing their singlet oxygen yield and therapeutic effects. In the same year, a team of scientists developed theranostic agents with customizable absorptions using Pdots of different structures, created via the reprecipitation method [435]. These agents showed promise as imaging-guided therapeutics for clinical cancer treatment and a range of biomedical applications. Recently, Wu et al. focused on enhancing the fluorescence intensity of Pdots by optimizing the stacking of conjugated polymer chains through low-temperature thermal annealing [436]. This treatment resulted in a fluorescence enhancement of approximately 11%–29%, while preserving the Pdots' stability and biosafety. Additionally, 975A2 and 9464D NB cell lines, derived from spontaneous tumors in TH-MYCN transgenic mice, were utilized to explore drug combinations aimed at boosting the antitumor immune response, employing both *in vivo* and *ex vivo* approaches. Intriguingly, this treatment strategy led to the recruitment of immune cells against Pdots and the activation of CD8 T and NK cells, indicating a potential synergistic effect in immunotherapy.

Whether it is a specific recognition probe or a non-specific recognition probe prepared based on Pdots materials or a nano-carrier with different properties constructed through different drug delivery routes, it can be summarized as follows: [A] carrier: (i) liposomes [437], which can undergo membrane fusion with target cells and enhance drug penetration; (ii) Lipid nanoparticles (Lipid NPs) [438]: ensuring local blood drug concentration and prolonging the half-life of drugs in the body; (iii) biocompatible materials coated with nanoparticles [439–442]: Various biological functions can be achieved, with commonly used materials including chitosan (CS), hyaluronic acid (HA), sodium alginate (SA), or polymers such as polyethylene glycol (PEG) or poly (ε-caprolactone) (PCL), or cell-penetrating peptides (CPP) or lipid raft structures; (iv) microneedles, constructing *in vitro* dressings [443, 444]: compared with intravascular injection, microneedles can greatly avoid blood dilution and metabolic stress of the organism, allowing higher blood drug concentration in local specific tissues to achieve the purpose of disease treatment. At the same time, microneedles can precisely deliver drugs deep into the target tissue and reduce pain; (v) hydrogels to create biological scaffolds [445]; (vi) dendritic macromolecules [446] –the last three methods mainly enhance the carrier's ability to carry and release drugs. [B] therapeutic effects: (i) direct contact [447], directly through the physical and chemical properties of

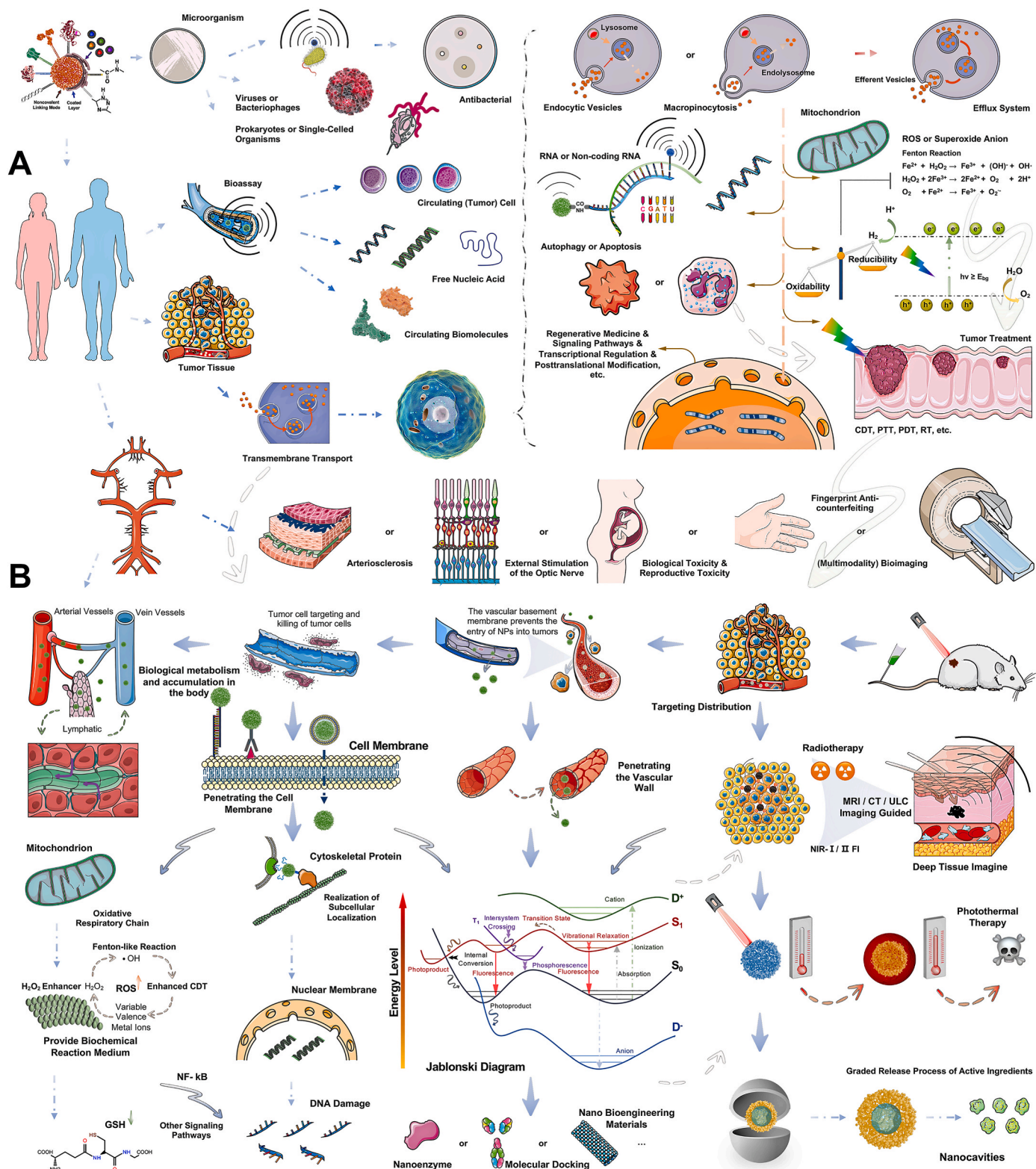


**Fig. 8.** Strategies for the application of semiconducting polymer dots (Pdots) in biomedical fields, the mechanisms used in disease diagnosis & treatment, and the multimodal therapy. Upper Left). Strategy for detection of histological parameters based on Pdots. Upper Right). Schematic diagram of transmembrane transport modes of Pdots. When Pdots enter the target cells, they can trigger various biological behaviors, such as cell proliferation, autophagy, or apoptosis. In addition, a nanobiological interface for the Fenton Reaction can be provided to generate ROS through a cascade reaction. Combined with Pdots' thermal conversion and radiation generation ability, it can achieve multi-dimensional therapeutic effects on tumors. Middle Part). Biotoxicity and other clinical applications of Pdots. Left Lower). Realization of the targeting function and subcellular spatial localization of functionalized Pdots. Right Lower). Schematic diagram of nanomedicine's construction strategy and therapeutic effect based on Pdots. Abbreviations: CDT, Chemodynamic therapy; PDT, photodynamic therapy; PAI, photoacoustic imaging technology; GSH, glutathione; NF-κB, nuclear factor-kappa B; PTT, photothermal therapy; PTT-CDT, photothermal-chemodynamic therapy; ROS, reactive oxygen species; RT, radiotherapy; SDT, sonodynamic therapy.

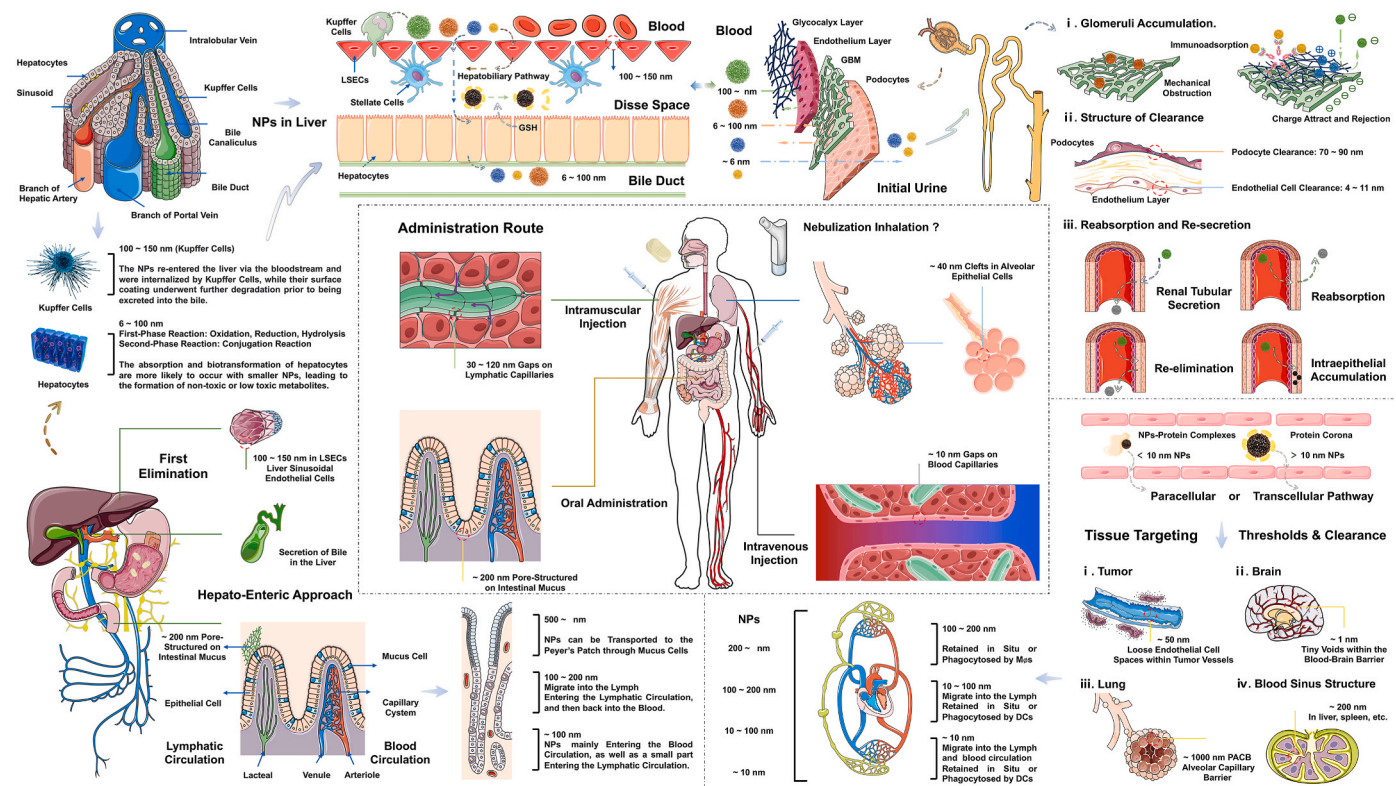


**Fig. 9. The implications of Pdots-based NPs for delivery, targeting, and clearance.** The transport, distribution, biological transformation, and metabolism of nanoscale drugs within the body are contingent upon their physicochemical properties (such as particle size, macroscopic physical morphology, surface charge, and density) as well as the diverse microenvironments encountered during their transit (including reticular structure, charge barrier, immune system response, interstitial space, and intrinsic barriers). i). The middle section - the predominant route of administration for nano drug carriers. ii). The lower right corner - the size thresholds of tissue interstice and appropriate administration route of nanoparticles with varying sizes. iii). The lower left corner - the oral administration route with great development potential. iv). The top half of the Figure - the impact of Pdots-based NPs on hepatic clearance and renal clearance. In terms of Pdots-based NPs, hepatic clearance serves as the primary degradation and metabolism pathways. Drawing inspiration from Ref. [457]. Copyright 2023 Springer Nature.

the material itself, changes the local microenvironment, mediates cell killing or inhibits oxidation; (ii) intracellular penetration [448], which changes intracellular homeostasis by molecular docking or binding to biologically active macromolecules; (iii) oxidation-reduction [449,450], internal doping of oxidizable variable valence metals or further construction into “nano-enzymes,” essentially providing an interface for biological reactions, generating large amounts of ROS through cascade reaction parameters; (iv) photodynamic therapy (PDT) [451]; (v) photothermal therapy (PTT) [452]; (vi) hydrogen production [453,454], which produces reducing substances and inhibits the level of ROS in cells; (vii) chemodynamic therapy (CDT) [126], and there are still unmet requirements to achieve a high antitumor efficiency, including the tumor accumulation of catalyst and enrichment of reactants of Fenton reaction; (viii) multimodal combined therapy [407,455,456], such as photothermal-chemodynamic therapy (PTT-CDT) (Fig. 8).

#### 6.4. Biotransformation and accumulation in vivo

Although nanomedicine based on nanomaterials has emerged as a pivotal discipline in modern medicine, the clinical trial failure rate of candidate drugs still exceeds 90% [458]. The primary and most pressing concern for researchers lies in the elimination of approximately 30% of these candidates due to uncontrollable toxicity or accumulation effects, primarily resulting from systemic administration. By gaining profound insights into the underlying mechanisms responsible for such toxicities or losses, we can revolutionize our approach towards abandoned drugs by ensuring precise delivery at the nanoscale, specifically to disease sites, rather than indiscriminately throughout the body [459,460]. This section aims to provide further guidance for future applications of

functionalized nanocarriers developed using Pdots by comprehensively understanding the aforementioned toxicological aspects.

According to the description in the 2nd chapter, functionalized nano drugs based on Pdots are primarily administered via tail vein injection in animal experiments, with a few instances of oral gavage or intramuscular injection (middle part of Fig. 9). Upon injection into the bloodstream, these NPs with a size distribution ranging from 8 to 32 nm (naked Pdots 8–32 nm; Pdots after modification 50–100 nm) undergo extravasation, penetration, retention, and distribution in tissues, which are collectively determined by NPs’ physicochemical properties and the microenvironment within the body. While Section 3.5 provides detailed information on achieving functionalization and targeting, NP transport is constrained by interstitial clearances present in the body, such as  $\sim 10$  nm intercellular clearance within capillary endothelial cells, enlarged endothelial fenestrations ( $\sim 50$  nm) found in tumor neovascularization, gaps measuring between 30–120 nm along lymphatic capillaries, and pore structures ( $\sim 200$  nm) within intestinal mucus (Fig. 9 lower right corner) [461–463]. Except for penetrating standard capillary endothelial clearances hard, Pdots-based nano drugs could easily penetrate other gap structures, leading to enrichment in target organs. Although most literature employs intravenous injection as a delivery method for Pdots-based medicines, we believe that developing oral formulations holds promise for future research directions. Furthermore, strict control over functionalized particle size may also open avenues for investigation through intramuscular injections. The surface of Pdots can be loaded with attenuated antigens or other functional macromolecules, enabling effective entry into lymphatic networks or local tumors’ tissue where they can modulate immune responses (development of the nano-vaccine) or influence tumor microenvironments (TME).

During *in vivo* transport of Pdots-based nano drugs, NPs in the bloodstream encounter high concentrations of plasma proteins (60–80 mg/mL) and inevitably undergo interactions with them [464,465]. The presence of elevated levels of plasma proteins leads to the formation of protein coronas on the outer surface of NPs, which significantly impacts their stability, targeting ability, translocation rate, as well as their biological transformation pathway and clearance efficiency within living organisms [466]. Notably, NPs with a particle size distribution ranging from 50 to 100 nm are more prone to being recognized as foreign entities by the immune system (Pdots after modification) [457]. Consequently, they become coated with immune proteins and subsequently cleared from circulation, significantly affecting drug functionality. Furthermore, this protein coating increases the hydrodynamic diameter (HD) and sedimentation coefficient of particles, elevating the risk for micro-thrombosis in capillaries [467]. However, ultrasmall NPs (~10 nm) have a higher tendency to form complexes with individual proteins initially before undergoing multiple steps of coating that result in dense protein coronas or even multilayer coronas over time [468]. Compared to larger-sized nanoparticles, these protein bindings exert a more pronounced influence on their *in vivo* transport dynamics. This consideration is also applicable when developing Pdots-based nano drugs and other nanocarriers since it necessitates biocompatibility and inertness towards plasma proteins at the surface chemistry level (Fig. 9). Furthermore, the barrier function of the cell membrane poses a significant challenge when NPs are localized around target cells. A retrospective analysis conducted by Chan et al., in 2016 revealed that regardless of nanoparticles' physicochemical properties or the local tumor microenvironment's pathophysiology, the median tumor targeting delivery efficiency was merely 0.7% [469]. This low delivery efficiency has prompted researchers to re-evaluate the cellular/molecular interaction between NPs and target cells [470,471]. In previous chapters, we discussed how different particle sizes and surface modification schemes influence the transmembrane transport of nanoparticles primarily through active transcellular pathways rather than passive paracellular pathways (Fig. 8). Larger-sized Pdots tend to undergo endocytosis, while smaller-sized ones are more likely to experience clathrin-mediated vesicular trafficking (section 6.1). Although small-sized nanoparticles appear to achieve better-targeting efficiency through other transmembrane pathways [such as the enhanced permeability and retention effect (EPR effect), active transshipment and retention effect (ART effect), and so on [472]], these theories fail to explain existing issues adequately.

Finally, the accumulation of nanomedicine nano-carriers in the body also emerges as a pivotal aspect. After nano drug administration, efficient clearance within the body significantly influences its biological safety and efficacy [457]. In terms of Pdots-based drugs, liver and kidney clearance serves as two primary degradation and metabolism pathways (Fig. 9-Upper Part). Firstly, Pdots-based nano drugs can effortlessly penetrate the 100–150 nm opening in liver sinusoidal endothelial cells (LSECs), thereby accessing the Disse Space [473]. Subsequently, under the influence of liver parenchymal epithelial cells, NPs undergo biodegradation and are transported to intrahepatic bile ducts before being excreted from the gastrointestinal tract [474,475]. However, it is crucial to note that large-sized Pdots NPs (150 ~ nm) face obstruction in penetrating the opening of LSECs, which may lead to pre-sinusoidal obstruction within intrahepatic vessels. Furthermore, NPs with sizes ranging from 100–150 nm accumulate in periportal spaces and are taken up by astrocytes, causing intrahepatic obstruction. Liver parenchymal epithelial cells absorb ultra-small-sized nanoparticles (~6 nm) [476]. Still, they cannot be degraded by lysosomal enzymes, leading to their accumulation within these cells and ultimately affecting their functionality. Moreover, appropriately sized Pdots-based NPs undergo first- (oxidation, reduction, and hydrolysis) and second-phase reactions (conjugation reaction) where aggregates modified on leading/side chains and dyes incorporated during early preparation processes experience further biological transformations resulting mainly in

degradation into less toxic substances; however, there exist instances where conversion into more poisonous substances occurs (Fig. 9 top left corner). On the other hand, renal clearance serves as the predominant pathway for ultrasmall Pdots NPs. The glomerular filtration function primarily relies on the constituents of the glomerular filtration membrane (GFM), including glycocalyx, endothelial cells (70–90 nm), glomerular basement membrane (GBM) (2–8 nm), and podocytes (4–11 nm) [477]. The entire kidney filtration threshold (KFT) is only 6 nm, indicating that large-sized Pdots NPs (100 ~ nm) cannot pass through the fenestrations of the glomerular endothelial layer and re-enter the bloodstream during the kidney filtration process. NPs with a size distribution between 6 and 100 nm can overcome the barrier of the endothelial layer but cannot traverse the gaps in the GBM. Although mechanical obstruction or immune deposition is possible, repulsion due to negative surface charge on most Pdots NPs could interact with the charge barrier, resulting in reduced kidney clearance. Ultra-small-sized NPs (~6 nm) can penetrate these barriers and be excreted into pro-urine; however, reabsorption by renal tubules and uptake by renal tubular epithelial cells should not be overlooked. Long-term exposure to high doses of NPs may still lead to renal tubular toxicity and fibrotic changes in renal parenchyma (Fig. 9 top right corner).

### 6.5. New directions in pdots-based nanomedicine

Nanomedicine, an innovative and rapidly advancing field at the nexus of nanotechnology and medical science, shows immense potential in transforming healthcare [388,478–480]. Pdots have notably risen as a multifaceted nanomaterial platform, finding applications in drug delivery, medical imaging, and various therapeutic interventions [455, 118,144,481,482]. Future directions in cancer nanomedicine are focused on enhancing therapeutic efficacy while minimizing off-target effects [483–485]. Here, we summarize current efforts being made: (i). Enhanced Drug Delivery Systems: Pdots offer unique advantages as drug carriers due to their tunable properties such as size, surface chemistry, and biocompatibility. Researchers are actively exploring strategies to improve drug loading efficiency and release kinetics using Pdots. Additionally, efforts are being made to develop stimuli responsive Pdots that can selectively release drugs at specific sites within the body. (ii). Targeted Imaging Agents: Pdots-based imaging agents hold immense potential for non-invasive diagnosis and monitoring of diseases. By functionalizing the surface of Pdots with targeting ligands or antibodies, researchers aim to achieve high specificity towards disease biomarkers. Furthermore, efforts are underway to enhance the brightness and stability of Pdots probes for improved imaging resolution. (iii). Therapeutic Applications: Beyond traditional drug delivery systems, Pdots themselves possess inherent therapeutic capabilities that can be harnessed for treating various diseases. For instance, photothermal therapy utilizing near-infrared-absorbing Pdots has shown promising results in cancer treatment by selectively destroying tumor cells while sparing healthy tissues. (iv). Combination Therapy Approaches: Combining multiple therapeutic modalities is an emerging trend in nanomedicine research aimed at synergistic effects against complex diseases like cancer or infections resistant to single treatments alone. Researchers are investigating novel approaches integrating different functionalities into a single nanoparticle system using Pdots as building blocks. (v). Biocompatibility Studies: As with any medical intervention involving nanoparticles, ensuring biocompatibility is crucial before clinical translation becomes feasible. Ongoing studies focus on evaluating long-term toxicity profiles of Pdots formulations through rigorous preclinical assessments, including biodistribution analysis and immunological response evaluations.

### 7. Achievement transformation

Pdots comprising primarily  $\pi$ -conjugated polymers and notable for their small size and high brightness, have been extensively applied in

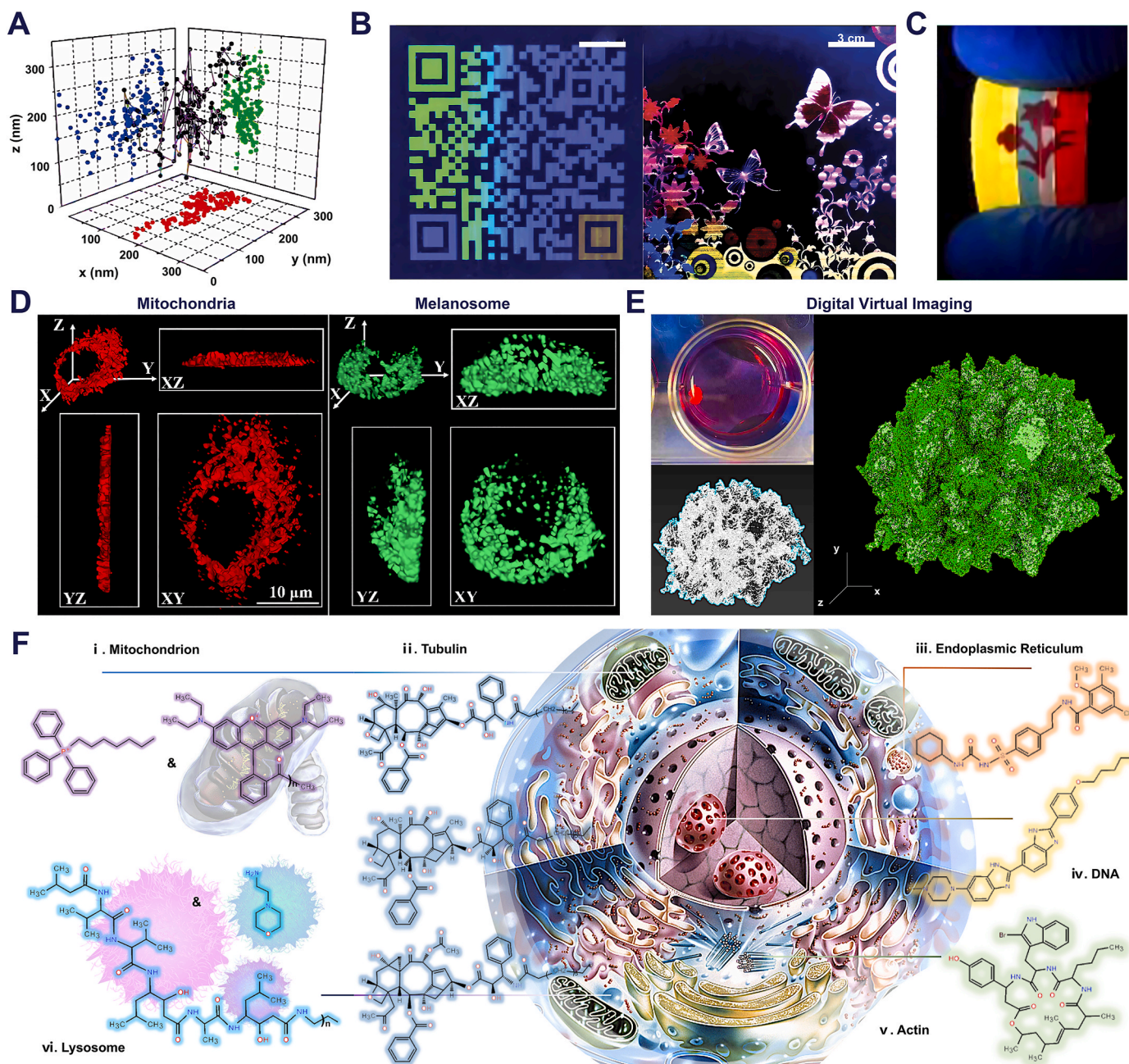


**Fig. 10. Translational applications of Pdots.** A). Single nanoparticles bioimaging and tracking. B). Full-color fluorescence patterning. Reprinted with permission from Ref. [219]. Copyright 2014 John Wiley and Sons Ltd. C). Inkjet printing and anti-counterfeiting applications. D). 3D and three-view imaging of melanosomes and mitochondria. E). Digital virtual imaging of liver organoid cell clusters. Reprinted with permission from Ref. [227]. Copyright 2023 Royal Society of Chemistry. Note: Reprinted with permission from Refs. [30,138], and [368]. Copyright 2014(A), 2017(C) and 2022(D) American Chemical Society. F). Commonly used chemical recognition groups for various subcellular structures. Such as: cytoskeleton proteins, mitochondria, lysosomes, nuclei, etc. Drawing inspiration from Ref. [497]. Copyright 2023 American Chemical Society.

fluorescence imaging and biosensing. Their ultra-small size (1–100 nm), along with stable physical and chemical properties, bright fluorescence, and enhanced properties due to internal doping, make them suitable for various translational applications. In the early 2000s, D. T. Chiu and colleagues began exploring Pdots' translational applications in diverse fields, as shown in previous figure legends (Fig. 6A) [25–27,221]. By 2009, Yu et al. were utilizing Pdots for single-cell tracking and flow cytometry analysis (Fig. 10A) [30]. In 2012, Chan et al. developed photoswitchable Pdots by conjugating photochromic spiropyran molecules to PFBT polymers [486]. In 2016, Kuo et al. introduced the use of photoswitchable Pdots as an optical 'painting' tool, enabling the selection of specific adherent cells based on fluorescence under a microscope

[487]. Using a focused 633-nm laser beam as a 'paintbrush,' they could selectively 'paint' individual Pdot-labeled cells, facilitating sorting and recovery for genetic analysis with high efficiency and purity [145]. In 2014, Taylor et al. updated the quantitative densitometric analysis approach for western blots, detailing the complete workflow from sample preparation to data analysis [488]. Applications in basic experiments in medicine are also seen in the following work [258,489,490]. Ye et al., in 2015, achieved a detection limit at the single-picogram level in dot blots and detected minute quantities of proteins using conventional western blot techniques [307]. In the same year, Chen et al. synthesized oxetane-functionalized Pdots (Ox-Pdots) for rapid visualization of latent fingerprints, showing greater stability than traditional

Pdots [491]. Subsequently, Chang et al. developed ink based on three primary color Pdots (RGB color model) for full fluorescence pattern printing (Fig. 10B) [219]. In 2017 and 2019, Tsai et al. created a dual visual reagent based on Pdots for anticounterfeiting, further expanding their use in flexible substrates and inkjet printing [55,138]. Then, in 2019, Yang et al. reported the first thermochromic-fluorescent ink based on semiconducting polymer dots, anticipating its wide use in advanced security marking technologies (Fig. 10C) [138]. In recent years, Pdots have emerged as an ideal theranostic platform for near-infrared (NIR) photothermal therapy, demonstrating exceptional capabilities in NIR-II fluorescence imaging and serving as photoactive membrane vesicles for precise cellular targeting [492,493]. Pdots exhibit promising potential in energy storage, exemplified by recent advancements in achieving high-performance quantum dot light-emitting devices. Furthermore, three-dimensional micropatterning of semiconducting polymers has been accomplished, enabling the formation of self-assembled microarchitectures with versatile dimensions ranging from dots to lines and networks [494], and combining multiple imaging methods to achieve multimodal imaging (Fig. 10 D & E). Later in 2022, the integration of green-emitting Pdots into diverse applications has been extensively investigated [495], showcasing notable accomplishments, and persisting challenges in this field. Moreover, meticulous manipulation of molecular structures has been explored to attain robust NIR-II fluorescence in Pdots [496]. Potential applications on Pdots have primarily centered on functional applications, such as substrate sensing detection and optical imaging. Challenges in nanomedicine development, understanding inherent biological behavior, achieving deep integration of information processing, and transforming results remain for Pdots, which may pave the way for the emergence of truly intelligent nanomaterials. The aim of these achievement transformations is to furnish novel ideas for designing and exploring the next generation of fluorescent probes and integrated nanomedical materials. The new generation of Pdots can interact with active macromolecules in the body, adapt to complex pathological and physiological microenvironments, and inherit the exceptional optical properties of classical fluorescent nanoprobes. And provide more convenient and powerful optical tools for explorers in more dimensions and levels.

## 8. Challenges and opportunities

Pdots represent a novel class of ultra-bright fluorescent probes for biological imaging. In recent years, researchers have been endeavoring to address the challenges of surface chemistry and biological coupling of Pdots, resulting in numerous outstanding works that elucidate these complexities. As early as 2010s, a serious of research article by Wu et al. summarized a straightforward and effective method for preparing Pdots, which overcame the challenges as mentioned above by introducing amphiphilic polymers combined with nanoprecipitation techniques [33, 40,176]. These nanoparticles are primarily composed of  $\pi$ -conjugated polymers. When they exhibit small particle sizes (between 1 and 100 nm) and high brightness, they are known as polymer dots (Pdots), which have been demonstrated to be practical in various applications such as fluorescence imaging and biosensing. In 2013, the experimental team also summarized the latest findings of the photophysical properties of Pdots, which showcased the advantages of these  $\pi$ -conjugated polymers as fluorescent labeling probes [3]. Furthermore, Aref et al. proposed some potential majorizations to the existing system in their work and discussed the feasibility of translating such diagnostic assays into clinical applications [498]. Due to their excellent properties, such as tunable luminescence, high brightness, excellent stability, and biocompatibility, Pdots have become a popular optical nanoscale platform [499,500]. In 2020, Yuan et al. provided a concise overview of the preparation and biological functionalization strategies of Pdots in a new review article [13]. In the same year, two types of nanoscale fluorescent Pdots with different emission wavelengths were introduced: CN-PPV (poly[2-methoxy-5-(2-ethylhexyloxy)-1,4-(1-cyanoethylene-1,4-phenylene)])

Pdots and PDFDP (poly{9,9-dihexyl-2,7-bis(1-cyano ethylene)fluorene}-{2,5-bis(-diphenylamine)-1,4-phenylene}) Pdots, for dual-color STED biological imaging and cell tracking. These findings herein indicate that Pdots are anticipated to emerge as an exceptional probe for dual-color STED nano replication in living cells [341]. In recent years, Pdots have garnered significant attention in applications spanning from fundamental analytical detection to advanced deep-tissue biological imaging, owing to their exceptional photostability, low cytotoxicity, and high fluorescence brightness. In 2020, Verma et al. comprehensively reviewed the advancement of Pdots in analytical detection and NIR-II fluorescence probes, including their clinical applications in point-of-care biosensing, fluorescence immunochromatographic strips, and multimodal imaging [133]. Presently, our research group remains committed to furthering the work mentioned above, with a primary focus on exploring Pdots in the development of “diagnosis and treatment integration” nanophotonic nanoprobes.

Regarding the spectral properties of Pdots, their preparation strategies require further optimization. Taking the extensively studied NIR nanoprobes as an example, the incorporation of side-chain groups and the doping of NIR dyes result in a broad emission spectrum for most available Pdots [6,27,455,501]. The full width at half maximum (FWHM) exhibited is approximately 2~3 times wider than that of inorganic Qdots emitted in the same optical region, thereby limiting their potential application in multi-channel imaging and multi-substrate detection analysis [49,502,503]. This suggests that researchers need to develop a new type of Pdots that can emit at different wavelengths with narrow spectral bandwidth. Furthermore, the most extensively reported Pdots exhibit emission in the visible range [504]. To develop new optical probes that emit in the NIR region, researchers often modify the side chains of the conjugated chain or dope the host structure with dyes using energy transfer strategies. This results in newly developed optical probes with multiple absorption or emission characteristic peaks, relatively complex monomer structures for each cycle, or leakage of encapsulated dyes. To a certain extent, this can lead to conclusions with low reproducibility and somewhat unstable physicochemical properties. This also suggests that researchers need to explore new types of polymers with relatively simple structures that have narrowband and NIR emission. In medical research and clinical translation, the biocompatibility and potential toxicity of Pdots still require further investigation. Although existing Pdots carriers meet the following three basic requirements: (i) the final hydrodynamic diameter (HD) is less than 5.5 nm, allowing for filtration in the blood sinus; (ii) the use of non-toxic agents in the preparation process; (iii) biodegradability [11,68,505,506]. However, the presence of charge barriers, the immune system, and long-term accumulation effects in the body cannot be ignored. In addition, the rigid polymer conjugate chain after depolymerization can cause unknown biological effects, which have already caused damage to liver and kidney functions and require extensive animal experiments or clinical trials to verify.

With the advancements in molecular biology and material science experimental techniques, the in vitro synthesis of nanoparticles and their functional modification have become established practical methods [507–510]. The emergence of novel technologies, the progression of computer technology, and the cross-disciplinary integration have injected vitality into the field of Pdots research. In this review, we also propose some insights [227,114,511]. For instance, can we construct a genuinely “enzyme active center” nano-enzyme based on Pdots’ surface chemical properties, simulate the structure and function of natural enzymes through “molecular docking” with substrates, and utilize materials at the nanoscale for molecular-level interactions with the assistance of cryo-electron microscopy technology and biomacromolecules’ spatial conformation simulation [512–514]. Furthermore, in practical applications, we might predict the potential emergence of stable new Pdots architectures through computer simulation and other methods, such as the development of more efficient NIR nanoprobes or the synthesis of more straightforward Pdots.

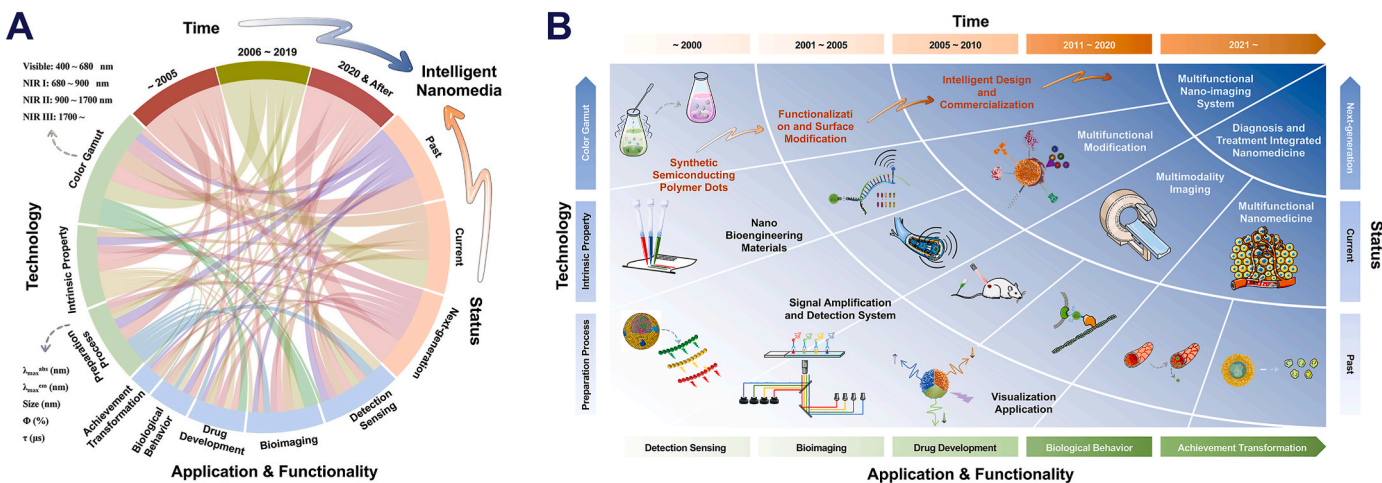


**Fig. 11. Prospects for Pdots.** A). Development context of optical nanomaterials based on Pdots within and beyond the optical imaging domain regarding the key milestones. B). Evolution and application of optical nanomaterials based on Pdots within and beyond optical imaging, analytical sensing, inherent properties, and achievement transformation at different stages.

Additionally, employing the integration of computer technology and imaging technology could facilitate the development of novel imaging technologies. In drug development, conformational targeting could potentially be achieved, with the aid of advanced instruments and equipment to observe, record, and quantify the changes occurring during the interaction between Pdots nano-carriers and target cells (Fig. 10F) [497]. This data will help us understand the physiological processes experienced by nano-carriers constructed based on Pdots in the body, as well as the metabolic kinetic parameters and related characteristics involved. Lastly, we can further explore the potential application value of Pdots in fields such as environmental protection, where they might be applied to water pollution control, waste gas purification, etc [515–517].

## 9. Conclusions

The investigation into semiconductor polymer dots (Pdots) has spanned nearly fifty years, yielding numerous outstanding contributions at various junctures. As illustrated in Fig. 11, we present the three stages of the Pdots development process. Initially, researchers primarily concentrated on exploring the intrinsic properties of Pdots, encompassing the optimization of preparation methods and physicochemical characteristics (indicated by the green semicircle on the left). In recent studies, the research has pivoted towards the development of Pdots for applications in substrate sensing & detection, biological imaging, and multifunctional nanomedicine carriers. As existing work accumulates and the performance requirements for optical nanoprobe escalates, future research could potentially focus more on analyzing NIR dyes, the conversion and application of achievements, and the biological behavior of Pdots (highlighted by the blue semicircle on the bottom).

The next generation of Pdots optical materials is demonstrating growing intelligence. As illustrated in Fig. 11, we present the development plan for Pdots, primarily focusing on the construction of multifunctional nanoscale imaging systems and the integration of diagnosis and treatment nanocarriers. In the field of optical imaging, AI simulations, multidisciplinary cross-integration, and other approaches are being increasingly employed to explore the preparation process, architectural design, and functional realization of Pdots materials. These methods play a vital role, from theoretical and computational analysis to practical research and development applications. Furthermore, multifunctional applications necessitate the combination of various materials across interdisciplinary fields, involving close collaboration between chemists, photophysicists, biologists, and clinicians. Intensified research in these critical fields will realize the functionality and practicality of

Pdots optical nanomaterials in diverse practical applications, paving a brighter path for their development.

## Figure section

This review article uses a variety of different drawing software. Such as: Adobe Photoshop (PS), Adobe Illustrator (AI), XMind (<https://xmind.cn>), R (<https://cran.r-project.org/>), and 3D Studio Max (Version 2021) & V-Ary Material Library for 3DS Max (Version 4.0). Chemical Structural Formulas: StoneMIND Collector (Version 1.6.0) or this software online website (<https://stonemind.stonewise.cn>). Source: PubMed (<https://pubmed.ncbi.nlm.nih.gov>) and Connected Papers (<https://www.connectedpapers.com>). Online Figure drawing website/studio: Genescloud.com. (<https://www.genescloud.cn/home>), FigDraw.com. (<https://www.figdraw.com>), and BioRender.com. (<https://www.biorender.com>). Figure High-definition Processing: BigJPG.com. (<https://bigjpg.com>).

## Notes

None. And if you need high-definition original Figures, please contact the authors of this review.

## CRediT authorship contribution statement

**Ze Zhang:** Writing – original draft, Methodology, Investigation, Conceptualization. **Chenhao Yu:** Writing – original draft, Data curation. **Yuyang Wu:** Writing – original draft, Data curation. **Zhe Wang:** Writing – original draft. **Haotian Xu:** Writing – original draft. **Yining Yan:** Writing – original draft. **Zhixin Zhan:** Writing – review & editing, Investigation, Conceptualization. **Shengyan Yin:** Writing – review & editing, Investigation, Conceptualization.

## Declaration of competing interest

All authors disclosed no relevant relationships.

## Data availability

No data was used for the research described in the article.

## Acknowledgements

This work was supported by the Jilin Provincial Science &

Technology Department (No.20220101057JC) and the Education Department Project of Jilin Province (No.JJKH20231128KJ). It also be supported by grants from the Doctor of Excellence Program (DEP) from The First Hospital of Jilin University (JDYY-DEP-2023014 & JDYY-DEP-2023032).

## References

- [1] O.S. Wolfbeis, An overview of nanoparticles commonly used in fluorescent bioimaging, *Chem. Soc. Rev.* 44 (14) (2015) 4743–68.
- [2] W.R. Algar, M. Massey, K. Rees, R. Higgins, K.D. Krause, G.H. Darwish, W. J. Peveler, Z. Xiao, H.Y. Tsai, R. Gupta, K. Lix, M.V. Tran, H. Kim, Photoluminescent nanoparticles for chemical and biological analysis and imaging, *Chem. Rev.* 121 (15) (2021) 9243–9358.
- [3] C. Wu, D.T. Chiu, Highly fluorescent semiconducting polymer dots for biology and medicine, *Angew. Chem. Int. Ed. Engl.* 52 (11) (2013) 3086–3109.
- [4] J. Yu, Y. Rong, C.T. Kuo, X.H. Zhou, D.T. Chiu, Recent advances in the development of highly luminescent semiconducting polymer dots and nanoparticles for biological imaging and medicine, *Anal. Chem.* 89 (1) (2017) 42–56.
- [5] Y. Jiang, K. Pu, Multimodal biophotonics of semiconducting polymer nanoparticles, *Acc. Chem. Res.* 51 (8) (2018) 1840–1849.
- [6] S. Jiang, J. Lin, P. Huang, Nanomaterials for NIR-II photoacoustic imaging, *Adv. Healthc. Mater.* 12 (16) (2023) e2202208.
- [7] Q. Wei, D. Xu, T. Li, X. He, J. Wang, Y. Zhao, L. Chen, Recent advances of NIR-II emissive semiconducting polymer dots for *in vivo* tumor fluorescence imaging and theranostics, *Biosensors* 12 (12) (2022) 1126.
- [8] S. Kundu, A. Patra, Nanoscale strategies for light harvesting, *Chem. Rev.* 117 (2) (2017) 712–757.
- [9] M. Massey, M. Wu, E.M. Conroy, W.R. Algar, Mind your P's and Q's: the coming of age of semiconducting polymer dots and semiconductor quantum dots in biological applications, *Curr. Opin. Biotechnol.* 34 (2015) 30–40.
- [10] Y. Wu, C. Shi, G. Wang, H. Sun, S. Yin, Recent advances in the development and applications of conjugated polymer dots, *J. Mater. Chem. B* 10 (16) (2022) 2995–3015.
- [11] N. Gupta, Y.H. Chan, S. Saha, M.H. Liu, Near-infrared-II semiconducting polymer dots for deep-tissue fluorescence imaging, *Chem. Asian. J.* 16 (3) (2021) 175–184.
- [12] Y. Rong, C. Wu, J. Yu, X. Zhang, F. Ye, M. Zeigler, M.E. Gallina, I.C. Wu, Y. Zhang, Y.H. Chan, W. Sun, K. Uvdal, D.T. Chiu, Multicolor fluorescent semiconducting polymer dots with narrow emissions and high brightness, *ACS Nano* 7 (1) (2013) 376–384.
- [13] Y. Yuan, W. Hou, W. Qin, C. Wu, Recent advances in semiconducting polymer dots as optical probes for biosensing, *Biomater. Sci.* 9 (2) (2021) 328–346.
- [14] Z. Wang, D. Han, H. Wang, M. Zheng, Y. Xu, H. Zhang, Organic semiconducting nanoparticles for biosensor: a review, *Biosensors* 13 (4) (2023) 494.
- [15] J. Sun, Q. Zhang, X. Dai, P. Ling, F. Gao, Engineering fluorescent semiconducting polymer nanoparticles for biological applications and beyond, *Chem. Commun.* 57 (16) (2021) 1989–2004.
- [16] R. Pepperkok, J. Ellenberg, High-throughput fluorescence microscopy for systems biology, *Nat. Rev. Mol. Cell Biol.* 7 (9) (2006) 690–696.
- [17] E. Betzig, G.H. Patterson, R. Sougrat, O.W. Lindwasser, S. Olenych, J. S. Bonifacino, M.W. Davidson, J. Lippincott-Schwartz, H.F. Hess, Imaging intracellular fluorescent proteins at nanometer resolution, *Science* 313 (5793) (2006) 1642–1645.
- [18] D. Seah, Z. Cheng, M. Vendrell, Fluorescent probes for imaging in humans: where are we now? *ACS Nano* 17 (20) (2023) 19478–19490.
- [19] L.D. Adair, E.J. New, Molecular fluorescent sensors for *in vivo* imaging, *Curr Opin Biotechnol.* 83 (2023) 102973.
- [20] H. Zhong, B. Zhao, J. Deng, Synthesis and application of fluorescent polymer micro- and nanoparticles, *Small* 19 (26) (2023) e2300961.
- [21] Y.C. Li, Q.H. Chen, X.Y. Pan, W. Lu, J. Zhang, New insight into the application of fluorescence platforms in tumor diagnosis: from chemical basis to clinical application, *Med. Res. Rev.* 43 (3) (2023) 570–613.
- [22] S. Borse, R. Rafique, Z.V.P. Murthy, T.J. Park, S.K. Kailasa, Applications of upconversion nanoparticles in analytical and biomedical sciences: a review, *Analyst* 147 (14) (2022) 3155–3179.
- [23] N.K. Younis, J.A. Ghoubaira, E.P. Bassil, H.N. Tantawi, A.H. Eid, Metal-based nanoparticles: promising tools for the management of cardiovascular diseases, *Nanomedicine* 36 (2021) 102433.
- [24] J. Pecher, S. Mecking, Nanoparticles of conjugated polymers, *Chem. Rev.* 110 (10) (2010) 6260–6279.
- [25] C. Wu, Y. Jin, T. Schneider, D.R. Burnham, P.B. Smith, D.T. Chiu, Ultrabright and bioorthogonal labeling of cellular targets using semiconducting polymer dots and click chemistry, *Angew. Chem. Int. Ed. Engl.* 49 (49) (2010) 9436–9440.
- [26] C. Wu, S.J. Hansen, Q. Hou, J. Yu, M. Zeigler, Y. Jin, D.R. Burnham, J.D. McNeill, J.M. Olson, D.T. Chiu, Design of highly emissive polymer dot bioconjugates for *in vivo* tumor targeting, *Angew. Chem. Int. Ed. Engl.* 50 (15) (2011) 3430–3434.
- [27] Y. Jin, F. Ye, M. Zeigler, C. Wu, D.T. Chiu, Near-infrared fluorescent dye-doped semiconducting polymer dots, *ACS Nano* 5 (2) (2011) 1468–1475.
- [28] A. Kaeser, A.P. Schenning, Fluorescent nanoparticles based on self-assembled pi-conjugated systems, *Adv. Mater.* 22 (28) (2010) 2985–2997.
- [29] C. Wu, C. Szymanski, Z. Cain, J. McNeill, Conjugated polymer dots for multiphoton fluorescence imaging, *J. Am. Chem. Soc.* 129 (43) (2007) 12904–12905.
- [30] J. Yu, C. Wu, S.P. Sahu, L.P. Fernando, C. Szymanski, J. McNeill, Nanoscale 3D tracking with conjugated polymer nanoparticles, *J. Am. Chem. Soc.* 131 (51) (2009) 18410–18414.
- [31] D. Tuncel, H.V. Demir, Conjugated polymer nanoparticles, *Nanoscale* 2 (4) (2010) 484–494.
- [32] F. Ye, C. Wu, Y. Jin, M. Wang, Y.H. Chan, J. Yu, W. Sun, S. Hayden, D.T. Chiu, A compact and highly fluorescent orange-emitting polymer dot for specific subcellular imaging, *Chem. Commun.* 48 (12) (2012) 1778–1780.
- [33] Y. Jin, F. Ye, C. Wu, Y.H. Chan, D.T. Chiu, Generation of functionalized and robust semiconducting polymer dots with polyelectrolytes, *Chem. Commun.* 48 (26) (2012) 3161–3163.
- [34] X. Zhang, J. Yu, C. Wu, Y. Jin, Y. Rong, F. Ye, D.T. Chiu, Importance of having low-density functional groups for generating high-performance semiconducting polymer dots, *ACS Nano* 6 (6) (2012) 5429–5439.
- [35] J. Yu, C. Wu, X. Zhang, F. Ye, M.E. Gallina, Y. Rong, I.C. Wu, W. Sun, Y.H. Chan, D.T. Chiu, Stable functionalization of small semiconducting polymer dots via covalent cross-linking and their application for specific cellular imaging, *Adv. Mater.* 24 (26) (2012) 3498–3504.
- [36] M.C. Baier, J. Huber, S. Mecking, Fluorescent conjugated polymer nanoparticles by polymerization in miniemulsion, *J. Am. Chem. Soc.* 131 (40) (2009) 14267–14273.
- [37] N. Kurokawa, H. Yoshikawa, N. Hirota, K. Hyodo, H. Masuhara, Size-dependent spectroscopic properties and thermochromic behavior in poly(substituted thiophene) nanoparticles, *Chemphyschem* 5 (10) (2004) 1609–1615.
- [38] K. Sun, H. Chen, L. Wang, S. Yin, H. Wang, G. Xu, D. Chen, X. Zhang, C. Wu, W. Qin, Size-dependent property and cell labeling of semiconducting polymer dots, *ACS Appl. Mater. Interfaces* 6 (13) (2014) 10802–10812.
- [39] E. Hittinger, A. Kokil, C. Weder, Synthesis and characterization of cross-linked conjugated polymer milli-, micro-, and nanoparticles, *Angew. Chem. Int. Ed. Engl.* 43 (14) (2004) 1808–1811.
- [40] C. Wu, C. Szymanski, J. McNeill, Preparation and encapsulation of highly fluorescent conjugated polymer nanoparticles, *Langmuir* 22 (7) (2006) 2956–2960.
- [41] K. Landfester, R. Montenegro, U. Scherf, R. Güntner, U. Asawapirom, S. Patil, D. Neher, T. Kietzke, Semiconducting polymer nanospheres in aqueous dispersion prepared by a miniemulsion process, *Adv. Mater.* 14 (9) (2002) 651–655.
- [42] T. Kietzke, D. Neher, K. Landfester, R. Montenegro, R. Güntner, U. Scherf, Novel approaches to polymer blends based on polymer nanoparticles, *Nat. Mater.* 2 (6) (2003) 408–412.
- [43] Y. He, X. Fan, J. Sun, R. Liu, Z. Fan, Z. Zhang, X. Chang, B. Wang, F. Gao, L. Wang, Flash nanoprecipitation of ultra-small semiconducting polymer dots with size tunability, *Chem. Commun.* 56 (17) (2020) 2594–2597.
- [44] L. Yao, G.O. Andreev, Y.K. Reshetnyak, O.A. Andreev, Fabrication of semiconductor nanowires by conjugation of quantum dots to actin filaments, *Anal. Bioanal. Chem.* 395 (5) (2009) 1563–1566.
- [45] Y. Zhang, J. Yu, M.E. Gallina, W. Sun, Y. Rong, D.T. Chiu, Highly luminescent, fluorinated semiconducting polymer dots for cellular imaging and analysis, *Chem. Commun.* 49 (74) (2013) 8256–8258.
- [46] W. Sun, F. Ye, M.E. Gallina, J. Yu, C. Wu, D.T. Chiu, Lyophilization of semiconducting polymer dot bioconjugates, *Anal. Chem.* 85 (9) (2013) 4316–4320.
- [47] K. Chang, Y. Tang, X. Fang, S. Yin, H. Xu, C. Wu, Incorporation of porphyrin to pi-conjugated backbone for polymer-dot-sensitized photodynamic therapy, *Biomacromolecules* 17 (6) (2016) 2128–2136.
- [48] Y. Li, H. Yu, Y. Qian, J. Hu, S. Liu, Amphiphilic star copolymer-based bimodal fluorogenic/magnetic resonance probes for concomitant bacteria detection and inhibition, *Adv. Mater.* 26 (39) (2014) 6734–6741.
- [49] L. Chen, D. Chen, Y. Jiang, J. Zhang, J. Yu, C.C. DuFort, S.R. Hingorani, X. Zhang, C. Wu, D.T. Chiu, A BODIPY-based donor/donor-acceptor system: towards highly efficient long-wavelength-excitable near-IR polymer dots with narrow and strong absorption features, *Angew. Chem. Int. Ed. Engl.* 58 (21) (2019) 7008–7012.
- [50] D. Chen, I.C. Wu, Z. Liu, Y. Tang, H. Chen, J. Yu, C. Wu, D.T. Chiu, Semiconducting polymer dots with bright near-band emission at 800 nm for biological applications, *Chem. Sci.* 8 (5) (2017) 3390–3398.
- [51] Z. Zhang, X. Fang, Z. Liu, H. Liu, D. Chen, S. He, J. Zheng, B. Yang, W. Qin, X. Zhang, C. Wu, Semiconducting polymer dots with dual-enhanced NIR-IIa fluorescence for through-skull mouse-brain imaging, *Angew. Chem. Int. Ed. Engl.* 59 (9) (2020) 3691–3698.
- [52] Z. Zhang, D. Chen, Z. Liu, D. Wang, J. Guo, J. Zheng, W. Qin, C. Wu, Near-infrared polymer dots with aggregation-induced emission for tumor imaging, *ACS Applied Polymer Materials* 2 (1) (2019) 74–79.
- [53] D. Wang, J. Qian, W. Qin, A. Qin, B.Z. Tang, S. He, Biocompatible and photostable AIE dots with red emission for *in vivo* two-photon bioimaging, *Sci. Rep.* 4 (2014) 4279.
- [54] A. Reisch, A.S. Klymchenko, Fluorescent polymer nanoparticles based on dyes: seeking brighter tools for bioimaging, *Small* 12 (15) (2016) 1968–1992.
- [55] W.K. Tsai, C.I. Wang, C.H. Liao, C.N. Yao, T.J. Kuo, M.H. Liu, C.P. Hsu, S.Y. Lin, C. Y. Wu, J.R. Pyle, J. Chen, Y.H. Chan, Molecular design of near-infrared fluorescent Pdots for tumor targeting: aggregation-induced emission versus anti-aggregation-caused quenching, *Chem. Sci.* 10 (1) (2019) 198–207.
- [56] L. Wei, D. Zhang, X. Zheng, X. Zeng, Y. Zeng, X. Shi, X. Su, L. Xiao, Fabrication of positively charged fluorescent polymer nanoparticles for cell imaging and gene delivery, *Nanotheranostics* 2 (2) (2018) 157–167.

- [57] S. Ozenler, M. Yucel, O. Tuncel, H. Kaya, S. Ozcelik, U.H. Yildiz, Single chain cationic polymer dot as a fluorescent probe for cell imaging and selective determination of hepatocellular carcinoma cells, *Anal. Chem.* 91 (16) (2019) 10357–10360.
- [58] K. Pu, N. Chattopadhyay, J. Rao, Recent advances of semiconducting polymer nanoparticles in in vivo molecular imaging, *J. Control Release* 240 (2016) 312–322.
- [59] J. Li, J. Rao, K. Pu, Recent progress on semiconducting polymer nanoparticles for molecular imaging and cancer phototherapy, *Biomaterials* 155 (2018) 217–235.
- [60] Z. Tian, J. Yu, C. Wu, C. Szymanski, J. McNeill, Amplified energy transfer in conjugated polymer nanoparticle tags and sensors, *Nanoscale* 2 (10) (2010) 1999–2011.
- [61] F. Ding, J. Feng, X. Zhang, J. Sun, C. Fan, Z. Ge, Responsive optical probes for deep-tissue imaging: photoacoustics and second near-infrared fluorescence, *Adv. Drug Deliv. Rev.* 173 (2021) 141–163.
- [62] X. Zhang, S. He, B. Ding, C. Qu, H. Chen, Y. Sun, R. Zhang, X. Lan, Z. Cheng, Synergistic strategy of rare-earth doped nanoparticles for NIR-II biomedical imaging, *J. Mater. Chem. B* 9 (44) (2021) 9116–9122.
- [63] M. Dai, Y.J. Yang, S. Sarkar, K.H. Ahn, Strategies to convert organic fluorophores into red/near-infrared emitting analogues and their utilization in bioimaging probes, *Chem. Soc. Rev.* 52 (18) (2023) 6344–6358.
- [64] F. Yang, Q. Zhang, S. Huang, D. Ma, Recent advances of near infrared inorganic fluorescent probes for biomedical applications, *J. Mater. Chem. B* 8 (35) (2020) 7856–7879.
- [65] Y. Liu, Y. Li, S. Koo, Y. Sun, Y. Liu, X. Liu, Y. Pan, Z. Zhang, M. Du, S. Lu, X. Qiao, J. Gao, X. Wang, Z. Deng, X. Meng, Y. Xiao, J.S. Kim, X. Hong, Versatile types of inorganic/organic NIR-IIa/IIb fluorophores: from strategic design toward molecular imaging and theranostics, *Chem. Rev.* 122 (1) (2022) 209–268.
- [66] W. Xu, D. Wang, B.Z. Tang, NIR-II AI<sup>E</sup>gens: a win-win integration towards bioapplications, *Angew. Chem. Int. Ed. Engl.* 60 (14) (2021) 7476–7487.
- [67] L. Chen, Y. Jiang, S. Xu, J. Zhang, S.R. Jung, J. Yu, X. Zhang, D.T. Chiu, BODIPY-based near-infrared semiconducting polymer dot for selective yellow laser-excited cell imaging, *RSC Adv* 13 (22) (2023) 15121–15125.
- [68] L. Feng, C. Zhu, H. Yuan, L. Liu, F. Lv, S. Wang, Conjugated polymer nanoparticles: preparation, properties, functionalization and biological applications, *Chem. Soc. Rev.* 42 (16) (2013) 6620–6633.
- [69] L.R. MacFarlane, H. Shaikh, J.D. Garcia-Hernandez, M. Vespa, T. Fukui, I. Manners, Functional nanoparticles through π-conjugated polymer self-assembly, *Nat. Rev. Mater.* 6 (1) (2020) 7–26.
- [70] K. Sonowal, L. Saikia, Functional groups assisted-photoinduced electron transfer-mediated highly fluorescent metal-organic framework quantum dot composite for selective detection of mercury (II) in water, *J. Environ. Sci.* 126 (2023) 531–544.
- [71] J. Sun, N. Chen, X. Chen, Q. Zhang, F. Gao, Two-photon fluorescent nanoprobe for glutathione sensing and imaging in living cells and zebrafish using a semiconducting polymer dots hybrid with dopamine and beta-cyclodextrin, *Anal. Chem.* 91 (19) (2019) 12414–12421.
- [72] J. Sun, P. Ling, F. Gao, A mitochondria-targeted ratiometric biosensor for pH monitoring and imaging in living cells with Congo-Red-Functionalized dual-emission semiconducting polymer dots, *Anal. Chem.* 89 (21) (2017) 11703–11710.
- [73] C.T. Kuo, I.C. Wu, L. Chen, J. Yu, L. Wu, D.T. Chiu, Improving the photostability of semiconducting polymer dots using buffers, *Anal. Chem.* 90 (20) (2018) 11785–11790.
- [74] A.H. Ashoka, I.O. Aparin, A. Reisch, A.S. Klymchenko, Brightness of fluorescent organic nanomaterials, *Chem. Soc. Rev.* 52 (14) (2023) 4525–4548.
- [75] Y. Jiang, Q. Hu, H. Chen, J. Zhang, D.T. Chiu, J. McNeill, Dual-mode superresolution imaging using charge transfer dynamics in semiconducting polymer dots, *Angew. Chem. Int. Ed. Engl.* 59 (37) (2020) 16173–16180.
- [76] Z. Meng, L. Guo, Q. Li, Peptide-coated semiconductor polymer dots for stem cells labeling and tracking, *Chemistry* 23 (28) (2017) 6836–6844.
- [77] X. Jiang, R. Yang, X. Lei, S. Xue, Z. Wang, J. Zhang, L. Yan, Z. Xu, Z. Chen, P. Zou, G. Wang, Design, synthesis, application and research progress of fluorescent probes, *J. Fluoresc.* (2023), <https://doi.org/10.1007/s10895-023-03344-7>.
- [78] L. Motiei, D. Margulies, Molecules that generate fingerprints: a new class of fluorescent sensors for chemical biology, medical diagnosis, and cryptography, *Acc. Chem. Res.* 56 (13) (2023) 1803–1814.
- [79] Y. Geng, Z. Wang, J. Zhou, M. Zhu, J. Liu, T.D. James, Recent progress in the development of fluorescent probes for imaging pathological oxidative stress, *Chem. Soc. Rev.* 52 (11) (2023) 3873–3926.
- [80] X. Yang, C. Li, P. Li, Q. Fu, Ratiometric optical probes for biosensing, *Theranostics* 13 (8) (2023) 2632–2656.
- [81] D.B. Sung, J.S. Lee, Natural-product-based fluorescent probes: recent advances and applications, *RSC Med. Chem.* 14 (3) (2023) 412–432.
- [82] Y. Yang, F. Gao, Y. Wang, H. Li, J. Zhang, Z. Sun, Y. Jiang, Fluorescent organic small molecule probes for bioimaging and detection applications, *Molecules* 27 (23) (2022) 8421.
- [83] B. Chen, Q. Yan, D. Li, J. Xie, Degradation mechanism and development of detection technologies of ATP-related compounds in aquatic products: recent advances and remaining challenges, *Crit. Rev. Food. Sci. Nutr.* (2023) 1–22.
- [84] L. Sun, H. Liu, Y. Ye, Y. Lei, R. Islam, S. Tan, R. Tong, Y.B. Miao, L. Cai, Smart nanoparticles for cancer therapy, *Signal Transduct. Target Ther.* 8 (1) (2023) 418.
- [85] A. Doustmanian, M. Fathi, M. Mazloomi, A. Salemi, M.R. Hamblin, R. Jahanban-Esfahlan, Molecular targets, therapeutic agents and multitasking nanoparticles to deal with cancer stem cells: a narrative review, *J. Control Release* 363 (2023) 57–83.
- [86] R.J. Hickman, P. Bannigan, Z. Bao, A. Aspuru-Guzik, C. Allen, Self-driving laboratories: a paradigm shift in nanomedicine development, *Matter* 6 (4) (2023) 1071–1081.
- [87] C. Fang, J. An, A. Bruno, X. Cai, J. Fan, J. Fujimoto, R. Golfieri, X. Hao, H. Jiang, L.R. Jiao, A.V. Kulkarni, H. Lang, C.R.A. Lesmana, Q. Li, L. Liu, Y. Liu, W. Lau, Q. Lu, K. Man, H. Maruyama, C. Mosconi, N. Ormeci, M. Pavlides, G. Rezende, J. H. Sohn, S. Treeprasertsuk, V. Vilgrain, H. Wen, S. Wen, X. Quan, R. Ximenes, Y. Yang, B. Zhang, W. Zhang, P. Zhang, S. Zhang, X. Qi, Consensus recommendations of three-dimensional visualization for diagnosis and management of liver diseases, *Hepatol. Int.* 14 (4) (2020) 437–453.
- [88] A.G. Hayes, P. Corlies, C. Tate, M. Barrington, J.F. Bell, J.N. Maki, M. Caplinger, M. Ravine, K.M. Kinch, K. Herkenhoff, B. Horgan, J. Johnson, M. Lemmon, G. Paar, M.S. Rice, E. Jensen, T.M. Kubacki, E. Cloutis, R. Deen, B.L. Ehlmann, E. Lakdawalla, R. Sullivan, A. Winhold, A. Parkinson, Z. Bailey, J. van Beek, P. Caballo-Perucha, E. Cisneros, D. Dixon, C. Donaldson, O.B. Jensen, J. Kuik, K. Lapo, A. Magee, M. Merusi, J. Mollerup, N. Scudder, C. Seeger, E. Stanish, M. Starr, M. Thompson, N. Turenne, K. Winchell, Pre-flight calibration of the mars 2020 rover mastcam zoom (Mastcam-Z) multispectral, stereoscopic imager, *Space Sci. Rev.* 217 (2) (2021) 29.
- [89] J. Albers, S. Pacile, M.A. Markus, M. Wiart, G. Vande Velde, G. Tromba, C. Dullin, X-ray-Based 3D virtual histology—adding the next dimension to histological analysis, *Mol. Imaging. Biol.* 20 (5) (2018) 732–741.
- [90] F. Hide, M.A. Diaz-Garcia, B.J. Schwartz, A.J. Heeger, New developments in the photonic applications of conjugated polymers, *Acc. Chem. Res.* 30 (10) (1997) 430–436.
- [91] J. Liu, X. Fang, Z. Liu, R. Li, Y. Yang, Y. Sun, Z. Zhao, C. Wu, Expansion microscopy with multifunctional polymer dots, *Adv. Mater.* 33 (25) (2021) e2007854.
- [92] C. Li, G. Chen, Y. Zhang, F. Wu, Q. Wang, Advanced fluorescence imaging technology in the near-infrared-II window for biomedical applications, *J. Am. Chem. Soc.* 142 (35) (2020) 14789–14804.
- [93] J. Huang, X. Chen, Y. Jiang, C. Zhang, S. He, H. Wang, K. Pu, Renal clearable polyfluorophore nanosensors for early diagnosis of cancer and allograft rejection, *Nat. Mater.* 21 (5) (2022) 598–607.
- [94] C. Yin, X. Zhen, H. Zhao, Y. Tang, Y. Ji, Y. Lyu, Q. Fan, W. Huang, K. Pu, Amphiphilic semiconducting oligomers for near-infrared photoacoustic and fluorescence imaging, *ACS Appl. Mater. Interfaces* 9 (14) (2017) 12332–12339.
- [95] Y. Lyu, D. Cui, J. Huang, W. Fan, Y. Miao, K. Pu, Near-infrared afterglow semiconducting nano-polycomplexes for the multiplex differentiation of cancer exosomes, *Angew. Chem. Int. Ed. Engl.* 58 (15) (2019) 4983–4987.
- [96] M. Zhang, J. Liu, G. Wang, Highly biocompatible nanoparticles of Au@ fluorescent polymers as novel contrast agent for in vivo bimodality NIR fluorescence/CT imaging, *Contrast Media Mol. Imaging* 2019 (2019) 8085039.
- [97] W. Sun, S. Hayden, Y. Jin, Y. Rong, J. Yu, F. Ye, Y.H. Chan, M. Zeigler, C. Wu, D. T. Chiu, A versatile method for generating semiconducting polymer dot nanocomposites, *Nanoscale* 4 (22) (2012) 7246–7249.
- [98] Y. Rong, J. Yu, X. Zhang, W. Sun, F. Ye, I.C. Wu, Y. Zhang, S. Hayden, Y. Zhang, C. Wu, D.T. Chiu, Yellow fluorescent semiconducting polymer dots with high brightness, small size, and narrow emission for biological applications, *ACS Macro. Lett.* 3 (10) (2014) 1051–1054.
- [99] Y. Feng, N. Wang, H. Ju, Highly efficient electrochemiluminescence of cyanovinylene-contained polymer dots in aqueous medium and its application in imaging analysis, *Anal. Chem.* 90 (2) (2018) 1202–1208.
- [100] J. Li, D. Cui, J. Huang, S. He, Z. Yang, Y. Zhang, Y. Luo, K. Pu, Organic semiconducting pro-nanostimulants for near-infrared photoactivatable cancer immunotherapy, *Angew. Chem. Int. Ed. Engl.* 58 (36) (2019) 12680–12687.
- [101] H. Chen, J. Yu, X. Men, J. Zhang, Z. Ding, Y. Jiang, C. Wu, D.T. Chiu, Reversible ratiometric NADH sensing using semiconducting polymer dots, *Angew. Chem. Int. Ed. Engl.* 60 (21) (2021) 12007–12012.
- [102] X. Men, F. Wang, H.B. Chen, Y.B. Liu, X.X. Men, Y. Yuan, Z. Zhang, D.Y. Gao, C. F. Wu, Z. Yuan, Ultrasmall semiconducting polymer dots with rapid clearance for second near-infrared photoacoustic imaging and photothermal cancer therapy, *Adv. Funct. Mater.* 30 (24) (2020) 1909673.
- [103] H. Chen, J. Zhang, K. Chang, X. Men, X. Fang, L. Zhou, D. Li, D. Gao, S. Yin, X. Zhang, Z. Yuan, C. Wu, Highly absorbing multispectral near-infrared polymer nanoparticles from one conjugated backbone for photoacoustic imaging and photothermal therapy, *Biomaterials* 144 (2017) 42–52.
- [104] Y. Han, T. Chen, Y. Li, L. Chen, L. Wei, L. Xiao, Single-particle enumeration-based sensitive glutathione S-transferase assay with fluorescent conjugated polymer nanoparticle, *Anal. Chem.* 91 (17) (2019) 11146–11153.
- [105] Y. Zhang, L. Pang, C. Ma, Q. Tu, R. Zhang, E. Saeed, A.E. Mahmoud, J. Wang, Small molecule-initiated light-activated semiconducting polymer dots: an integrated nanoplateform for targeted photodynamic therapy and imaging of cancer cells, *Anal. Chem.* 86 (6) (2014) 3092–3099.
- [106] F. Luo, M. Zhu, Y. Liu, J. Sun, F. Gao, Ratiometric and visual determination of copper ions with fluorescent nanohybrids of semiconducting polymer nanoparticles and carbon dots, *Spectrochim. Acta A Mol. Biomol. Spectrosc.* 295 (2023) 122574.
- [107] B. McCarthy, A. Cudykier, R. Singh, N. Levi-Polyachenko, S. Soker, Semiconducting polymer nanoparticles for photothermal ablation of colorectal cancer organoids, *Sci. Rep.* 11 (1) (2021) 1532.
- [108] E. McCabe-Lankford, B. McCarthy, M.A. Berwick, K. Salafian, L. Galarza-Paez, S. Sarkar, J. Sloop, G. Donati, A.J. Brown, N. Levi-Polyachenko, Binding of targeted semiconducting photothermal polymer nanoparticles for intraperitoneal detection and treatment of colorectal cancer, *Nanotheranostics* 4 (3) (2020) 107–118.

- [109] N. Wang, L. Chen, W. Chen, H. Ju, Potential- and color-resolved electrochemiluminescence of polymer dots for array imaging of multiplex MicroRNAs, *Anal. Chem.* 93 (12) (2021) 5327–5333.
- [110] X. Shi, Q. Li, C. Zhang, H. Pei, G. Wang, H. Zhou, L. Fan, K. Yang, B. Jiang, F. Wang, R. Zhu, Semiconducting polymer nano-radiotherapeutic for combined radio-photothermal therapy of pancreatic tumor, *J. Nanobiotechnology* 19 (1) (2021) 337.
- [111] H. Lu, C.H. Chang, B.R. Wu, N.C. Wu, J.Z. Liang, C.A. Dai, A.C. Yang, Reaching nearly 100% quantum efficiencies in thin solid films of semiconducting polymers via molecular confinements under large segmental stresses, *ACS Nano* 16 (5) (2022) 8273–8282.
- [112] N. Zhang, Z.Y. Zhao, H. Gao, Y. Yu, J.B. Pan, H.Y. Chen, J.J. Xu, An ultrasensitive electrochemiluminescence assay for nucleic acid detection based on carboxyl functionalized polymer dots, *J. Electroanal. Chem.* 900 (2021) 115743.
- [113] G. Song, X. Zheng, Y. Wang, X. Xia, S. Chu, J. Rao, A magneto-optical nanoplatform for multimodality imaging of tumors in mice, *ACS Nano* 13 (7) (2019) 7750–7758.
- [114] D. Chen, W. Qi, Y. Liu, Y. Yang, T. Shi, Y. Wang, X. Fang, Y. Wang, L. Xi, C. Wu, Near-infrared II semiconducting polymer dots: chain packing modulation and high-contrast vascular imaging in deep tissues, *ACS Nano* 17 (17) (2023) 17082–17094.
- [115] X. Zhang, J. Yu, Y. Rong, F. Ye, D.T. Chiu, K. Uvdal, High-intensity near-IR fluorescence in semiconducting polymer dots achieved by cascade FRET strategy, *Chem. Sci.* 4 (5) (2013) 2143–2151.
- [116] S.Y. Liou, C.S. Ke, J.H. Chen, Y.W. Luo, S.Y. Kuo, Y.H. Chen, C.C. Fang, C.Y. Wu, C.M. Chiang, Y.H. Chan, Tuning the emission of semiconducting polymer dots from green to near-infrared by alternating donor monomers and their applications for *in vivo* biological imaging, *ACS Macro. Lett.* 5 (1) (2016) 154–157.
- [117] Y. Liu, J.F. Liu, D.D. Chen, X.S. Wang, Z.B. Liu, H. Liu, L.H. Jiang, C.F. Wu, Y. P. Zou, Quinoxaline-based semiconducting polymer dots for *in vivo* NIR-II fluorescence imaging, *Macromolecules* 52 (15) (2019) 5735–5740.
- [118] Z. Xie, Y. Yang, Y. He, C. Shu, D. Chen, J. Zhang, J. Chen, C. Liu, Z. Sheng, H. Liu, J. Liu, X. Gong, L. Song, S. Dong, *In vivo* assessment of inflammation in carotid atherosclerosis by noninvasive photoacoustic imaging, *Theranostics* 10 (10) (2020) 4694–4704.
- [119] H. Zhu, Y. Fang, Q. Miao, X. Qi, D. Ding, P. Chen, K. Pu, Regulating near-infrared photodynamic properties of semiconducting polymer nanotheranostics for optimized cancer therapy, *ACS Nano* 11 (9) (2017) 8998–9009.
- [120] H. Zhu, J. Li, X. Qi, P. Chen, K. Pu, Oxygenic hybrid semiconducting nanoparticles for enhanced photodynamic therapy, *Nano Lett.* 18 (1) (2018) 586–594.
- [121] Y. Zhang, F. Ye, W. Sun, J. Yu, I.C. Wu, Y. Rong, Y. Zhang, D.T. Chiu, Light-induced crosslinkable semiconducting polymer dots, *Chem. Sci.* 6 (3) (2015) 2102–2109.
- [122] K. Sun, Y. Yang, H. Zhou, S. Yin, W. Qin, J. Yu, D.T. Chiu, Z. Yuan, X. Zhang, C. Wu, Ultrabright polymer-dot transducer enabled wireless glucose monitoring via a smartphone, *ACS Nano* 12 (6) (2018) 5176–5184.
- [123] G. Hong, Y. Zou, A.L. Antaris, S. Diao, D. Wu, K. Cheng, X. Zhang, C. Chen, B. Liu, Y. He, J.Z. Wu, J. Yuan, B. Zhang, Z. Tao, C. Fukunaga, H. Dai, Ultrafast fluorescence imaging *in vivo* with conjugated polymer fluorophores in the second near-infrared window, *Nat. Commun.* 5 (2014) 4206.
- [124] Z. Ding, X. Dou, G. Wu, C. Wang, J. Xie, Nanoscale semiconducting polymer dots with rhodamine spirolactam as fluorescent sensor for mercury ions in living systems, *Talanta* 259 (2023) 124494.
- [125] K. Shou, Y. Tang, H. Chen, S. Chen, L. Zhang, A. Zhang, Q. Fan, A. Yu, Z. Cheng, Diketopyrrolopyrrole-based semiconducting polymer nanoparticles for *in vivo* second near-infrared window imaging and image-guided tumor surgery, *Chem. Sci.* 9 (12) (2018) 3105–3110.
- [126] M. Chen, Y. Yang, L. Tang, S. He, W. Guo, G. Ge, Z. Zeng, X. Li, G. Li, W. Xiong, S. X. Wu, Iron-rich semiconducting polymer dots for the combination of ferroptosis-starvation and phototherapeutic cancer therapy, *Adv. Healthc. Mater.* 12 (26) (2023) e2300839.
- [127] X. Men, H. Chen, C. Sun, Y. Liu, R. Wang, X. Zhang, C. Wu, Z. Yuan, Thermosensitive polymer dot nanocomposites for trimodal computed tomography/photoacoustic/fluorescence imaging-guided synergistic chemophotothermal therapy, *ACS Appl. Mater. Interfaces* 12 (46) (2020) 51174–51184.
- [128] X. Men, X. Geng, Z. Zhang, H. Chen, M. Du, Z. Chen, G. Liu, C. Wu, Z. Yuan, Biomimetic semiconducting polymer dots for highly specific NIR-II fluorescence imaging of glioma, *Mater. Today Bio* 16 (2022) 100383.
- [129] S. He, S. Wu, Ratiometric fluorescent semiconducting polymer dots for temperature sensing, *Analyst* 148 (4) (2023) 863–868.
- [130] C. Zheng, L. Ding, Y. Wu, X. Tan, Y. Zeng, X. Zhang, X. Liu, J. Liu, A near-infrared turn-on fluorescence probe for glutathione detection based on nanocomposites of semiconducting polymer dots and MnO<sub>2</sub> nanosheets, *Anal. Bioanal. Chem.* 412 (29) (2020) 8167–8176.
- [131] B. Zhang, F. Wang, H. Zhou, D. Gao, Z. Yuan, C. Wu, X. Zhang, Polymer dots compartmentalized in liposomes as a photocatalyst for *in situ* hydrogen therapy, *Angew. Chem. Int. Ed. Engl.* 58 (9) (2019) 2744–2748.
- [132] C. Riahin, A. Meares, N.N. Esemoto, M. Ptaszek, M. LaScola, N. Pandala, E. Lavik, M. Yang, G. Stacey, D. Hu, J.C. Traeger, G. Orr, Z. Rosenzweig, Hydroporphyrin-doped near-infrared-emitting polymer dots for cellular fluorescence imaging, *ACS Appl. Mater. Interfaces* 14 (18) (2022) 20790–20801.
- [133] M. Verma, Y.H. Chan, S. Saha, M.H. Liu, Recent developments in semiconducting polymer dots for analytical detection and NIR-II fluorescence imaging, *ACS Appl. Bio. Mater.* 4 (3) (2021) 2142–2159.
- [134] S. Li, K. Chang, K. Sun, Y. Tang, N. Cui, Y. Wang, W. Qin, H. Xu, C. Wu, Amplified singlet oxygen generation in semiconductor polymer dots for photodynamic cancer therapy, *ACS Appl. Mater. Interfaces* 8 (6) (2016) 3642–3644.
- [135] Y. Li, N. Zhang, W.W. Zhao, D.C. Jiang, J.J. Xu, H.Y. Chen, Polymer dots for photoelectrochemical bioanalysis, *Anal. Chem.* 89 (9) (2017) 4945–4950.
- [136] C.P. Chen, Y.C. Huang, S.Y. Liou, P.J. Wu, S.Y. Kuo, Y.H. Chan, Near-infrared fluorescent semiconducting polymer dots with high brightness and pronounced effect of positioning alkyl chains on the comonomers, *ACS Appl. Mater. Interfaces* 6 (23) (2014) 21585–21595.
- [137] Y.H. Chen, S.Y. Kuo, W.K. Tsai, C.S. Ke, C.H. Liao, C.P. Chen, Y.T. Wang, H. W. Chen, Y.H. Chan, Dual colorimetric and fluorescent imaging of latent fingerprints on both porous and nonporous surfaces with near-infrared fluorescent semiconducting polymer dots, *Anal. Chem.* 88 (23) (2016) 11616–11623.
- [138] W.K. Tsai, Y.S. Lai, P.J. Tseng, C.H. Liao, Y.H. Chan, Dual colorimetric and fluorescent authentication based on semiconducting polymer dots for anticonteering applications, *ACS Appl. Mater. Interfaces* 9 (36) (2017) 30918–30924.
- [139] F. Ye, C. Wu, Y. Jin, Y.H. Chan, X. Zhang, D.T. Chiu, Ratiometric temperature sensing with semiconducting polymer dots, *J. Am. Chem. Soc.* 133 (21) (2011) 8146–8149.
- [140] C.C. Fang, C.C. Chou, Y.Q. Yang, T. Wei-Kai, Y.T. Wang, Y.H. Chan, Multiplexed detection of tumor markers with multicolor polymer dot-based immunochromatography test strip, *Anal. Chem.* 90 (3) (2018) 2134–2140.
- [141] M. Ethirajan, Y. Chen, P. Joshi, R.K. Pandey, The role of porphyrin chemistry in tumor imaging and photodynamic therapy, *Chem. Soc. Rev.* 40 (1) (2011) 340–362.
- [142] W. Hou, Y. Yuan, Z. Sun, S. Guo, H. Dong, C. Wu, Ratiometric fluorescent detection of intracellular singlet oxygen by semiconducting polymer dots, *Anal. Chem.* 90 (24) (2018) 14629–14634.
- [143] J. Sun, H. Mei, S. Wang, F. Gao, Two-photon semiconducting polymer dots with dual-emission for ratiometric fluorescent sensing and bioimaging of tyrosinase activity, *Anal. Chem.* 88 (14) (2016) 7372–7377.
- [144] X. Dai, J. Ma, Q. Zhang, Q. Xu, L. Yang, F. Gao, Simultaneous inhibition of planktonic and biofilm bacteria by self-adapting semiconducting polymer dots, *J. Mater. Chem. B* 9 (33) (2021) 6658–6667.
- [145] C.T. Kuo, H.S. Peng, Y. Rong, J. Yu, W. Sun, B. Fujimoto, D.T. Chiu, Optically encoded semiconducting polymer dots with single-wavelength excitation for barcoding and tracking of single cells, *Anal. Chem.* 89 (11) (2017) 6232–6238.
- [146] X. Dou, Q. Wang, T. Zhu, Z. Ding, J. Xie, Construction of effective nanosensor by combining semiconducting polymer dots with diphenylcarbazide for specific recognition of trace Cr (VI) ion in water and vitro, *Nanomaterials* 12 (15) (2022) 2663.
- [147] Y. Jiang, J. Zhang, S.R. Jung, H. Chen, S. Xu, D.T. Chiu, High-precision mapping of membrane proteins on synaptic vesicles using spectrally encoded super-resolution imaging, *Angew. Chem. Int. Ed. Engl.* 62 (8) (2023) e202217889.
- [148] A.M. Hassan, X. Wu, J.W. Jarrett, S. Xu, J. Yu, D.R. Miller, E.P. Perillo, Y.L. Liu, D. T. Chiu, H.C. Yeh, A.K. Dunn, Polymer dots enable deep *in vivo* multiphoton fluorescence imaging of microvasculature, *Biomed. Opt. Express* 10 (2) (2019) 584–599.
- [149] C.S. Ke, C.C. Fang, J.Y. Yan, P.J. Tseng, J.R. Pyle, C.P. Chen, S.Y. Lin, J. Chen, X. Zhang, Y.H. Chan, Molecular engineering and design of semiconducting polymer dots with narrow-band, near-infrared emission for *in vivo* biological imaging, *ACS Nano* 11 (3) (2017) 3166–3177.
- [150] X. Chen, Z. Liu, R. Li, C. Shan, Z. Zeng, B. Xue, W. Yuan, C. Mo, P. Xi, C. Wu, Y. Sun, Multicolor super-resolution fluorescence microscopy with blue and carmine small photoblinking polymer dots, *ACS Nano* 11 (8) (2017) 8084–8091.
- [151] H.Y. Liu, P.J. Wu, S.Y. Kuo, C.P. Chen, E.H. Chang, C.Y. Wu, Y.H. Chan, Quinoxaline-based polymer dots with ultrabright red to near-infrared fluorescence for *in vivo* biological imaging, *J. Am. Chem. Soc.* 137 (32) (2015) 10420–10429.
- [152] J. Ou, H. Tan, Z. Chen, X. Chen, FRET-based semiconducting polymer dots for pH sensing, *Sensors* 19 (6) (2019).
- [153] I.C. Wu, J. Yu, F. Ye, Y. Rong, M.E. Gallina, B.S. Fujimoto, Y. Zhang, Y.H. Chan, W. Sun, X.H. Zhou, C. Wu, D.T. Chiu, Squaraine-based polymer dots with narrow, bright near-infrared fluorescence for biological applications, *J. Am. Chem. Soc.* 137 (1) (2015) 173–178.
- [154] L. Chen, L. Wu, J. Yu, C.T. Kuo, T. Jian, I.C. Wu, Y. Rong, D.T. Chiu, Highly photostable wide-dynamic-range pH sensitive semiconducting polymer dots enabled by dendronizing the near-IR emitters, *Chem. Sci.* 8 (10) (2017) 7236–7245.
- [155] Z. Zhang, Y. Yuan, Z. Liu, H. Chen, D. Chen, X. Fang, J. Zheng, W. Qin, C. Wu, Brightness enhancement of near-infrared semiconducting polymer dots for *in vivo* whole-body cell tracking in deep organs, *ACS Appl. Mater. Interfaces* 10 (32) (2018) 26928–26935.
- [156] Z. Hashim, M. Green, P.H. Chung, K. Suhling, A. Prott, A. Phinikaridou, R. Botnar, R.A. Khanbeigi, M. Thanou, L.A. Dailey, N.J. Commander, C. Rowland, J. Scott, D. Jenner, Gd-containing conjugated polymer nanoparticles: bimodal nanoparticles for fluorescence and MRI imaging, *Nanoscale* 6 (14) (2014) 8376–8386.
- [157] Y.H. Chan, C. Wu, F. Ye, Y. Jin, P.B. Smith, D.T. Chiu, Development of ultrabright semiconducting polymer dots for ratiometric pH sensing, *Anal. Chem.* 83 (4) (2011) 1448–1455.
- [158] W.B. Wu, G.X. Feng, S.D. Xu, B. Liu, A photostable far-red/near-infrared conjugated polymer photosensitizer with aggregation-induced emission for image-guided cancer cell ablation, *Macromolecules* 49 (14) (2016) 5017–5025.

- [159] M.H. Liu, Z. Zhang, Y.C. Yang, Y.H. Chan, Polymethine-based semiconducting polymer dots with narrow-band emission and absorption/emission maxima at NIR-II for bioimaging, *Angew. Chem. Int. Ed. Engl.* 60 (2) (2021) 983–989.
- [160] M.H. Liu, T.C. Chen, J.R. Vicente, C.N. Yao, Y.C. Yang, C.P. Chen, P.W. Lin, Y. C. Ho, J. Chen, S.Y. Lin, Y.H. Chan, Cyanine-based polymer dots with long-wavelength excitation and near-infrared fluorescence beyond 900 nm for in vivo biological imaging, *ACS Appl. Bio. Mater.* 3 (6) (2020) 3846–3858.
- [161] M.H. Elsayed, M. Abdellah, Y.H. Hung, J. Jayakumar, L.Y. Ting, A.M. Elewa, C. L. Chang, W.C. Lin, K.L. Wang, M. Abdel-Hafiez, H.W. Hung, M. Horie, H.H. Chou, Hydrophobic and hydrophilic conjugated polymer dots as binary photocatalysts for enhanced visible-light-driven hydrogen evolution through forster resonance energy transfer, *ACS Appl. Mater. Interfaces* 13 (47) (2021) 56554–56565.
- [162] J. Sun, S. Wang, F. Gao, Covalent surface functionalization of semiconducting polymer dots with beta-cyclodextrin for fluorescent ratiometric assay of cholesterol through host-guest inclusion and FRET, *Langmuir* 32 (48) (2016) 12725–12731.
- [163] L. Xiong, A.J. Shuhendler, J. Rao, Self-luminescing BRET-FRET near-infrared dots for in vivo lymph-node mapping and tumour imaging, *Nat. Commun.* 3 (2012) 1193.
- [164] Y. Lyu, X. Zhen, Y. Miao, K. Pu, Reaction-based semiconducting polymer nanoprobes for photoacoustic imaging of protein sulfenic acids, *ACS Nano* 11 (1) (2017) 358–367.
- [165] Y. Jiang, P.K. Upputuri, C. Xie, Y. Lyu, L. Zhang, Q. Xiong, M. Pramanik, K. Pu, Broadband absorbing semiconducting polymer nanoparticles for photoacoustic imaging in second near-infrared window, *Nano Lett.* 17 (8) (2017) 4964–4969.
- [166] X. Zhen, C. Xie, Y. Jiang, X. Ai, B. Xing, K. Pu, Semiconducting photothermal nanoagonist for remote-controlled specific cancer therapy, *Nano Lett.* 18 (2) (2018) 1498–1505.
- [167] X. Zhen, C. Zhang, C. Xie, Q. Miao, K.L. Lim, K. Pu, Intraparticle energy level alignment of semiconducting polymer nanoparticles to amplify chemiluminescence for ultrasensitive in vivo imaging of reactive oxygen species, *ACS Nano* 10 (6) (2016) 6400–6409.
- [168] Y. Jiang, P.K. Upputuri, C. Xie, Z. Zeng, A. Sharma, X. Zhen, J. Li, J. Huang, M. Pramanik, K. Pu, Metabolizable semiconducting polymer nanoparticles for second near-infrared photoacoustic imaging, *Adv. Mater.* 31 (11) (2019) e1808166.
- [169] D. Cui, J. Li, X. Zhao, K. Pu, R. Zhang, Semiconducting polymer nanoreporters for near-infrared chemiluminescence imaging of immunoactivation, *Adv. Mater.* 32 (6) (2020) e1906314.
- [170] Q. Miao, C. Xie, X. Zhen, Y. Lyu, H. Duan, X. Liu, J.V. Jokerst, K. Pu, Molecular afterglow imaging with bright, biodegradable polymer nanoparticles, *Nat. Biotechnol.* 35 (11) (2017) 1102–1110.
- [171] A. Creamer, A.L. Fiego, A. Agliano, L. Prados-Martin, H. Hogset, A. Najer, D. A. Richards, J.P. Wojciechowski, J.E.J. Foote, N. Kim, A. Monahan, J. Tang, A. Shamsabadi, L.N.C. Rochet, I.A. Thanasi, L.R. de la Ballina, C.L. Rapley, S. Turnock, E.A. Love, L. Bugeon, M.J. Dallman, M. Heeney, G. Kramer-Marek, V. Chudasama, F. Fenaroli, M.M. Stevens, Modular synthesis of semiconducting graft copolymers to achieve "clickable" fluorescent nanoparticles with long circulation and specific cancer targeting, *Adv. Mater.* (2023) e2300413, <https://doi.org/10.1002/adma.202300413>.
- [172] P.J. Wu, J.L. Chen, C.P. Chen, Y.H. Chan, Photoactivated ratiometric copper(II) ion sensing with semiconducting polymer dots, *Chem. Commun.* 49 (9) (2013) 898–900.
- [173] C. Xie, X. Zhen, Q. Miao, Y. Lyu, K. Pu, Self-assembled semiconducting polymer nanoparticles for ultrasensitive near-infrared afterglow imaging of metastatic tumors, *Adv. Mater.* 30 (21) (2018) e1801331.
- [174] K.F. Hsu, S.P. Su, H.F. Lu, M.H. Liu, Y.J. Chang, Y.J. Lee, H.K. Chiang, C.P. Hsu, C. W. Lu, Y.H. Chan, TADF-based NIR-II semiconducting polymer dots for in vivo 3D bone imaging, *Chem. Sci.* 13 (34) (2022) 10074–10081.
- [175] Y.C. Huang, C.P. Chen, P.J. Wu, S.Y. Kuo, Y.H. Chan, Coumarin dye-embedded semiconducting polymer dots for ratiometric sensing of fluoride ions in aqueous solution and bio-imaging in cells, *J. Mater. Chem. B* 2 (37) (2014) 6188–6191.
- [176] C. Wu, J. McNeill, Swelling-controlled polymer phase and fluorescence properties of polyfluorene nanoparticles, *Langmuir* 24 (11) (2008) 5855–5861.
- [177] J. Zhang, J. Yu, Y. Jiang, D.T. Chiu, Ultrabright Pdots with a large absorbance cross section and high quantum yield, *ACS Appl. Mater. Interfaces* 14 (11) (2022) 13631–13637.
- [178] J.C. Yang, Y.C. Ho, Y.H. Chan, Ultrabright fluorescent polymer dots with thermochromic characteristics for full-color security marking, *ACS Appl. Mater. Interfaces* 11 (32) (2019) 29341–29349.
- [179] A. Chabok, M. Shamsipur, A. Yeganeh-Faal, F. Molaabasi, K. Molaei, M. Sarparast, A highly selective semiconducting polymer dots-based "off-on" fluorescent nanoprobe for iron, copper and histidine detection and imaging in living cells, *Talanta* 194 (2019) 752–762.
- [180] Z. Zhang, Y. Wu, N. Lin, S. Yin, Z. Meng, Monitoring clinical-pathological grading of hepatocellular carcinoma using MicroRNA-guided semiconducting polymer dots, *ACS Appl. Mater. Interfaces* 14 (6) (2022) 7717–7730.
- [181] Y. Jiang, K. Pu, Molecular fluorescence and photoacoustic imaging in the second near-infrared optical window using organic contrast agents, *Adv. Biosyst.* 2 (5) (2018) e1700262.
- [182] G.S. Hong, A.L. Antaris, H.J. Dai, Near-infrared fluorophores for biomedical imaging, *Nature Biomedical Engineering* 1 (1) (2017).
- [183] Y. Duan Kenry, B. Liu, Recent advances of optical imaging in the second near-infrared window, *Adv. Mater.* 30 (47) (2018) e1802394.
- [184] R. Dutta, A. Bala, A. Sen, M.R. Spinazze, H. Park, W. Choi, Y. Yoon, S. Kim, Optical enhancement of indirect bandgap 2D transition metal dichalcogenides for multi-functional optoelectronic sensors, *Adv. Mater.* 35 (46) (2023) e2303272.
- [185] T. Yan, M. Su, Z. Wang, J. Zhang, Second near-infrared plasmonic nanomaterials for photoacoustic imaging and photothermal therapy, *Small* 19 (30) (2023) e2300539.
- [186] Y. Naciri, A. Hsini, Z. Ajmal, J.A. Navio, B. Bakiz, A. Albourine, M. Ezahri, A. Benlhachemi, Recent progress on the enhancement of photocatalytic properties of BiPO(4) using pi-conjugated materials, *Adv. Colloid Interface Sci.* 280 (2020) 102160.
- [187] A. Alo, L.W.T. Barros, G. Nagamine, J.C. Lemus, J. Planelles, J.L. Movilla, J. I. Clemente, H.J. Lee, W.K. Bae, L.A. Padilha, Beyond universal volume scaling: tailoring two-photon absorption in nanomaterials by heterostructure design, *Nano Lett.* 23 (15) (2023) 7180–7187.
- [188] H.S. Ra, S.H. Lee, S.J. Jeong, S. Cho, J.S. Lee, Advances in heterostructures for optoelectronic devices: materials, properties, conduction mechanisms, device applications, *Small Methods* (2023) e2300245.
- [189] L.X. Zhang, M.Y. Qi, Z.R. Tang, Y.J. Xu, Heterostructure-engineered semiconductor quantum dots toward photocatalyzed-redox cooperative coupling reaction, *Research* 6 (2023) 73.
- [190] H. Yan, Z. Chen, Y. Zheng, C. Newman, J.R. Quinn, F. Dotz, M. Kastler, A. Facchetti, A high-mobility electron-transporting polymer for printed transistors, *Nature* 457 (7230) (2009) 679–686.
- [191] S. Gunes, H. Neugebauer, N.S. Sariciftci, Conjugated polymer-based organic solar cells, *Chem. Rev.* 107 (4) (2007) 1324–1338.
- [192] A. Liu, S. Wang, H. Song, Y. Liu, L. Gedda, K. Edwards, L. Hammarstrom, H. Tian, Excited-state and charge-carrier dynamics in binary conjugated polymer dots towards efficient photocatalytic hydrogen evolution, *Phys. Chem. Chem. Phys.* 25 (4) (2023) 2935–2945.
- [193] Y.X. Li, S.P. Su, C.H. Yang, M.H. Liu, P.H. Lo, Y.C. Chen, C.P. Hsu, Y.J. Lee, H. K. Chiang, Y.H. Chan, Molecular design of ultrabright semiconducting polymer dots with high NIR-II fluorescence for 3D tumor mapping, *Adv. Healthc. Mater.* 10 (24) (2021) e2100993.
- [194] S. Zhu, R. Tian, A.L. Antaris, X. Chen, H. Dai, Near-infrared-II molecular dyes for cancer imaging and surgery, *Adv. Mater.* 31 (24) (2019) e1900321.
- [195] J. Ouyang, L. Sun, Z. Zeng, C. Zeng, F. Zeng, S. Wu, Nanoaggregate probe for breast cancer metastasis through multispectral optoacoustic tomography and aggregation-induced NIR-I/II fluorescence imaging, *Angew. Chem. Int. Ed. Engl.* 59 (25) (2020) 10111–10121.
- [196] Y. Su, B. Yu, S. Wang, H. Cong, Y. Shen, NIR-II bioimaging of small organic molecule, *Biomaterials* 271 (2021) 120717.
- [197] F. Ding, Y. Zhan, X. Lu, Y. Sun, Recent advances in near-infrared II fluorophores for multifunctional biomedical imaging, *Chem. Sci.* 9 (19) (2018) 4370–4380.
- [198] X. Zhang, S. Bloch, W. Akers, S. Achilefu, Near-infrared molecular probes for in vivo imaging, *Curr. Protoc. Cytom.* Chapter 12 (2012). Unit12 27.
- [199] F. Ding, Y. Fan, Y. Sun, F. Zhang, Beyond 1000 nm emission wavelength: recent advances in organic and inorganic emitters for deep-tissue molecular imaging, *Adv. Healthc. Mater.* 8 (14) (2019) e1900260.
- [200] M. Beija, C.A. Afonso, J.M. Martinho, Synthesis and applications of Rhodamine derivatives as fluorescent probes, *Chem. Soc. Rev.* 38 (8) (2009) 2410–2433.
- [201] S. Zeng, X. Liu, Y.S. Kafutti, H. Kim, J. Wang, X. Peng, H. Li, J. Yoon, Fluorescent dyes based on rhodamine derivatives for bioimaging and therapeutics: recent progress, challenges, and prospects, *Chem. Soc. Rev.* 52 (16) (2023) 5607–5651.
- [202] M. Sibrian-Vazquez, J.O. Escobedo, M. Lowry, R.M. Strongin, Progress toward red and near-infrared (NIR) emitting saccharide sensors, *Pure Appl. Chem.* 84 (11) (2012) 2443–2456.
- [203] J.B. Grimm, A.N. Tkachuk, L. Xie, H. Choi, B. Mohar, N. Falco, K. Schaefer, R. Patel, Q. Zheng, Z. Liu, J. Lippincott-Schwartz, T.A. Brown, L.D. Lavis, A general method to optimize and functionalize red-shifted rhodamine dyes, *Nat. Methods* 17 (8) (2020) 815–821.
- [204] X. Zhou, R. Lai, J.R. Beck, H. Li, C.I. Stains, Nebraska Red: a phosphinate-based near-infrared fluorophore scaffold for chemical biology applications, *Chem. Commun.* 52 (83) (2016) 12290–12293.
- [205] M. Dai, H. Lee, Y.J. Yang, M. Santra, C.W. Song, Y.W. Jun, Y.J. Reo, W.J. Kim, K. H. Ahn, Synthesis of near-infrared-emitting benzorhodamines and their applications to bioimaging and photothermal therapy, *Chemistry* 26 (50) (2020) 11549–11557.
- [206] L.G. Wang, I. Munhenzva, M. Sibrian-Vazquez, J.O. Escobedo, C.H. Kitts, F. R. Fronczek, R.M. Strongin, Altering fundamental trends in the emission of xanthene dyes, *J. Org. Chem.* 84 (5) (2019) 2585–2595.
- [207] Y. Jung, J. Jung, Y. Huh, D. Kim, Benzo[g]coumarin-Based fluorescent probes for bioimaging applications, *J. Anal. Methods Chem.* 2018 (2018) 5249765.
- [208] H.N. Lv, P.F. Tu, Y. Jiang, Benzocoumarins: isolation, synthesis, and biological activities, *Mini Rev. Med. Chem.* 14 (7) (2014) 603–622.
- [209] L. Han, R. Kang, X. Zu, Y. Cui, J. Gao, Novel coumarin sensitizers based on 2-(thiophen-2-yl)thiazole pi-bridge for dye-sensitized solar cells, *Photochem. Photobiol. Sci.* 14 (11) (2015) 2046–2053.
- [210] H.J. Feng, R.R. Li, Y.C. Song, X.Y. Li, B. Liu, Novel D-π-A-π-A coumarin dyes for highly efficient dye-sensitized solar cells: effect of π-bridge on optical, electrochemical, and photovoltaic performance, *Journal of Power Sources* 345 (2017) 59–66.
- [211] K.C. Avhad, D.S. Patil, Y.K. Gawale, S. Chitrambalam, M.C. Sreenath, I.H. Joe, N. Sekar, Large Stokes shifted far-red to NIR-emitting D-π-A coumarins: combined synthesis, experimental, and computational investigation of spectroscopic and non-linear optical properties, *ChemistrySelect* 3 (16) (2018) 4393–4405.

- [212] S. Singha, D. Kim, B. Roy, S. Sambasivan, H. Moon, A.S. Rao, J.Y. Kim, T. Joo, J. W. Park, Y.M. Rhee, T. Wang, K.H. Kim, Y.H. Shin, J. Jung, K.H. Ahn, A structural remedy toward bright dipolar fluorophores in aqueous media, *Chem. Sci.* 6 (7) (2015) 4335–4342.
- [213] Y. Zhang, C. Roux, A. Rouchaud, A. Meddahi-Pelle, V. Gueguen, C. Mangeney, F. Sun, G. Pavon-Djavid, Y. Luo, Recent advances in Fe-based bioresorbable stents: materials design and biosafety, *Bioact. Mater.* 31 (2024) 333–354.
- [214] W. Guo, M. Chen, Y. Yang, G. Ge, L. Tang, S. He, Z. Zeng, X. Li, G. Li, W. Xiong, S. Wu, Biocompatibility and biological effects of surface-modified conjugated polymer nanoparticles, *Molecules* 28 (5) (2023).
- [215] Y. Luo, Y. Han, X. Hu, M. Yin, C. Wu, Q. Li, N. Chen, Y. Zhao, Live-cell imaging of octaarginine-modified polymer dots via single particle tracking, *Cell Prolif* 52 (2) (2019) e12556.
- [216] J.V. Carratala, A. Aris, E. Garcia-Fruitos, N. Ferrer-Miralles, Design strategies for positively charged endolysins: insights into Artlysin development, *Biotechnol. Adv.* 69 (2023) 108250.
- [217] L. Miao, Y. Wei, X. Lu, M. Jiang, Y. Liu, P. Li, Y. Ren, H. Zhang, W. Chen, B. Han, W. Lu, Interaction of 2D nanomaterial with cellular barrier: membrane attachment and intracellular trafficking, *Adv. Drug Deliv. Rev.* 204 (2024) 115131.
- [218] M.E. Rad, C. Soylukan, P.K. Kulabhusan, B.N. Gunaydin, M. Yuce, Material and design toolkit for drug delivery: state of the art, trends, and challenges, *ACS Appl. Mater. Interfaces* 15 (48) (2023) 55201–55231.
- [219] K. Chang, Z. Liu, H. Chen, L. Sheng, S.X. Zhang, D.T. Chiu, S. Yin, C. Wu, W. Qin, Conjugated polymer dots for ultra-stable full-color fluorescence patterning, *Small* 10 (21) (2014) 4270–4275.
- [220] L. Guo, J. Ge, P. Wang, Polymer dots as effective phototheranostic agents, *Photochem. Photobiol.* 94 (5) (2018) 916–934.
- [221] C. Wu, T. Schneider, M. Zeigler, J. Yu, P.G. Schiro, D.R. Burnham, J.D. McNeill, D. T. Chiu, Bioconjugation of ultrabright semiconducting polymer dots for specific cellular targeting, *J. Am. Chem. Soc.* 132 (43) (2010) 15410–15417.
- [222] X. Shen, D. Pan, Q. Gong, Z. Gu, K. Luo, Enhancing drug penetration in solid tumors via nanomedicine: evaluation models, strategies and perspectives, *Bioact. Mater.* 32 (2024) 445–472.
- [223] M. Singh, B.K. Jana, P. Pal, I. Singha, A. Rajkumari, P. Chowrasia, V. Nath, B. Mazumder, Nanoparticles in pancreatic cancer therapy: a detailed and elaborated review on patent literature, *Expert. Opin. Ther. Pat.* 33 (10) (2023) 681–699.
- [224] Q. Zhou, J. Xiang, N. Qiu, Y. Wang, Y. Piao, S. Shao, J. Tang, Z. Zhou, Y. Shen, Tumor Abnormality-Oriented Nanomedicine Design, *Chem. Rev.* 123 (18) (2023) 10920–10989.
- [225] S. Guo, D. Gu, Y. Yang, J. Tian, X. Chen, Near-infrared photodynamic and photothermal co-therapy based on organic small molecular dyes, *J. Nanobiotechnology* 21 (1) (2023) 348.
- [226] X. Bai, K. Wang, L. Chen, J. Zhou, J. Wang, Semiconducting polymer dots as fluorescent probes for in vitro biosensing, *J. Mater. Chem. B* 10 (33) (2022) 6248–6262.
- [227] Z. Zhang, Y. Wu, Z. Xuan, H. Xu, S. Yin, Z. Meng, Self-assembly of three-dimensional liver organoids: virtual reconstruction via endocytosed polymer dots for refactoring the fine structure, *Biomater. Sci.* 11 (24) (2023) 7867–7883.
- [228] Y. Yuan, Z. Zhang, W. Hou, W. Qin, Z. Meng, C. Wu, In vivo dynamic cell tracking with long-wavelength excitable and near-infrared fluorescent polymer dots, *Biomaterials* 254 (2020) 120139.
- [229] D. Chen, Q. Li, Z. Meng, L. Guo, Y. Tang, Z. Liu, S. Yin, W. Qin, Z. Yuan, X. Zhang, C. Wu, Bright polymer dots tracking stem cell engraftment and migration to injured mouse liver, *Theranostics* 7 (7) (2017) 1820–1834.
- [230] G. Aguilar-Hernandez, B.A. Lopez-Romero, M. Nicolas-Garcia, Y. Nolasco-Gonzalez, H.S. Garcia-Galindo, E. Montalvo-Gonzalez, Nanosuspensions as carriers of active ingredients: chemical composition, development methods, and their biological activities, *Food Res. Int.* 174 (Pt 1) (2023) 113583.
- [231] H. Sajjad, A. Sajjad, R.T. Hayat, M.M. Khan, M. Zia, Copper oxide nanoparticles: in vitro and in vivo toxicity, mechanisms of action and factors influencing their toxicology, *Comp. Biochem. Physiol. C Toxicol. Pharmacol.* 271 (2023) 109682.
- [232] L. Xuan, Z. Ju, M. Skonieczna, P.K. Zhou, R. Huang, Nanoparticles-induced potential toxicity on human health: applications, toxicity mechanisms, and evaluation models, *MedComm* 4 (4) (2023) e327, 2020.
- [233] M. Qi, X. Wang, J. Chen, Y. Liu, Y. Liu, J. Jia, L. Li, T. Yue, L. Gao, B. Yan, B. Zhao, M. Xu, Transformation, absorption and toxicological mechanisms of silver nanoparticles in the gastrointestinal tract following oral exposure, *ACS Nano* 17 (10) (2023) 8851–8865.
- [234] N.H.A. Nguyen, P. Falagan-Lotsch, Mechanistic insights into the biological effects of engineered nanomaterials: a focus on gold nanoparticles, *Int. J. Mol. Sci.* 24 (4) (2023).
- [235] I. Nandi Shubhangi, S.K. Rai, P. Chandra, MOF-based nanocomposites as transduction matrices for optical and electrochemical sensing, *Talanta* 266 (Pt 2) (2024) 125124.
- [236] Z. Yang, J. Guo, L. Wang, J. Zhang, L. Ding, H. Liu, X. Yu, Nanozyme-enhanced electrochemical biosensors: mechanisms and applications, *Small* (2023) e2307815.
- [237] A. Klebes, H.C. Ates, R.D. Verboket, G.A. Urban, F. von Stetten, C. Dincer, S. M. Früh, Emerging multianalyte biosensors for the simultaneous detection of protein and nucleic acid biomarkers, *Biosens. Bioelectron.* 244 (2024) 115800.
- [238] A.V. Kalinichev, S.E. Zieger, K. Koren, Optical sensors (optodes) for multiparameter chemical imaging: classification, challenges, and prospects, *Analyst* 149 (1) (2023) 29–45.
- [239] T. Sun, B. Feng, J. Huo, Y. Xiao, W. Wang, J. Peng, Z. Li, C. Du, W. Wang, G. Zou, L. Liu, Artificial intelligence meets flexible sensors: emerging smart flexible sensing systems driven by machine learning and artificial synapses, *Nanomicro. Lett.* 16 (1) (2023) 14.
- [240] E. Beswick, T. Fawcett, Z. Hassan, D. Forbes, R. Dakin, J. Newton, S. Abrahams, A. Carson, S. Chandran, D. Perry, S. Pal, A systematic review of digital technology to evaluate motor function and disease progression in motor neuron disease, *J. Neurol.* 269 (12) (2022) 6254–6268.
- [241] Y. Yuan, B. Liu, H. Li, M. Li, Y. Song, R. Wang, T. Wang, H. Zhang, Flexible wearable sensors in medical monitoring, *Biosensors* 12 (12) (2022) 1069.
- [242] T. Naghd, S. Ardalan, Z. Asghari Adib, A.R. Sharifi, H. Golmohammadi, Moving toward smart biomedical sensing, *Biosens. Bioelectron.* 223 (2023) 115009.
- [243] J. Zhang, M. Zhou, X. Li, Y. Fan, J. Li, K. Lu, H. Wen, J. Ren, Recent advances of fluorescent sensors for bacteria detection-A review, *Talanta* 254 (2023) 124133.
- [244] S.A. Patil, S. Grossman, R. Kenney, L.J. Balcer, S. Galetta, Where's the vision? The importance of visual outcomes in neurologic disorders: the 2021 H. Houston Merritt lecture, *Neurology* 100 (5) (2023) 244–253.
- [245] S. Akgonullu, A. Denizli, Plasmonic nanosensors for pharmaceutical and biomedical analysis, *J. Pharm. Biomed. Anal.* 236 (2023) 115671.
- [246] Y. Nie, G. Fu, Y. Leng, Nuclear delivery of nanoparticle-based drug delivery systems by nuclear localization signals, *Cells* 12 (12) (2023).
- [247] S. Sargazi, I. Fatima, M. Hassan Kiani, V. Mohammadzadeh, R. Arshad, M. Bilal, A. Rahdar, A.M. Diez-Pascual, R. Behzadmehr, Fluorescent-based nanosensors for selective detection of a wide range of biological macromolecules: a comprehensive review, *Int. J. Biol. Macromol.* 206 (2022) 115–147.
- [248] W. Sun, J. Yu, R. Deng, Y. Rong, B. Fujimoto, C. Wu, H. Zhang, D.T. Chiu, Semiconducting polymer dots doped with europium complexes showing ultranarrow emission and long luminescence lifetime for time-gated cellular imaging, *Angew. Chem. Int. Ed. Engl.* 52 (43) (2013) 11294–11297.
- [249] K. Sun, Y. Tang, Q. Li, S. Yin, W. Qin, J. Yu, D.T. Chiu, Y. Liu, Z. Yuan, X. Zhang, C. Wu, In vivo dynamic monitoring of small molecules with implantable polymer-dot transducer, *ACS Nano* 10 (7) (2016) 6769–6781.
- [250] S.Y. Kuo, H.H. Li, P.J. Wu, C.P. Chen, Y.C. Huang, Y.H. Chan, Dual colorimetric and fluorescent sensor based on semiconducting polymer dots for ratiometric detection of lead ions in living cells, *Anal. Chem.* 87 (9) (2015) 4765–4771.
- [251] C. Cordovilla, T.M. Swager, Strain release in organic photonic nanoparticles for protease sensing, *J. Am. Chem. Soc.* 134 (16) (2012) 6932–6935.
- [252] P.J. Wu, S.Y. Kuo, Y.C. Huang, C.P. Chen, Y.H. Chan, Polydiacetylene-enclosed near-infrared fluorescent semiconducting polymer dots for bioimaging and sensing, *Anal. Chem.* 86 (10) (2014) 4831–4839.
- [253] P.Y. You, F.C. Li, M.H. Liu, Y.H. Chan, Colorimetric and fluorescent dual-mode immunoassay based on plasmon-enhanced fluorescence of polymer dots for detection of PSA in whole blood, *ACS Appl. Mater. Interfaces* 11 (10) (2019) 9841–9849.
- [254] D. Fang, S. Zhang, H. Dai, Y. Lin, An ultrasensitive ratiometric electrochemiluminescence immunosensor combining photothermal amplification for ovarian cancer marker detection, *Biosens. Bioelectron.* 146 (2019) 111768.
- [255] H. Chen, J. Yu, J. Zhang, K. Sun, Z. Ding, Y. Jiang, Q. Hu, C. Wu, D.T. Chiu, Monitoring metabolites using an NAD(P)H-sensitive polymer dot and a metabolite-specific enzyme, *Angew. Chem. Int. Ed. Engl.* 60 (35) (2021) 19331–19336.
- [256] N. Wang, X. Cao, D. Sun, X. Li, G. Tian, J. Feng, P. Wei, A polymer dot-based NADH-sensitive electrochemiluminescence biosensor for analysis of metabolites in serum, *Talanta* 267 (2024) 125149.
- [257] Y.Q. Yang, Y.C. Yang, M.H. Liu, Y.H. Chan, FRET-created traffic light immunoassay based on polymer dots for PSA detection, *Anal. Chem.* 92 (1) (2020) 1493–1501.
- [258] M. Schuller, A. Meister, M. Green, L.A. Dailey, Investigating conjugated polymer nanoparticle formulations for lateral flow immunoassays, *RSC Adv* 11 (47) (2021) 29816–29825.
- [259] K. Lix, M.V. Tran, M. Massey, K. Rees, E.R. Sauve, Z.M. Hudson, W.R. Algar, Dextran functionalization of semiconducting polymer dots and conjugation with tetrameric antibody complexes for bioanalysis and imaging, *ACS Appl. Bio. Mater.* 3 (1) (2020) 432–440.
- [260] C. Lou, H. Yang, Y. Hou, H. Huang, J. Qiu, C. Wang, Y. Sang, H. Liu, L. Han, Microfluidic platforms for real-time in situ monitoring of biomarkers for cellular processes, *Adv. Mater.* (2023) e2307051, <https://doi.org/10.1002/adma.202307051>.
- [261] W. Sun, J.B. Yu, F.M. Ye, Y. Rong, D.T. Chiu, Highly fluorescent semiconducting polymer dots for single-molecule imaging and biosensing, *Biosensing and Nanomedicine* Vi 8812, 2013.
- [262] J. Wang, S. Zhang, H. Dai, H. Zheng, Z. Hong, Y. Lin, Dual-readout immunosensor constructed based on brilliant photoelectrochemical and photothermal effect of polymer dots for sensitive detection of sialic acid, *Biosens. Bioelectron.* 142 (2019) 111567.
- [263] G. Gao, E.S. Sumrall, S. Pitchiya, M. Bitzer, S. Alberti, N.G. Walter, Biomolecular condensates in kidney physiology and disease, *Nat. Rev. Nephrol.* 19 (12) (2023) 756–770.
- [264] K. Soltyś, A. Tarczewska, D. Bystranowska, Modulation of biomolecular phase behavior by metal ions, *Biochim. Biophys. Acta Mol. Cell Res.* 1870 (8) (2023) 119567.
- [265] Y.H. Chan, Y. Jin, C. Wu, D.T. Chiu, Copper(II) and iron(II) ion sensing with semiconducting polymer dots, *Chem. Commun.* 47 (10) (2011) 2820–2822.
- [266] L. Feng, L. Guo, X. Wang, Preparation, properties and applications in cell imaging and ions detection of conjugated polymer nanoparticles with alkoxyl bonding fluorene core, *Biosens. Bioelectron.* 87 (2017) 514–521.

- [267] Q. Li, K. Sun, K. Chang, J. Yu, D.T. Chiu, C. Wu, W. Qin, Ratiometric luminescent detection of bacterial spores with terbium chelated semiconducting polymer dots, *Anal. Chem.* 85 (19) (2013) 9087–9091.
- [268] W. Xu, S. Lu, M. Xu, Y. Jiang, Y. Wang, X. Chen, Simultaneous imaging of intracellular pH and O<sub>2</sub>) using functionalized semiconducting polymer dots, *J. Mater. Chem. B* 4 (2) (2016) 292–298.
- [269] X.M. Shi, L.P. Mei, N. Zhang, W.W. Zhao, J.J. Xu, H.Y. Chen, A polymer dots-based photoelectrochemical pH sensor: simplicity, high sensitivity, and broad-range pH measurement, *Anal. Chem.* 90 (14) (2018) 8300–8303.
- [270] H. Gao, N. Zhang, Y. Li, W. Zhao, Y.W. Quan, Y.X. Cheng, H.Y. Chen, J.J. Xu, Trace Ir(III) complex enhanced electrochemiluminescence of AlE-active Pdots in aqueous media, *Sci. China-Chem.* 63 (5) (2020) 715–721.
- [271] G. Li, H. Gao, N. Wang, Z. Li, H. Ju, Ratiometric fluorescent detection of MiRNA-21 via pH-regulated adsorption of DNA on polymer dots and exonuclease III-assisted amplification, *Anal. Chim. Acta* 1232 (2022) 340450.
- [272] W. You, Y. Li, K. Liu, X. Mi, Y. Li, X. Guo, Z. Li, Latest assessment methods for mitochondrial homeostasis in cognitive diseases, *Neural. Regen. Res.* 19 (4) (2024) 754–768.
- [273] C.N. Okoye, S.A. Koren, A.P. Wojtovich, Mitochondrial complex I ROS production and redox signaling in hypoxia, *Redox. Biol.* 67 (2023) 102926.
- [274] S. Liu, B. Huang, J. Cao, Y. Wang, H. Xiao, Y. Zhu, H. Zhang, ROS fine-tunes the function and fate of immune cells, *Int. Immunopharmacol.* 119 (2023) 110069.
- [275] S. Lin, C. Ye, Z. Lin, L. Huang, D. Li, Recent progress of near-infrared fluorescent probes in the determination of reactive oxygen species for disease diagnosis, *Talanta* 268 (Pt 1) (2024) 125264.
- [276] K. Jomova, R. Raptova, S.Y. Alomar, S.H. Alwasel, E. Nepovimova, K. Kuca, M. Valko, Reactive oxygen species, toxicity, oxidative stress, and antioxidants: chronic diseases and aging, *Arch. Toxicol.* 97 (10) (2023) 2499–2574.
- [277] W. Zhao, P. Zhuang, Y. Chen, Y. Wu, M. Zhong, Y. Liu, "Double-edged sword" effect of reactive oxygen species (ROS) in tumor development and carcinogenesis, *Physiol. Res.* 72 (3) (2023) 301–307.
- [278] S. Li, J. Chen, G. Chen, Q. Li, K. Sun, Z. Yuan, W. Qin, H. Xu, C. Wu, Semiconductor polymer dots induce proliferation in human gastric mucosal and adenocarcinoma cells, *Macromol. Biosci.* 15 (3) (2015) 318–327.
- [279] L. Cai, L. Deng, X. Huang, J. Ren, Catalytic chemiluminescence polymer dots for ultrasensitive in vivo imaging of intrinsic reactive oxygen species in mice, *Anal. Chem.* 90 (11) (2018) 6929–6935.
- [280] Y. Xu, L. Xiao, Efficient suppression of amyloid-beta peptide aggregation and cytotoxicity with photosensitive polymer nanodots, *J. Mater. Chem. B* 8 (26) (2020) 5776–5782.
- [281] A. Liu, L. Gedda, M. Axelsson, M. Pavliuk, K. Edwards, L. Hammarstrom, H. Tian, Panchromatic ternary polymer dots involving sub-picosecond energy and charge transfer for efficient and stable photocatalytic hydrogen evolution, *J. Am. Chem. Soc.* 143 (7) (2021) 2875–2885.
- [282] A. Ortiz-Perez, M. Zhang, L.W. Fitzpatrick, C. Izquierdo-Lozano, L. Albertazzi, Advanced optical imaging for the rational design of nanomedicines, *Adv. Drug Deliv. Rev.* 204 (2024) 115138.
- [283] J. Li, F. Cheng, H. Huang, L. Li, J.J. Zhu, Nanomaterial-based activatable imaging probes: from design to biological applications, *Chem. Soc. Rev.* 44 (21) (2015) 7855–7880.
- [284] D. Crosby, S. Bhatia, K.M. Brindle, L.M. Coussens, C. Dive, M. Emberton, S. Esener, R.C. Fitzgerald, S.S. Gambhir, P. Kuhn, T.R. Rebbeck, S. Balasubramanian, Early detection of cancer, *Science* 375 (6586) (2022) eaay9040.
- [285] M. Yang, J. Huang, J. Fan, J. Du, K. Pu, X. Peng, Chemiluminescence for bioimaging and therapeutics: recent advances and challenges, *Chem. Soc. Rev.* 49 (19) (2020) 6800–6815.
- [286] D.E. Lee, H. Koo, I.C. Sun, J.H. Ryu, K. Kim, I.C. Kwon, Multifunctional nanoparticles for multimodal imaging and theragnosis, *Chem. Soc. Rev.* 41 (7) (2012) 2656–2672.
- [287] K.A. Myers, C. Janetopoulos, Recent advances in imaging subcellular processes, *F1000Res* 5 (2016).
- [288] R. Han, Z. Li, Y. Fan, Y. Jiang, Recent advances in super-resolution fluorescence imaging and its applications in biology, *J. Genet. Genomics.* 40 (12) (2013) 583–595.
- [289] L. Sun, F. Bian, D. Xu, Y. Luo, Y. Wang, Y. Zhao, Tailoring biomaterials for biomimetic organs-on-chips, *Mater. Horiz.* 10 (11) (2023) 4724–4745.
- [290] E. Tolstik, S.E. Lehnart, C. Soeller, K. Lorenz, L. Sacconi, Cardiac multiscale bioimaging: from nano- through micro- to mesoscales, *Trends. Biotechnol.* 42 (2) (2023) 212–227.
- [291] D. Shima, N. Sunaguchi, T. Yuasa, M. Ando, K. Mori, R. Gupta, S. Ichihara, X-Ray dark-field imaging (XDF)-a promising tool for 3D virtual histopathology, *Mol. Imaging. Biol.* 23 (4) (2021) 481–494.
- [292] F.J. Verweij, L. Balaj, C.M. Boulanger, D.R.F. Carter, E.B. Compeer, G. D'Angelo, S. El Andaloussi, J.G. Goetz, J.C. Gross, V. Hyenne, E.M. Kramer-Albers, C.P. Lai, X. Loyer, A. Marki, S. Momma, E.N.M. Nolte-'t Hoen, D.M. Pegtel, H. Peinado, G. Raposo, K. Rilla, H. Tahara, C. Thery, M.E. van Royen, R.E. Vandebroucke, A. M. Wehman, K. Witwer, Z. Wu, R. Wubbolts, G. van Niel, The power of imaging to understand extracellular vesicle biology in vivo, *Nat. Methods* 18 (9) (2021) 1013–1026.
- [293] Y. Su, S. Liu, Y. Guan, Z. Xie, M. Zheng, X. Jing, Renal clearable Hafnium-doped carbon dots for CT/Fluorescence imaging of orthotopic liver cancer, *Biomaterials* 255 (2020) 120110.
- [294] M.M. Vandevenne, E. Favuzza, M. Veta, E. Lucenteforte, T.T. Berendschot, R. Mencucci, R.M. Nuijts, G. Virgili, M.M. Dickman, Artificial intelligence for detecting keratoconus, *Cochrane, Database Syst. Rev.* 11 (11) (2023) CD014911.
- [295] C. Jensen, Y. Teng, Is it time to start transitioning from 2D to 3D cell culture? *Front Mol. Biosci.* 7 (2020) 33.
- [296] A.W. Browne, C. Arnesano, N. Harutyunyan, T. Khuu, J.C. Martinez, H.A. Pollack, D.S. Koos, T.C. Lee, S.E. Fraser, R.A. Moats, J.G. Aparicio, D. Cobrinik, Structural and functional characterization of human stem-cell-derived retinal organoids by live imaging, *Invest. Ophthalmol. Vis. Sci.* 58 (9) (2017) 3311–3318.
- [297] C. Wu, B. Bull, C. Szymanski, K. Christensen, J. McNeill, Multicolor conjugated polymer dots for biological fluorescence imaging, *ACS Nano* 2 (11) (2008) 2415–2423.
- [298] G. Hong, S. Diao, A.L. Antaris, H. Dai, Carbon nanomaterials for biological imaging and nanomedicinal therapy, *Chem. Rev.* 115 (19) (2015) 10816–10906.
- [299] X. Fang, X. Chen, R. Li, Z. Liu, H. Chen, Z. Sun, B. Ju, Y. Liu, S.X. Zhang, D. Ding, Y. Sun, C. Wu, Multicolor photo-crosslinkable AlEgens toward compact nanodots for subcellular imaging and STED nanoscopy, *Small* 13 (41) (2017) 1702128.
- [300] K. Pu, A.J. Shuhendler, J.V. Jokerst, J. Mei, S.S. Gambhir, Z. Bao, J. Rao, Semiconducting polymer nanoparticles as photoacoustic molecular imaging probes in living mice, *Nat. Nanotechnol.* 9 (3) (2014) 233–239.
- [301] K. Pu, J. Mei, J.V. Jokerst, G. Hong, A.L. Antaris, N. Chattopadhyay, A. J. Shuhendler, T. Kuroswaya, Y. Zhou, S.S. Gambhir, Z. Bao, J. Rao, Diketopyrrolopyrrole-based semiconducting polymer nanoparticles for in vivo photoacoustic imaging, *Adv. Mater.* 27 (35) (2015) 5184–5190.
- [302] B. Dunn, M. Hanafi, J. Hummel, J.R. Cressman, R. Veneziano, P.V. Chitnis, NIR-II nanoprobes: a review of components-based approaches to next-generation bioimaging probes, *Bioengineering* 10 (8) (2023) 954.
- [303] M. Zhou, S. Liang, D. Liu, K. Ma, Y. Peng, Z. Wang, Engineered nanoprobes for immune activation monitoring, *ACS Nano* 16 (12) (2022) 19940–19958.
- [304] D.R. Miller, A.M. Hassan, J.W. Jarrett, F.A. Medina, E.P. Perillo, K. Hagan, S. M. Shams Kazmi, T.A. Clark, C.T. Sullender, T.A. Jones, B.V. Zemelman, A. K. Dunn, In vivo multiphoton imaging of a diverse array of fluorophores to investigate deep neurovascular structure, *Biomed. Opt. Express* 8 (7) (2017) 3470–3481.
- [305] D.R. Miller, J.W. Jarrett, A.M. Hassan, A.K. Dunn, Deep tissue imaging with multiphoton fluorescence microscopy, *Curr. Opin. Biomed. Eng.* 4 (2017) 32–39.
- [306] S. Deng, L. Li, J. Zhang, Y. Wang, Z. Huang, H. Chen, Semiconducting polymer dots for point-of-care biosensing and in vivo bioimaging: a concise review, *Biosensors* 13 (1) (2023).
- [307] F. Ye, P.B. Smith, D.T. Chiu, Ultrasensitive protein detection on dot blots and western blots with semiconducting polymer dots, *Methods Mol. Biol.* 1314 (2015) 131–137.
- [308] J. Li, Y. Li, S. Tang, Y. Zhang, J. Zhang, Y. Li, L. Xiong, Toxicity, uptake and transport mechanisms of dual-modal polymer dots in penny grass (*Hydrocotyle vulgaris* L.), *Environ. Pollut.* 265 (Pt A) (2020) 114877.
- [309] Y.C. Chen, Y.H. Syu, J.Y. Huang, C.Y. Lin, Y.H. Chan, Hybrid polymer dot-magnetic nanoparticle based immunoassay for dual-mode multiplexed detection of two mycotoxins, *Chem. Commun.* 59 (66) (2023) 9968–9971.
- [310] L. Peng, Y. Liu, J. Zhang, Z. Zhang, Z. Liu, X. Fang, Y. Wang, C. Wu, Surface plasmon-enhanced NIR-II fluorescence in a multilayer nanoprobe for through-skull mouse brain imaging, *ACS Appl. Mater. Interfaces* 14 (34) (2022) 38575–38583.
- [311] Y. Lu, W. Song, Z. Tang, W. Shi, S. Gao, J. Wu, Y. Wang, H. Pan, Y. Wang, H. Huang, The preparation of Golgi apparatus-targeted polymer dots encapsulated with carbon nanodots of bright near-infrared fluorescence for long-term bioimaging, *Molecules* 28 (17) (2023).
- [312] Y. Yang, Q. Jiang, F. Zhang, Nanocrystals for deep-tissue in vivo luminescence imaging in the near-infrared region, *Chem. Rev.* 124 (2) (2024) 554–628.
- [313] Y. Wang, J.N. Staudinger, T.L. Mindt, G. Gasser, Theranostics with photodynamic therapy for personalized medicine: to see and to treat, *Theranostics* 13 (15) (2023) 5501–5544.
- [314] C. Li, Y. Pang, Y. Xu, M. Lu, L. Tu, Q. Li, A. Sharma, Z. Guo, X. Li, Y. Sun, Near-infrared metal agents assisting precision medicine: from strategic design to bioimaging and therapeutic applications, *Chem. Soc. Rev.* 52 (13) (2023) 4392–4442.
- [315] K. Zhang, F.R. Chen, L. Wang, J. Hu, Second near-infrared (NIR-II) window for imaging-navigated modulation of brain structure and function, *Small* 19 (14) (2023) e2206044.
- [316] H.S. Peng, D.T. Chiu, Soft fluorescent nanomaterials for biological and biomedical imaging, *Chem. Soc. Rev.* 44 (14) (2015) 4699–4722.
- [317] S.L. Li, X.Y. Wang, R. Hu, H. Chen, M. Li, J.W. Wang, Y.X. Wang, L.B. Liu, F.T. Lv, X.J. Liang, S. Wang, Near-infrared (NIR)-Absorbing conjugated polymer dots as highly effective photothermal materials for therapy, 2016 cancer therapy, *Chemistry of Materials* 28 (23) (2016) 8669–8675.
- [318] S. Chen, S. Cui, R. Du, M. Liu, W.K. Tsai, F. Guo, Q. Wu, L. Zhao, Y. Zhang, Simultaneous near-infrared and green fluorescence from single conjugated polymer dots with aggregation-induced emission fluorogen for cell imaging, *J. Mater. Chem. B* 6 (47) (2018) 7871–7876.
- [319] Y. Liu, J. Liu, D. Chen, X. Wang, Z. Zhang, Y. Yang, L. Jiang, W. Qi, Z. Ye, S. He, Q. Liu, L. Xi, Y. Zou, C. Wu, Fluorination enhances NIR-II fluorescence of polymer dots for quantitative brain tumor imaging, *Angew. Chem. Int. Ed. Engl.* 59 (47) (2020) 21049–21057.
- [320] Y. Dai, F. Zhang, K. Chen, Z. Sun, Z. Wang, Y. Xue, M. Li, Q. Fan, Q. Shen, Q. Zhao, An activatable phototheranostic nanoplatform for tumor specific NIR-II fluorescence imaging and synergistic NIR-II photothermal-chemodynamic therapy, *Small* 19 (22) (2023) e2206053.
- [321] W. Denk, J.H. Strickler, W.W. Webb, Two-photon laser scanning fluorescence microscopy, *Science* 248 (4951) (1990) 73–76.

- [322] N.D. Bhattacharyya, W. Kyaw, M.M. McDonald, R. Dhenni, A.K. Grootveld, Y. Xiao, R. Chai, W.H. Khoo, L.C. Danserau, C.M. Sergio, P. Timpong, W.M. Lee, P. I. Croucher, T.G. Phan, Minimally invasive longitudinal intravital imaging of cellular dynamics in intact long bone, *Nat. Protoc.* 18 (12) (2023) 3856–3880.
- [323] S. Li, X.-F. Jiang, Q.-H. Xu, Polyfluorene based conjugated polymer nanoparticles for two-photon live cell imaging, *Sci. China Chem.* 61 (1) (2017) 88–96.
- [324] X. Lou, Z. Zhao, B.Z. Tang, Organic dots based on AIogens for two-photon fluorescence bioimaging, *Small* 12 (47) (2016) 6430–6450.
- [325] M.E. Darvin, Optical methods for non-invasive determination of skin penetration: current trends, advances, possibilities, prospects, and translation into *in vivo* human studies, *Pharmaceutics* 15 (9) (2023).
- [326] S. Uderhardt, G. Neag, N.G. R, Dynamic multiplex tissue imaging in inflammation research, *Annu. Rev. Pathol.* (2023), <https://doi.org/10.1146/annurev-pathmechdis-070323-124158>.
- [327] T.C. He, W.B. Hu, H.F. Shi, Q.F. Pan, G.H. Ma, W. Huang, Q.L. Fan, X.D. Lin, Strong nonlinear optical phosphorescence from water-soluble polymer dots: towards the application of two-photon bioimaging, *Dyes and Pigments* 123 (2015) 218–221.
- [328] Z. Liu, Z. Sun, W. Di, W. Qin, Z. Yuan, C. Wu, Brightness calibrates particle size in single particle fluorescence imaging, *Opt. Lett.* 40 (7) (2015) 1242–1245.
- [329] A.M. Hassan, X. Wu, J.W. Jarrett, S.H. Xu, D.R. Miller, J.B. Yu, E.P. Perillo, Y. L. Liu, D.T. Chiu, H.C. Yeh, A.K. Dunn, Polymer dots enable deep multiphoton fluorescence imaging of cerebrovascular architecture. Multiphoton Microscopy in the Biomedical Sciences XVIII 10498, 2018 104982Y.
- [330] Q. Zhang, X. Hu, X. Dai, P. Ling, J. Sun, H. Chen, F. Gao, General strategy to achieve color-tunable ratiometric two-photon integrated single semiconducting polymer dot for imaging hypochlorous acid, *ACS Nano* 15 (8) (2021) 13633–13645.
- [331] D.M. Mayder, C.M. Tonge, G.D. Nguyen, M.V. Tran, G. Tom, G.H. Darwish, R. Gupta, K. Lix, S. Kamal, W.R. Algar, S.A. Burke, Z.M. Hudson, Polymer dots with enhanced photostability, quantum yield, and two-photon cross-section using structurally constrained deep-blue fluorophores, *J. Am. Chem. Soc.* 143 (41) (2021) 16976–16992.
- [332] Q. Zhang, Z. Zhang, X. Hu, J. Sun, F. Gao, Dual-targeting into the mitochondria of cancer cells for ratiometric investigation of the dynamic fluctuation of sulfur dioxide and formaldehyde with two-photon integrated semiconducting polymer dots, *ACS Appl. Mater. Interfaces* 14 (1) (2022) 179–190.
- [333] S. Samanta, K. Lai, F. Wu, Y. Liu, S. Cai, X. Yang, J. Qu, Z. Yang, Xanthene, cyanine, oxazine and BODIPY: the four pillars of the fluorophore empire for super-resolution bioimaging, *Chem. Soc. Rev.* 52 (20) (2023) 7197–7261.
- [334] C. Zhang, Z. Tian, R. Chen, F. Rowan, K. Qiu, Y. Sun, J.L. Guan, J. Diao, Advanced imaging techniques for tracking drug dynamics at the subcellular level, *Adv. Drug Deliv. Rev.* 199 (2023) 114978.
- [335] R. Zhai, B. Fang, Y. Lai, B. Peng, H. Bai, X. Liu, L. Li, W. Huang, Small-molecule fluorogenic probes for mitochondrial nanoscale imaging, *Chem. Soc. Rev.* 52 (3) (2023) 942–972.
- [336] W. Zou, L. Yang, H. Lu, M. Li, D. Ji, J. Slone, T. Huang, Application of super-resolution microscopy in mitochondria-dynamic diseases, *Adv. Drug Deliv. Rev.* 200 (2023) 115043.
- [337] S. Calovi, F.N. Soria, J. Tonnesen, Super-resolution STED microscopy in live brain tissue, *Neurobiol. Dis.* 156 (2021) 105420.
- [338] Y. Liu, Z. Peng, X. Peng, W. Yan, Z. Yang, J. Qu, Shedding new lights into STED microscopy: emerging nanoprobe for imaging, *Front. Chem.* 9 (2021) 641330.
- [339] R. Sharma, M. Singh, R. Sharma, Recent advances in STED and RESOLFT super-resolution imaging techniques, *Spectrochim. Acta A Mol. Biomol. Spectrosc.* 231 (2020) 117715.
- [340] W. Jahr, P. Velicky, J.G. Danzl, Strategies to maximize performance in STimulated Emission Depletion (STED) nanoscopy of biological specimens, *Methods* 174 (2020) 27–41.
- [341] Y. Wu, H. Ruan, Z. Dong, R. Zhao, J. Yu, X. Tang, X. Kou, X. Zhang, M. Wu, F. Luo, J. Yuan, X. Fang, Fluorescent polymer dot-based multicolor stimulated emission depletion nanoscopy with a single laser beam pair for cellular tracking, *Anal. Chem.* 92 (17) (2020) 12088–12096.
- [342] T. Dertinger, A. Pallaoro, G. Braun, S. Ly, T.A. Laurence, S. Weiss, Advances in super-resolution optical fluctuation imaging (SOFI), *Q. Rev. Biophys.* 46 (2) (2013) 210–221.
- [343] S. Cox, G.E. Jones, Imaging cells at the nanoscale, *Int. J. Biochem. Cell. Biol.* 45 (8) (2013) 1669–1678.
- [344] T. Dertinger, R. Colyer, G. Iyer, S. Weiss, J. Enderlein, Fast, background-free, 3D super-resolution optical fluctuation imaging (SOFI), *Proc. Natl. Acad. Sci. U.S.A.* 106 (52) (2009) 22287–22292.
- [345] T. Dertinger, J. Xu, O.F. Naini, R. Vogel, S. Weiss, SOFI-based 3D superresolution sectioning with a widefield microscope, *Opt. Nanoscopy* 1 (2) (2012) 2.
- [346] Z. Liu, J. Liu, Z. Zhang, Z. Sun, X. Shao, J. Guo, L. Xi, Z. Yuan, X. Zhang, D.T. Chiu, C. Wu, Narrow-band polymer dots with pronounced fluorescence fluctuations for dual-color super-resolution imaging, *Nanoscale* 12 (14) (2020) 7522–7526.
- [347] J. Ihli, D.C. Green, C. Lynch, M.A. Holden, P.A. Lee, S. Zhang, I.K. Robinson, S.E. D. Webb, F.C. Meldrum, Super-resolution microscopy reveals shape and distribution of dislocations in single-crystal nanocomposites, *Angew. Chem. Int. Ed. Engl.* 58 (48) (2019) 17328–17334.
- [348] J. Tam, D. Merino, Stochastic optical reconstruction microscopy (STORM) in comparison with stimulated emission depletion (STED) and other imaging methods, *J. Neurochem.* 135 (4) (2015) 643–658.
- [349] D. Baddeley, J. Bewersdorf, Biological insight from super-resolution microscopy: what we can learn from localization-based images, *Annu. Rev. Biochem.* 87 (2018) 965–989.
- [350] Y. Jiang, M. Novoa, T. Nongnual, R. Powell, T. Bruce, J. McNeill, Improved superresolution imaging using telegraph noise in organic semiconductor nanoparticles, *Nano Lett.* 17 (6) (2017) 3896–3901.
- [351] Z. Ye, L. Wei, Y. Li, L. Xiao, Efficient modulation of beta-amyloid peptide fibrillation with polymer nanoparticles revealed by super-resolution optical microscopy, *Anal. Chem.* 91 (13) (2019) 8582–8590.
- [352] D. Kamiyama, B. Huang, Development in the STORM, *Dev. Cell.* 23 (6) (2012) 1103–1110.
- [353] M. Igarashi, M. Nozumi, L.G. Wu, F. Cella Zanacchi, I. Katona, L. Barna, P. Xu, M. Zhang, F. Xue, E. Boyden, New observations in neuroscience using superresolution microscopy, *J. Neurosci.* 38 (44) (2018) 9459–9467.
- [354] Z. Yao, X. Wang, J. Liu, S. Zhou, Z. Zhang, S. He, J. Liu, C. Wu, X. Fang, Photoswitchable semiconducting polymer dots for pattern encoding and superresolution imaging, *Chem. Commun.* 59 (17) (2023) 2469–2472.
- [355] B. Park, D. Oh, J. Kim, C. Kim, Functional photoacoustic imaging: from nano- and micro- to macro-scale, *Nano. Converg.* 10 (1) (2023) 29.
- [356] A.A. Oraevsky, B. Clingman, J. Zalev, A.T. Stavros, W.T. Yang, J.R. Parikh, Clinical optoacoustic imaging combined with ultrasound for coregistered functional and anatomical mapping of breast tumors, *Photoacoustics* 12 (2018) 30–45.
- [357] B. Sridharan, H.G. Lim, Advances in photoacoustic imaging aided by nano contrast agents: special focus on role of lymphatic system imaging for cancer theranostics, *J. Nanobiotechnology* 21 (1) (2023) 437.
- [358] H. Hu, J. Zhao, K. Ma, J. Wang, X. Wang, T. Mao, C. Xiang, H. Luo, Y. Cheng, M. Yu, Y. Qin, K. Yang, Q. Li, Y. Sun, S. Wang, Sonodynamic therapy combined with phototherapy: novel synergistic strategy with superior efficacy for antitumor and antiinfection therapy, *J. Control Release* 359 (2023) 188–205.
- [359] M. Xu, Z. Chen, J. Zheng, Q. Zhao, Z. Yuan, Artificial intelligence-aided optical imaging for cancer theranostics, *Semin. Cancer Biol.* 94 (2023) 62–80.
- [360] H. Assi, R. Cao, M. Castelino, B. Cox, F.J. Gilbert, J. Grohl, K. Gurusamy, L. Hacker, A.M. Ivory, J. Joseph, F. Knieling, M.J. Leahy, L. Lilaj, S. Manohar, I. Meglinski, C. Moran, A. Murray, A.A. Oraevsky, M.D. Pagel, M. Pramanik, J. Raymond, M.K.A. Singh, W.C. Vogt, L. Wang, S. Yang, I. Members Of, S. E. Bohndiek, A review of a strategic roadmapping exercise to advance clinical translation of photoacoustic imaging: from current barriers to future adoption, *Photoacoustics* 32 (2023) 100539.
- [361] J. Zhang, H.B. Chen, T. Zhou, L.M. Wang, D.Y. Gao, X.J. Zhang, Y.B. Liu, C.F. Wu, Z. Yuan, A PIID-DTBT based semi-conducting polymer dots with broad and strong optical absorption in the visible-light region: highly effective contrast agents for multiscale and multi-spectral photoacoustic imaging, *Nano Research* 10 (1) (2017) 64–76.
- [362] Z. Yuan, J. Zhang, Semiconducting polymer dot as a highly-effective contrast agent for photoacoustic imaging. *Photons Plus Ultrasound: Imaging and Sensing* 2018 10494, 2018.
- [363] K. Chang, Y. Liu, D. Hu, Q. Qi, D. Gao, Y. Wang, D. Li, X. Zhang, H. Zheng, Z. Sheng, Z. Yuan, Highly stable conjugated polymer dots as multifunctional agents for photoacoustic imaging-guided photothermal therapy, *ACS Appl. Mater. Interfaces* 10 (8) (2018) 7012–7021.
- [364] Y. Lyu, Y. Fang, Q. Miao, X. Zhen, D. Ding, K. Pu, Intraparticle molecular orbital engineering of semiconducting polymer nanoparticles as amplified theranostics for *in vivo* photoacoustic imaging and photothermal therapy, *ACS Nano* 10 (4) (2016) 4472–4481.
- [365] T. Stahl, R. Bofinger, I. Lam, K.J. Fallon, P. Johnson, O. Ogunlade, V. Vassileva, R. B. Pedley, P.C. Beard, H.C. Hailes, H. Bronstein, A.B. Tabor, Tunable semiconducting polymer nanoparticles with INDT-based conjugated polymers for photoacoustic molecular imaging, *Bioconjug. Chem.* 28 (6) (2017) 1734–1740.
- [366] B. Guo, J. Chen, N. Chen, E. Middha, S. Xu, Y. Pan, M. Wu, K. Li, C. Liu, B. Liu, High-resolution 3D NIR-II photoacoustic imaging of cerebral and tumor vasculatures using conjugated polymer nanoparticles as contrast agent, *Adv. Mater.* 31 (25) (2019) e1808355.
- [367] B. Guo, Z. Feng, D. Hu, S. Xu, E. Middha, Y. Pan, C. Liu, H. Zheng, J. Qian, Z. Sheng, B. Liu, Precise deciphering of brain vasculatures and microscopic tumors with dual NIR-II fluorescence and photoacoustic imaging, *Adv. Mater.* 31 (30) (2019) e1902504.
- [368] A. Sun, Y. Ji, Y. Li, W. Xie, Z. Liu, T. Li, T. Jin, W. Qi, K. Li, C. Wu, L. Xi, Multicolor photoacoustic volumetric imaging of subcellular structures, *ACS Nano* 16 (2) (2022) 3231–3238.
- [369] X. Zhen, K. Pu, X. Jiang, Photoacoustic imaging and photothermal therapy of semiconducting polymer nanoparticles: signal amplification and second near-infrared construction, *Small* 17 (6) (2021) e2004723.
- [370] X. Huang, N. Lan, Y. Zhang, W. Zeng, H. He, X. Liu, Benzobisthiadiazole and its derivative-based semiconducting polymer nanoparticles for second near-infrared photoacoustic imaging, *Front. Chem.* 10 (2022) 842712.
- [371] J. Sobhanan, A. Anas, V. Biju, Nanomaterials for fluorescence and multimodal bioimaging, *Chem. Rec.* 23 (3) (2023) e202200253.
- [372] M.E. Graziotto, C.J. Kidman, L.D. Adair, S.A. James, H.H. Harris, E.J. New, Towards multimodal cellular imaging: optical and X-ray fluorescence, *Chem. Soc. Rev.* 52 (23) (2023) 8295–8318.
- [373] X. Hu, Y. Tang, Y. Hu, F. Lu, X. Lu, Y. Wang, J. Li, Y. Li, Y. Ji, W. Wang, D. Ye, Q. Fan, W. Huang, Gadolinium-chelated conjugated polymer-based nanotheranostics for photoacoustic/magnetic resonance/NIR-II fluorescence imaging-guided cancer photothermal therapy, *Theranostics* 9 (14) (2019) 4168–4181.
- [374] A. Petkidis, V. Andriasyan, U.F. Greber, Machine learning for cross-scale microscopy of viruses, *Cell. Rep. Methods* 3 (9) (2023) 100557.

- [375] D. Qiu, Y. Cheng, X. Wang, Medical image super-resolution reconstruction algorithms based on deep learning: a survey, *Comput. Methods Programs Biomed.* 238 (2023) 107590.
- [376] J.B. Belge, P. Mulders, L. Van Diermen, P. Sienraert, B. Sabbe, C.C. Abbott, I. Tendolkar, D. Schrijvers, P. van Eijndhoven, Reviewing the neurobiology of electroconvulsive therapy on a micro- meso- and macro-level, *Prog. Neuropsychopharmacol. Biol. Psychiatry* 127 (2023) 110809.
- [377] C. Gong, C. Jing, X. Chen, C.M. Pun, G. Huang, A. Saha, M. Nieuwoudt, H.X. Li, Y. Hu, S. Wang, Generative AI for brain image computing and brain network computing: a review, *Front Neurosci* 17 (2023) 1203104.
- [378] N. Chinam, M. Bekkali, M. Kallas, J. Li, Virtual occlusal records acquired by using intraoral scanners: a review of factors that influence maxillo-mandibular relationship accuracy, *J. Prosthodont.* 32 (S2) (2023) 192–207.
- [379] S.A. Alajaji, Z.H. Khouri, M. Elgharib, M. Saeed, A.R.H. Ahmed, M.B. Khan, T. Tavares, M. Jessri, A.C. Puche, H. Hoorfar, I. Stojanov, J.J. Scuibba, A. S. Sultan, Generative adversarial networks in digital histopathology: current applications, limitations, ethical considerations, and future directions, *Mod. Pathol.* 37 (1) (2024) 100369.
- [380] D. Kanschik, R.R. Bruno, G. Wolff, M. Kelm, C. Jung, Virtual and augmented reality in intensive care medicine: a systematic review, *Ann. Intensive Care* 13 (1) (2023) 81.
- [381] A. Waqas, M.M. Bui, E.F. Glassy, I. El Naqa, P. Borkowski, A.A. Borkowski, G. Rasool, Revolutionizing digital pathology with the power of generative artificial intelligence and foundation models, *Lab. Invest.* 103 (11) (2023) 100255.
- [382] M. Eisenstein, AI under the microscope: the algorithms powering the search for cells, *Nature* 623 (7989) (2023) 1095–1097.
- [383] P. Paul-Gilloteaux, Bioimage informatics: investing in software usability is essential, *PLoS Biol.* 21 (7) (2023) e3002213.
- [384] D. Bayer, S. Antonucci, H.P. Muller, R. Saad, L. Dupuis, V. Rasche, T.M. Bockers, A.C. Ludolph, J. Kassubek, F. Roselli, Disruption of orbitofrontal-hypothalamic projections in a murine ALS model and in human patients, *Transl. Neurodegener.* 10 (1) (2021) 17.
- [385] R. Menze, B. Hesse, M. Kusmierzuk, D. Chen, T. Weitkamp, S. Bettink, B. Scheller, Synchrotron microtomography reveals insights into the degradation kinetics of bio-degradable coronary magnesium scaffolds, *Bioact. Mater.* 32 (2024) 1–11.
- [386] S. Sacco, R. Ornello, Headache research in 2023: advancing therapy and technology, *Lancet Neurol* 23 (1) (2024) 17–19.
- [387] M. Karelina, J.J. Noh, R.O. Dror, How accurately can one predict drug binding modes using AlphaFold models? *Elife* 12 (2023) RP9386.
- [388] L.M. Liz-Marzan, A.E. Nel, C.J. Brinker, W.C.W. Chan, C. Chen, X. Chen, D. Ho, T. Hu, K. Kataoka, N.A. Kotov, W.J. Parak, M.M. Stevens, What do we mean when we say nanomedicine? *ACS Nano* 16 (9) (2022) 13257–13259.
- [389] M. Liang, J. Lu, M. Kovochich, T. Xia, S.G. Ruehm, A.E. Nel, F. Tamanoi, J.I. Zink, Multifunctional inorganic nanoparticles for imaging, targeting, and drug delivery, *ACS Nano* 2 (5) (2008) 889–896.
- [390] Y. Zhang, F. Wang, C. Liu, Z. Wang, L. Kang, Y. Huang, K. Dong, J. Ren, X. Qu, Nanozyme decorated metal-organic frameworks for enhanced photodynamic therapy, *ACS Nano* 12 (1) (2018) 651–661.
- [391] B. Pelaz, C. Alexiou, R.A. Alvarez-Puebla, F. Alves, A.M. Andrews, S. Ashraf, L. P. Balogh, L. Ballerini, A. Bestetti, C. Brendel, S. Bosi, M. Carril, W.C. Chan, C. Chen, X. Chen, X. Chen, Z. Cheng, D. Cui, J. Du, C. Dullin, A. Escudero, N. Feliu, M. Gao, M. George, Y. Gogotsi, A. Grunweller, Z. Gu, N.J. Halas, N. Hampf, R.K. Hartmann, M.C. Hersam, P. Hunziker, J. Jian, X. Jiang, P. Jungebluth, P. Kadhiresan, K. Kataoka, A. Khademhosseini, J. Kopecik, N. A. Kotov, H.F. Krug, D.S. Lee, C.M. Lehr, K.W. Leong, X.J. Liang, M. Ling Lim, L. M. Liz-Marzan, X. Ma, P. Macchiarini, H. Meng, H. Mohwald, P. Mulvaney, A. E. Nel, S. Nie, P. Nordlander, T. Okano, J. Oliveira, T.H. Park, R.M. Penner, M. Prato, V. Puntes, V.M. Rotello, A. Samarakoon, R.E. Schaak, Y. Shen, S. Sjoqvist, A.G. Skirtach, M.G. Soliman, M.M. Stevens, H.W. Sung, B.Z. Tang, R. Tietze, B.N. Udagama, J.S. VanEpps, T. Weil, P.S. Weiss, I. Willner, Y. Wu, L. Yang, Z. Yue, Q. Zhang, Q. Zhang, X.E. Zhang, Y. Zhao, X. Zhou, W.J. Parak, Diverse applications of nanomedicine, *ACS Nano* 11 (3) (2017) 2313–2381.
- [392] A.E.M.D.D. Nel, Transformational impact of nanomedicine: reconciling outcome with promise, *Nano Lett.* 20 (8) (2020) 5601–5603.
- [393] Z. Tang, Y. Xiao, N. Kong, C. Liu, W. Chen, X. Huang, D. Xu, J. Ouyang, C. Feng, C. Wang, J. Wang, H. Zhang, W. Tao, Nano-bio interfaces effect of two-dimensional nanomaterials and their applications in cancer immunotherapy, *Acta Pharm. Sin. B* 11 (11) (2021) 3447–3464.
- [394] Y. Zhu, X. Cai, J. Li, Z. Zhong, Q. Huang, C. Fan, Synchrotron-based X-ray microscopic studies for bioeffects of nanomaterials, *Nanomedicine* 10 (3) (2014) 515–524.
- [395] F. Ye, C. Wu, W. Sun, J. Yu, X. Zhang, Y. Rong, Y. Zhang, I.C. Wu, Y.H. Chan, D. T. Chiu, Semiconducting polymer dots with monofunctional groups, *Chem. Commun.* 50 (42) (2014) 5604–5607.
- [396] H. Chen, X. Fang, Y. Jin, X. Hu, M. Yin, X. Men, N. Chen, C. Fan, D.T. Chiu, Y. Wan, C. Wu, Semiconducting polymer nanocavities: porogenic synthesis, tunable host-guest interactions, and enhanced drug/siRNA delivery, *Small* 14 (21) (2018) e1800239.
- [397] M.J. Ko, S. Min, H. Hong, W. Yoo, J. Joo, Y.S. Zhang, H. Kang, D.H. Kim, Magnetic nanoparticles for ferropotosis cancer therapy with diagnostic imaging, *Bioact. Mater.* 32 (2024) 66–97.
- [398] S. Batool, S. Sohail, F. Ud Din, A.H. Alamri, A.S. Alqahtani, M.A. Alshahrani, M. A. Alshehri, H.G. Choi, A detailed insight of the tumor targeting using nanocarrier drug delivery system, *Drug Deliv* 30 (1) (2023) 2183815.
- [399] Q. Hu, H. Zuo, J.C. Hsu, C. Zeng, Z. Tian, Z. Sun, W. Cai, Z. Tang, W. Chen, The emerging landscape for combating resistance associated with energy-based therapies via nanomedicine, *Adv Mater* (2023) e2308286.
- [400] N. Wu, Z. Zhang, J. Zhou, Z. Sun, Y. Deng, G. Lin, M. Ying, X. Wang, K.T. Yong, C. Wu, G. Xu, The biocompatibility studies of polymer dots on pregnant mice and fetuses, *Nanotheranostics* 1 (3) (2017) 261–271.
- [401] Y. Han, X. Li, H. Chen, X. Hu, Y. Luo, T. Wang, Z. Wang, Q. Li, C. Fan, J. Shi, L. Wang, Y. Zhao, C. Wu, N. Chen, Real-time imaging of endocytosis and intracellular trafficking of semiconducting polymer dots, *ACS Appl. Mater. Interfaces* 9 (25) (2017) 21200–21208.
- [402] T. Han, Y. Wang, S. Ma, M. Li, N. Zhu, S. Tao, J. Xu, B. Sun, Y. Jia, Y. Zhang, S. Zhu, B. Yang, Near-infrared carbonized polymer dots for NIR-II bioimaging, *Adv. Sci.* 9 (30) (2022) e2203474.
- [403] Q. Zhang, J. Sun, R. Zhang, X. Chen, N. Chen, F. Gao, Trichromatic-emission and dual-ratio semiconducting polymer dots as fluorescent probe for simultaneous quantification of Cu(2+) and pH in vitro and in vivo, *Chem. Commun.* 56 (61) (2020) 8647–8650.
- [404] X. Zhao, J. Li, D. Liu, M. Yang, W. Wang, S. Zhu, B. Yang, Self-enhanced carbonized polymer dots for selective visualization of lysosomes and real-time apoptosis monitoring, *iScience* 23 (4) (2020) 100982.
- [405] X. Guo, Q. Gong, J. Borowiec, S. Zhang, S. Han, M. Zhang, M. Willis, T. Kreouzis, K. Yu, Energetics of nonradiative surface trap states in nanoparticles monitored by time-of-flight photoconduction measurements on nanoparticle-polymer blends, *ACS Appl. Mater. Interfaces* 11 (40) (2019) 37184–37192.
- [406] X. Dai, Y. Xie, W. Feng, Y. Chen, Nanomedicine-enabled chemical regulation of reactive X species for versatile disease treatments, *Angew. Chem. Int. Ed. Engl.* 62 (50) (2023) e202309160.
- [407] Y. Dai, X. Li, Y. Xue, K. Chen, G. Jiao, L. Zhu, M. Li, Q. Fan, Y. Dai, Q. Zhao, Q. Shen, Self-delivery of metal-coordinated NIR-II nanoaddjutants for multimodal imaging-guided photothermal-chemodynamic amplified immunotherapy, *Acta Biomater.* 166 (2023) 496–511.
- [408] D. Zhang, Z. Cai, N. Liao, S. Lan, M. Wu, H. Sun, Z. Wei, J. Li, X. Liu, pH/hypoxia programmable triggered cancer photo-chemotherapy based on a semiconducting polymer dot hybridized mesoporous silica framework, *Chem. Sci.* 9 (37) (2018) 7390–7399.
- [409] V. Ratziu, M. Hompesch, M. Petricean, C. Serdjebi, J.S. Iyer, A.V. Parwani, D. Tai, E. Bugianesi, K. Cusi, S.L. Friedman, E. Lawitz, M. Romero-Gomez, D. Schuppan, R. Loomba, V. Paradis, C. Behling, A.J. Sanyal, Artificial intelligence-assisted digital pathology for non-alcoholic steatohepatitis: current status and future directions, *J. Hepatol.* 80 (2) (2023) 335–351.
- [410] C. Aging Biomarker, H. Bao, J. Cao, M. Chen, M. Chen, W. Chen, X. Chen, Y. Chen, Y. Chen, Y. Chen, Z. Chen, J.K. Chhetri, Y. Ding, J. Feng, J. Guo, M. Guo, C. He, Y. Jia, H. Jiang, Y. Jing, D. Li, J. Li, J. Li, Q. Liang, R. Liang, F. Liu, X. Liu, Z. Liu, O.J. Luo, J. Lv, J. Ma, K. Mao, J. Nie, X. Qiao, X. Sun, X. Tang, J. Wang, Q. Wang, S. Wang, X. Wang, Y. Wang, Y. Wang, R. Wu, K. Xia, F.H. Xiao, L. Xu, Y. Xu, H. Yan, L. Yang, R. Yang, Y. Yang, Y. Ying, L. Zhang, W. Zhang, W. Zhang, W. Zhang, X. Zhang, Z. Zhang, M. Zhou, R. Zhou, Q. Zhu, Z. Zhu, F. Cao, Z. Cao, P. Chan, C. Chen, G. Chen, H.Z. Chen, J. Chen, W. Ci, B.S. Ding, Q. Ding, F. Gao, J.J. Han, K. Huang, Z. Ju, Q.P. Kong, J. Li, J. Li, X. Li, B. Liu, F. Liu, L. Liu, Q. Liu, Q. Liu, X. Liu, Y. Liu, X. Luo, S. Ma, X. Ma, Z. Mao, J. Nie, Y. Peng, J. Qu, J. Ren, R. Ren, M. Song, Z. Songyang, Y.E. Sun, Y. Sun, M. Tian, S. Wang, S. Wang, X. Wang, X. Wang, Y.J. Wang, Y. Wang, C.C.L. Wong, A.P. Xiang, Y. Xiao, Z. Xie, D. Xu, J. Ye, R. Yue, C. Zhang, H. Zhang, L. Zhang, W. Zhang, Y. Zhang, Y.W. Zhang, Z. Zhang, T. Zhao, Y. Zhao, D. Zhu, W. Zou, G. Pei, G.H. Liu, Biomarkers of aging, *Sci. China Life Sci.* 66 (5) (2023) 893–1066.
- [411] G. Ravegnini, F. Gorini, E. De Crescenzo, A. De Leo, D. De Biase, M. Di Stanislao, P. Hrelia, S. Angelini, P. De Iaco, A.M. Perrone, Can miRNAs be useful biomarkers in improving prognostic stratification in endometrial cancer patients? An update review, *Int. J. Cancer* 150 (7) (2022) 1077–1090.
- [412] G.B. Lerner, S. Virmani, J.M. Henderson, J.M. Francis, L.H. Beck Jr., A conceptual framework linking immunology, pathology, and clinical features in primary membranous nephropathy, *Kidney Int* 100 (2) (2021) 289–300.
- [413] S. Rogalla, C.H. Contag, Early cancer detection at the epithelial surface, *Cancer J* 21 (3) (2015) 179–187.
- [414] A. Hanifi, X. Bi, X. Yang, B. Kavukcuoglu, P.C. Lin, E. DiCarlo, R.G. Spencer, M. P. Bostrom, N. Pleshko, Infrared fiber optic probe evaluation of degenerative cartilage correlates to histological grading, *Am. J. Sports Med.* 40 (12) (2012) 2853–2861.
- [415] J. Krohn, P. Svenmarker, C.T. Xu, S.J. Mork, S. Andersson-Engels, Transscleral optical spectroscopy of uveal melanoma in enucleated human eyes, *Invest. Ophthalmol. Vis. Sci.* 53 (9) (2012) 5379–5385.
- [416] M.P. O'Brien, M. Pennmata, U. Palukuru, P. West, X. Yang, M.P. Bostrom, T. Freeman, N. Pleshko, Monitoring the progression of spontaneous articular cartilage healing with infrared spectroscopy, *Cartilage* 6 (3) (2015) 174–184.
- [417] Q. Zhu, A. Ricci Jr., P. Hegde, M. Kane, E. Cronin, A. Merkulov, Y. Xu, B. Tavakoli, S. Tannenbaum, Assessment of functional differences in malignant and benign breast lesions and improvement of diagnostic accuracy by using US-guided diffuse optical tomography in conjunction with conventional US, *Radiology* 280 (2) (2016) 387–397.
- [418] G.C. Cockerham, K. Bijwaard, Z.M. Sheng, A.A. Hidayat, R.L. Font, I.W. McLean, Primary graft failure : a clinicopathologic and molecular analysis, *Ophthalmology* 107 (11) (2000) 2083–2090. ;discussion 2090–1.
- [419] R. Ren, S. Cai, X. Fang, X. Wang, Z. Zhang, M. Damiani, C. Hudlerova, A. Rosa, J. Hope, N.J. Cook, P. Gorenkin, A. Erofeev, P. Novak, A. Badhan, M. Crone, P. Freemont, G.P. Taylor, L. Tang, C. Edwards, A. Shevchuk, P. Cherepanov, Z. Luo, W. Tan, Y. Korchev, A.P. Ivanov, J.B. Edel, Multiplexed detection of viral

- antigen and RNA using nanopore sensing and encoded molecular probes, *Nat. Commun.* 14 (1) (2023) 7362.
- [420] M. Chen, Z. Feng, X. Fan, J. Sun, W. Geng, T. Wu, J. Sheng, J. Qian, Z. Xu, Long-term monitoring of intravital biological processes using fluorescent protein-assisted NIR-II imaging, *Nat. Commun.* 13 (1) (2022) 6643.
- [421] Z. Yang, L. Li, A.J. Jin, W. Huang, X. Chen, Rational design of semiconducting polymer brushes as cancer theranostics, *Mater. Horiz.* 7 (6) (2020) 1474–1494.
- [422] A.A. Shemetov, M.V. Monakhov, Q. Zhang, J.E. Canton-Josh, M. Kumar, M. Chen, M.E. Matlashov, X. Li, W. Yang, L. Nie, D.M. Shcherbakova, Y. Kozorovitskiy, J. Yao, N. Ji, V.V. Verkhusha, A near-infrared genetically encoded calcium indicator for *in vivo* imaging, *Nat. Biotechnol.* 39 (3) (2021) 368–377.
- [423] L. Tang, B.P. Nadappuram, P. Cadinu, Z. Zhao, L. Xue, L. Yi, R. Ren, J. Wang, A. P. Ivanov, J.B. Edel, Combined quantum tunnelling and dielectrophoretic trapping for molecular analysis at ultra-low analyte concentrations, *Nat. Commun.* 12 (1) (2021) 913.
- [424] R. Liang, J. Wang, X. Wu, L. Dong, R. Deng, K. Wang, M. Sullivan, S. Liu, M. Wu, J. Tao, X. Yang, J. Zhu, Multifunctional biodegradable polymer nanoparticles with uniform sizes: generation and *in vitro* anti-melanoma activity, *Nanotechnology* 24 (45) (2013) 455302.
- [425] J.F. Maya-Vetencourt, G. Manfredi, M. Mete, E. Colombo, M. Bramini, S. Di Marco, D. Shmal, G. Mantero, M. Dipalo, A. Rocchi, M.L. DiFrancesco, E. D. Papaleo, A. Russo, J. Barsotti, C. Eleftheriou, F. Di Maria, V. Cossu, F. Piazza, L. Emionite, F. Ticconi, C. Marini, G. Sambuceti, G. Pertile, G. Lanzani, F. Benfenati, Subretinally injected semiconducting polymer nanoparticles rescue vision in a rat model of retinal dystrophy, *Nat. Nanotechnol.* 15 (8) (2020) 698–708.
- [426] M.A. Ansari, T. Tripathi, B. Venkidasamy, A. Monziani, G. Rajakumar, M. N. Alomary, S.A. Alyahya, O. Onimus, N. D’Souza, M.A. Barkat, E.A. Al-Suhaimi, R. Samynathan, M. Thiruvengadam, Multifunctional nanocarriers for Alzheimer’s disease: befriending the barriers, *Mol. Neurobiol.* (2023), <https://doi.org/10.1007/s12035-023-03730-z>.
- [427] S. Yuan, T. Ma, Y.N. Zhang, N. Wang, Z. Baloch, K. Ma, Novel drug delivery strategies for antidepressant active ingredients from natural medicinal plants: the state of the art, *J. Nanobiotechnology* 21 (1) (2023) 391.
- [428] X. Chu, M. Duan, H. Hou, Y. Zhang, P. Liu, H. Chen, Y. Liu, S.L. Li, Recent strategies of carbon dot-based nanodrugs for enhanced emerging antitumor modalities, *J. Mater. Chem. B* 11 (38) (2023) 9128–9154.
- [429] X. Li, S. Zhang, X. Zhang, Y. Hou, X. Meng, G. Li, F. Xu, L. Teng, Y. Qi, F. Sun, Y. Li, Folate receptor-targeting semiconducting polymer dots hybrid mesoporous silica nanoparticles against rheumatoid arthritis through synergistic photothermal therapy, photodynamic therapy, and chemotherapy, *Int. J. Pharm.* 607 (2021) 120947.
- [430] Y. Tang, H. Chen, K. Chang, Z. Liu, Y. Wang, S. Qu, H. Xu, C. Wu, Photo-cross-linkable polymer dots with stable sensitizer loading and amplified singlet oxygen generation for photodynamic therapy, *ACS Appl. Mater. Interfaces* 9 (4) (2017) 3419–3431.
- [431] J. Cruz Navarro, L.L. Ponce Mejia, C. Robertson, A precision medicine agenda in traumatic brain injury, *Front Pharmacol* 13 (2022) 713100.
- [432] M. Wolter, E.T. Grant, M. Boudaud, A. Steinle, G.V. Pereira, E.C. Martens, M. S. Desai, Leveraging diet to engineer the gut microbiome, *Nat. Rev. Gastroenterol. Hepatol.* 18 (12) (2021) 885–902.
- [433] J.K. Hockings, J.A. Castrillon, F. Cheng, Pharmacogenomics meets precision cardio-oncology: is there synergistic potential? *Hum. Mol. Genet.* 29 (R2) (2020) R177–R185.
- [434] M.D. Qian, W.Y. Hou, D.D. Chen, X.S. Li, Q.D. Chen, C.F. Wu, Metalloporphyrin loaded semiconducting polymer dots as potent photosensitizers via triplet-triplet energy transfer, *J. Photochem. Photobiol. A-Chem.* 383 (2019).
- [435] K. Chang, D. Gao, Q. Qi, Y. Liu, Z. Yuan, Engineering biocompatible benzodithiophene-based polymer dots with tunable absorptions as high-efficiency theranostic agents for multiscale photoacoustic imaging-guided photothermal therapy, *Biomater. Sci.* 7 (4) (2019) 1486–1492.
- [436] Y. Wu, H. Yang, C. Shi, H. Sun, S. Yin, G. Wang, Luminescence-enhanced conjugated polymer dots through thermal treatment for cell imaging, *Biomater. Sci.* 10 (17) (2022) 4764–4772.
- [437] D. Meisner, M. Mezei, Liposome ocular delivery systems, *Adv. Drug Deliv. Rev.* 16 (1) (1995) 75–93.
- [438] W. Mehner, K. Mäder, Solid lipid nanoparticles Production, characterization and applications, *Adv. Drug Deliv. Rev.* 64 (2012) 83–101.
- [439] H. Dang, C. Dong, L. Zhang, Sustained latanoprost release from PEGylated solid lipid nanoparticle-laden soft contact lens to treat glaucoma, *Pharm. Dev. Technol.* 27 (2) (2022) 127–133.
- [440] E.B. Souto, R.H. Muller, Lipid nanoparticles: effect on bioavailability and pharmacokinetic changes, *Handb. Exp. Pharmacol.* 197 (2010) 115–141.
- [441] J.W. Lee, J.H. Park, J.R. Robinson, Bioadhesive-based dosage forms: the next generation, *J. Pharm. Sci.* 89 (7) (2000) 850–866.
- [442] Z. Liu, Y. Jiao, Y. Wang, C. Zhou, Z. Zhang, Polysaccharides-based nanoparticles as drug delivery systems, *Adv. Drug Deliv. Rev.* 60 (15) (2008) 1650–1662.
- [443] W.B. Zhao, K.K. Liu, Y. Wang, F.K. Li, R. Guo, S.Y. Song, C.X. Shan, Antibacterial carbon dots: mechanisms, design, and applications, *Adv. Healthc. Mater.* 12 (23) (2023) e2300324.
- [444] X. Ma, Q. Zhou, B. Gao, Recent advances of biosensors on microneedles, *Anal. Methods* 15 (43) (2023) 5711–5730.
- [445] C.L. Bourlais, L. Acar, H. Zia, P.A. Sado, T. Needham, R. Leverage, Ophthalmic drug delivery systems—recent advances, *Prog. Retin. Eye Res.* 17 (1) (1998) 33–58.
- [446] D. Dhumal, B. Maron, E. Malach, Z. Lyu, L. Ding, D. Marson, E. Laurini, A. Tintaru, B. Ralahy, S. Giorgio, S. Prich, Z. Hayouka, L. Peng, Dynamic self-assembling supramolecular dendrimer nanosystems as potent antibacterial candidates against drug-resistant bacteria and biofilms, *Nanoscale* 14 (26) (2022) 9286–9296.
- [447] Q. Cui, T. Liu, X. Li, L. Zhao, Q. Wu, X. Wang, K. Song, D. Ge, Validation of the mechano-bactericidal mechanism of nanostructured surfaces with finite element simulation, *Colloids Surf. B-Biointerfaces* 206 (2021) 111929.
- [448] K.Y. Zheng, M.I. Setyawati, D.T. Leong, J.P. Xie, Antimicrobial silver nanomaterials, *Coord. Chem. Rev.* 357 (2018) 1–17.
- [449] N. Kashef, Y.Y. Huang, M.R. Hamblin, Advances in antimicrobial photodynamic inactivation at the nanoscale, *Nanophotonics* 6 (5) (2017) 853–879.
- [450] C.A. Juan, J.M. Perez de la Lastra, F.J. Plou, E. Perez-Lebna, The chemistry of reactive oxygen species (ROS) revisited: outlining their role in biological macromolecules (DNA, lipids and proteins) and induced pathologies, *Int. J. Mol. Sci.* 22 (9) (2021) 4642.
- [451] X. Wang, F. Lv, T. Li, Y. Han, Z. Yi, M. Liu, J. Chang, C. Wu, Electrospun micropatterned nanocomposites incorporated with Cu(2)S nanoflowers for skin tumor therapy and wound healing, *ACS Nano* 11 (11) (2017) 11337–11349.
- [452] S. Link, M.A. El-Sayed, Shape and size dependence of radiative, non-radiative and photothermal properties of gold nanocrystals, *Int. Rev. Phys. Chem.* 19 (3) (2000) 409–453.
- [453] S. Wang, B. Cai, H. Tian, Efficient generation of hydrogen peroxide and formate by an organic polymer dots photocatalyst in alkaline conditions, *Angew. Chem. Int. Ed. Engl.* 61 (23) (2022) e202202733.
- [454] L. Wang, R. Fernandez-Teran, L. Zhang, D.L. Fernandes, L. Tian, H. Chen, H. Tian, Organic polymer dots as photocatalysts for visible light-driven hydrogen generation, *Angew. Chem. Int. Ed. Engl.* 55 (40) (2016) 12306–12310.
- [455] L. Ding, Y. Wu, M. Wu, Q. Zhao, H. Li, J. Liu, X. Liu, X. Zhang, Y. Zeng, Engineered red blood cell biomimetic nanovesicle with oxygen self-supply for near-infrared-II fluorescence-guided synergistic chemo-photodynamic therapy against hypoxic tumors, *ACS Appl. Mater. Interfaces* 13 (44) (2021) 52435–52449.
- [456] H. Shen, C. Jiang, W. Li, Q. Wei, R.A. Ghiladi, Q. Wang, Synergistic photodynamic and photothermal antibacterial activity of *in situ* grown bacterial cellulose/MoS (2)-chitosan nanocomposite materials with visible light illumination, *ACS Appl. Mater. Interfaces* 13 (26) (2021) 31193–31205.
- [457] M. Xu, Y. Qi, G. Liu, Y. Song, X. Jiang, B. Du, Size-dependent *in vivo* transport of nanoparticles: implications for delivery, targeting, and clearance, *ACS Nano* 17 (21) (2023) 20825–20849.
- [458] D. Sun, W. Gao, H. Hu, S. Zhou, Why 90% of clinical drug development fails and how to improve it?, *Acta Pharm. Sin. B* 12 (7) (2022) 3049–3062.
- [459] W. Poon, B.R. Kingston, B. Ouyang, W. Ngo, W.C.W. Chan, A framework for designing delivery systems, *Nat. Nanotechnol.* 15 (10) (2020) 819–829.
- [460] B.J. Nelson, S. Pane, Delivering drugs with microrobots, *Science* 382 (6675) (2023) 1120–1122.
- [461] P. Baluk, J. Fuxe, H. Hashizume, T. Romano, E. Lashnits, S. Butz, D. Vestweber, M. Corada, C. Molendini, E. Dejana, D.M. McDonald, Functionally specialized junctions between endothelial cells of lymphatic vessels, *J. Exp. Med.* 204 (10) (2007) 2349–2362.
- [462] S.K. Hobbs, W.L. Monsky, F. Yuan, W.G. Roberts, L. Griffith, V.P. Torchilin, R. K. Jain, Regulation of transport pathways in tumor vessels: role of tumor type and microenvironment, *Proc. Natl. Acad. Sci. U.S.A.* 95 (8) (1998) 4607–4612.
- [463] J. Linnankoski, J. Makela, J. Palmgren, T. Mauriala, C. Vedin, A.L. Ungell, L. Lazarova, P. Artursson, A. Urtti, M. Yliperttila, Paracellular porosity and pore size of the human intestinal epithelium in tissue and cell culture models, *J. Pharm. Sci.* 99 (4) (2010) 2166–2175.
- [464] T. Cedervall, I. Lynch, S. Lindman, T. Berggard, E. Thulin, H. Nilsson, K. A. Dawson, S. Linse, Understanding the nanoparticle-protein corona using methods to quantify exchange rates and affinities of proteins for nanoparticles, *Proc. Natl. Acad. Sci. U.S.A.* 104 (7) (2007) 2050–2055.
- [465] M.P. Monopoli, C. Aberg, A. Salvati, K.A. Dawson, Biomolecular coronas provide the biological identity of nanosized materials, *Nat. Nanotechnol.* 7 (12) (2012) 779–786.
- [466] G. Caracciolo, O.C. Farokhzad, M. Mahmoodi, Biological identity of nanoparticles *in vivo*: clinical implications of the protein corona, *Trends Biotechnol.* 35 (3) (2017) 257–264.
- [467] M.A. Dobrovolskaia, A.K. Patri, J. Zheng, J.D. Clogston, N. Ayub, P. Aggarwal, B. W. Neun, J.B. Hall, S.E. McNeil, Interaction of colloidal gold nanoparticles with human blood: effects on particle size and analysis of plasma protein binding profiles, *Nanomedicine* 5 (2) (2009) 106–117.
- [468] J. Piella, N.G. Bastus, V. Puntes, Size-dependent protein-nanoparticle interactions in citrate-stabilized gold nanoparticles: the emergence of the protein corona, *Bioconjug. Chem.* 28 (1) (2017) 88–97.
- [469] S. Wilhelm, A.J. Tavares, Q. Dai, S. Ohta, J. Audet, H.F. Dvorak, W.C.W. Chan, Analysis of nanoparticle delivery to tumours, *Nat. Rev. Mater.* 1 (5) (2016) 16014.
- [470] X. Li, Z. Huang, Z. Liao, A. Liu, S. Huo, Transformable nanodrugs for overcoming the biological barriers in the tumor environment during drug delivery, *Nanoscale* 15 (19) (2023) 8532–8547.
- [471] C. Qiu, F. Xia, J. Zhang, Q. Shi, Y. Meng, C. Wang, H. Pang, L. Gu, C. Xu, Q. Guo, J. Wang, Advanced Strategies for Overcoming Endosomal/Lysosomal Barrier in Nanodrug Delivery, vol. 6, Research (Wash D C), 2023, p. 148.
- [472] L.N.M. Nguyen, Z.P. Lin, S. Sindhwan, P. MacMillan, S.M. Mladjenovic, B. Stordy, W. Ngo, W.C.W. Chan, The exit of nanoparticles from solid tumours, *Nat. Mater.* 22 (10) (2023) 1261–1272.

- [473] E. Felli, S. Selicean, S. Guixe-Muntet, C. Wang, J. Bosch, A. Berzigotti, J. Gracia-Sancho, Mechanobiology of portal hypertension, *JHEP Rep* 5 (11) (2023) 100869.
- [474] Y.N. Zhang, W. Poon, A.J. Tavares, I.D. McGilvray, W.C.W. Chan, Nanoparticle-liver interactions: cellular uptake and hepatobiliary elimination, *J. Control Release* 240 (2016) 332–348.
- [475] H. Wang, C.A. Thorling, X. Liang, K.R. Bridle, J.E. Grice, Y. Zhu, D.H.G. Crawford, Z.P. Xu, X. Liu, M.S. Roberts, Diagnostic imaging and therapeutic application of nanoparticles targeting the liver, *J. Mater. Chem. B* 3 (6) (2015) 939–958.
- [476] H.S. Choi, W. Liu, P. Misra, E. Tanaka, J.P. Zimmer, B. Itty Ipe, M.G. Bawendi, J. V. Frangioni, Renal clearance of quantum dots, *Nat. Biotechnol.* 25 (10) (2007) 1165–1170.
- [477] Y. Huang, M. Yu, J. Zheng, Proximal tubules eliminate endocytosed gold nanoparticles through an organelle-extrusion-mediated self-renewal mechanism, *Nat. Nanotechnol.* 18 (6) (2023) 637–646.
- [478] Z. Jin, Q. Gao, K. Wu, J. Ouyang, W. Guo, X.J. Liang, Harnessing inhaled nanoparticles to overcome the pulmonary barrier for respiratory disease therapy, *Adv. Drug. Deliv. Rev.* 202 (2023) 115111.
- [479] L. Zhang, B.Z. Zhai, Y.J. Wu, Y. Wang, Recent progress in the development of nanomaterials targeting multiple cancer metabolic pathways: a review of mechanistic approaches for cancer treatment, *Drug Deliv* 30 (1) (2023) 1–18.
- [480] Y. Li, Y. Guo, K. Zhang, R. Zhu, X. Chen, Z. Zhang, W. Yang, Cell death pathway regulation by functional nanomedicines for robust antitumor immunity, *Adv. Sci.* 11 (3) (2024) e2306580.
- [481] Y. Liu, G. Yang, Y. Hui, S. Ranaweera, C.X. Zhao, Microfluidic nanoparticles for drug delivery, *Small* 18 (36) (2022) e2106580.
- [482] W. Zhou, Y. Chen, Y. Zhang, X. Xin, R. Li, C. Xie, Q. Fan, Iodine-rich semiconducting polymer nanoparticles for CT/fluorescence dual-modal imaging-guided enhanced photodynamic therapy, *Small* 16 (5) (2020) e1905641.
- [483] X. Song, H. Qian, Y. Yu, Nanoparticles mediated the diagnosis and therapy of glioblastoma: bypass or cross the blood-brain barrier, *Small* 19 (45) (2023) e2302613.
- [484] K. Liu, Y. Yao, S. Xue, M. Zhang, D. Li, T. Xu, F. Zhi, Y. Liu, D. Ding, Recent advances of tumor microenvironment-responsive nanomedicines-energized combined phototherapy of cancers, *Pharmaceutics* 15 (10) (2023) 2480.
- [485] J.S. Ni, Y. Li, W. Yue, B. Liu, K. Li, Nanoparticle-based cell trackers for biomedical applications, *Theranostics* 10 (4) (2020) 1923–1947.
- [486] Y.H. Chan, M.E. Gallina, X. Zhang, I.C. Wu, Y. Jin, W. Sun, D.T. Chiu, Reversible photoswitching of spiropyran-conjugated semiconducting polymer dots, *Anal. Chem.* 84 (21) (2012) 9431–9438.
- [487] C.T. Kuo, A.M. Thompson, M.E. Gallina, F. Ye, E.S. Johnson, W. Sun, M. Zhao, J. Yu, I.C. Wu, B. Fujimoto, C.C. DuFort, M.A. Carlson, S.R. Hingorani, A. L. Paguirigan, J.P. Radich, D.T. Chiu, Optical painting and fluorescence activated sorting of single adherent cells labelled with photoswitchable Pdots, *Nat. Commun.* 7 (2016) 11468.
- [488] S.C. Taylor, A. Posch, The design of a quantitative western blot experiment, *Biomed. Res. Int.* 2014 (2014) 361590.
- [489] F. Ye, P.B. Smith, C. Wu, D.T. Chiu, Ultrasensitive detection of proteins on Western blots with semiconducting polymer dots, *Macromol. Rapid Commun.* 34 (9) (2013) 785–790.
- [490] S.K. Lee, J. Baek, K.F. Jensen, High throughput synthesis of uniform biocompatible polymer beads with high quantum dot loading using microfluidic jet-mode breakup, *Langmuir* 30 (8) (2014) 2216–2222.
- [491] H. Chen, K. Chang, X. Men, K. Sun, X. Fang, C. Ma, Y. Zhao, S. Yin, W. Qin, C. Wu, Covalent patterning and rapid visualization of latent fingerprints with photo-cross-linkable semiconductor polymer dots, *ACS Appl. Mater. Interfaces* 7 (26) (2015) 14477–14484.
- [492] Y. Yang, X. Fan, L. Li, Y. Yang, A. Nuernisha, D. Xue, C. He, J. Qian, Q. Hu, H. Chen, J. Liu, W. Huang, Semiconducting polymer nanoparticles as theranostic system for near-infrared-II fluorescence imaging and photothermal therapy under safe laser fluence, *ACS Nano* 14 (2) (2020) 2509–2521.
- [493] J. Li, K. Pu, Development of organic semiconducting materials for deep-tissue optical imaging, phototherapy and photoactivation, *Chem. Soc. Rev.* 48 (1) (2019) 38–71.
- [494] J.I. Shin, S.J. Cho, J. Jeon, K.H. Lee, J.J. Wie, Three-dimensional micropatterning of semiconducting polymers via capillary force-assisted evaporative self-assembly, *Soft Matter* 15 (19) (2019) 3854–3863.
- [495] F. Sajjad, H. Jin, Y. Han, L. Wang, L. Bao, T. Chen, Y. Yan, Y. Qiu, Z.L. Chen, Incorporation of green emission polymer dots into pyropheophorbide-alpha enhance the PDT effect and biocompatibility, *Photodiagnosis Photodyn. Ther.* 37 (2022) 102562.
- [496] X. Su, Z. Bao, W. Xie, D. Wang, T. Han, D. Wang, B.Z. Tang, Precise planar-twisted molecular engineering to construct semiconducting polymers with balanced absorption and quantum yield for efficient phototheranostics, *Research* 6 (2023) 194.
- [497] X. Duan, M. Zhang, Y.H. Zhang, Organic fluorescent probes for live-cell super-resolution imaging, *Front Optoelectron* 16 (1) (2023) 34.
- [498] A.R. Aref, M. Campisi, E. Ivanova, A. Portell, D. Larios, B.P. Piel, N. Mathur, C. Zhou, R.V. Coakley, A. Bartels, M. Bowden, Z. Herbert, S. Hill, S. Gilhooley, J. Carter, I. Canadas, T.C. Thai, S. Kitajima, V. Chiono, C.P. Paweletz, D.A. Barbee, R.D. Kamm, R.W. Jenkins, 3D microfluidic ex vivo culture of organotypic tumor spheroids to model immune checkpoint blockade, *Lab. Chip.* 18 (20) (2018) 3129–3143.
- [499] R.W. Jenkins, A.R. Aref, P.H. Lizotte, E. Ivanova, S. Stinson, C.W. Zhou, M. Bowden, J. Deng, H. Liu, D. Miao, M.X. He, W. Walker, G. Zhang, T. Tian, C. Cheng, Z. Wei, S. Palakurthi, M. Bittinger, H. Vitzthum, J.W. Kim, A. Merlino, M. Quinn, C. Venkataramani, J.A. Kaplan, A. Portell, P.C. Gokhale, B. Phillips, A. Smart, A. Rotem, R.E. Jones, L. Keogh, M. Anguiano, L. Stapleton, Z. Jia, M. Barzily-Rokni, I. Canadas, T.C. Thai, M.R. Hammond, R. Vlahos, E.S. Wang, H. Zhang, S. Li, G.J. Hanna, W. Huang, M.P. Hoang, A. Piris, J.P. Eliane, A. O. Stemmer-Rachamimov, L. Cameron, M.J. Su, P. Shah, B. Izar, M. Thakuria, N. R. LeBoeuf, G. Rabinowitz, V. Gundu, S. Parangi, J.M. Cleary, B.C. Miller, S. Kitajima, R. Thummalapalli, B. Miao, T.U. Barbee, V. Sivathanu, J. Wong, W. G. Richards, P. Bueno, C.H. Yoon, J. Miret, M. Herlyn, L.A. Garraway, E.M. Van Allen, G.J. Freeman, P.T. Kirschmeier, J.H. Lorch, P.A. Ott, F.S. Hodin, K. T. Flaherty, R.D. Kamm, G.M. Boland, K.K. Wong, D. Dornan, C.P. Paweletz, D. A. Barbee, Ex vivo profiling of PD-1 blockade using organotypic tumor spheroids, *Cancer Discov* 8 (2) (2018) 196–215.
- [500] H. Aboulkheyr Es, A.R. Aref, M.E. Warkiani, Generation and culture of organotypic breast carcinoma spheroids for the study of drug response in a 3D microfluidic device, *Methods Mol. Biol.* 2535 (2022) 49–57.
- [501] D. Ding, J. Liu, G. Feng, K. Li, Y. Hu, B. Liu, Bright far-red/near-infrared conjugated polymer nanoparticles for in vivo bioimaging, *Small* 9 (18) (2013) 3093–3102.
- [502] U. Resch-Genger, M. Grabolle, S. Cavaliere-Jaricot, R. Nitschke, T. Nann, Quantum dots versus organic dyes as fluorescent labels, *Nat. Methods* 5 (9) (2008) 763–775.
- [503] X. Lim, The nanolight revolution is coming, *Nature* 531 (7592) (2016) 26–28.
- [504] F. Xiao, X. Fang, H. Li, H. Xue, Z. Wei, W. Zhang, Y. Zhu, L. Lin, Y. Zhao, C. Wu, L. Tian, Light-harvesting fluorescent spherical nucleic acids self-assembled from a DNA-grafted conjugated polymer for amplified detection of nucleic acids, *Angew. Chem. Int. Ed. Engl.* 61 (12) (2022) e202115812.
- [505] A. Eftekhari, C. Kryschi, D. Pamies, S. Gülec, E. Ahmadian, D. Janas, S. Davaran, R. Khalilov, Natural and synthetic nanovectors for cancer therapy, *Nanotheranostics* 7 (3) (2023) 236–257.
- [506] J. Gu, X. Li, D. Hu, Y. Liu, G. Zhang, X. Jia, W. Huang, K. Xi, Green synthesis of amphiphilic carbon dots from organic solvents: application in fluorescent polymer composites and bio-imaging, *RSC Adv* 8 (23) (2018) 12556–12561.
- [507] X. Gao, C. Li, Nanopropes visualizing gliomas by crossing the blood brain tumor barrier, *Small* 10 (3) (2014) 426–440.
- [508] S.N. Tammam, H.M.E. Azzazy, A. Lamprecht, How successful is nuclear targeting by nanocarriers? *J. Control Release* 229 (2016) 140–153.
- [509] J. He, C. Li, L. Ding, Y. Huang, X. Yin, J. Zhang, J. Zhang, C. Yao, M. Liang, R. P. Pirraco, J. Chen, Q. Lu, R. Baldridge, Y. Zhang, M. Wu, R.L. Reis, Y. Wang, Tumor targeting strategies of smart fluorescent nanoparticles and their applications in cancer diagnosis and treatment, *Adv. Mater.* 31 (40) (2019) e1902409.
- [510] N. Dhas, M.C. Garcia, R. Kudarha, A. Pandey, A.N. Nikam, D. Gopalan, G. Fernandes, S. Soman, S. Kulkarni, R.N. Seetharam, R. Tiwari, S. Waikar, C. Pardeshi, S. Mutalik, Advancements in cell membrane camouflaged nanoparticles: a bioinspired platform for cancer therapy, *J. Control Release* 346 (2022) 71–97.
- [511] Y. Luo, M. Yin, C. Mu, X. Hu, H. Xie, J. Li, T. Cao, N. Chen, J. Wu, C. Fan, Engineering female germline stem cells with exocytotic polymer dots, *Adv. Mater.* 35 (24) (2023) e2210458.
- [512] H. Zhao, C. Xu, T. Wang, J. Liu, Biomimetic construction of artificial selenoenzymes, *Biomimetics* 8 (1) (2023) 54.
- [513] R.K. Sindhu, A. Najda, P. Kaur, M. Shah, H. Singh, P. Kaur, S. Cavaliere, M. Jaroszuk-Sierocińska, M.H. Rahman, Potentiality of nanoenzymes for cancer treatment and other diseases: current status and future challenges, *Materials* 14 (20) (2021) 5965.
- [514] Z. Yu, R. Lou, W. Pan, N. Li, B. Tang, Nanoenzymes in disease diagnosis and therapy, *Chem. Commun.* 56 (99) (2020) 15513–15524.
- [515] B. Cai, M. Axelsson, S. Zhan, M.V. Pavliuk, S. Wang, J. Li, H. Tian, Organic polymer dots photocatalyze CO<sub>2</sub> reduction in aqueous solution, *Angew. Chem. Int. Ed. Engl.* 62 (45) (2023) e202312276.
- [516] J.E. Jeong, J.J. Sutton, H.S. Ryu, M. Kang, E.J. Tay, T.L. Nguyen, K.C. Gordon, S. H. Shim, H.Y. Woo, Resonant Raman-active polymer dot barcodes for multiplex cell mapping, *ACS Nano* 17 (5) (2023) 4800–4812.
- [517] M.V. Pavliuk, M. Lorenzi, D.R. Morado, L. Gedda, S. Wrede, S.H. Mejias, A. Liu, M. Senger, S. Glover, K. Edwards, G. Berggren, H. Tian, Polymer dots as photoactive membrane vesicles for [FeFe]-Hydrogenase self-assembly and solar-driven hydrogen evolution, *J. Am. Chem. Soc.* 144 (30) (2022) 13600–13611.